Université de Montréal

New Grafted PLA-g-PEG Polymeric Nanoparticles Used to Improve Bioavailability of Oral Drugs.

par
Mohamed Mokhtar

Faculté de pharmacie

Thèse présentée à la Faculté de pharmacie
en vue de l'obtention du grade de Ph.D.
en Science Pharmaceutiques
option Technologie Pharmaceutique

February, 2015

Université de Montréal
Facluté des études supérieures
Cette thèse intitulée:

New Grafted PEG-g-PLA Polymeric Nanoparticle used to Improve Bioavailability of Oral Drugs.

Présentée par
Mohamed Mokhtar

a été évaluée par un jury composé des personnes suivantes :

Dr. Valérie Gaëlle, Roullin , Président-rapporteur

Dr. Patrice Hildgen, Directeur de recherche

Dr. Patrick Gosselin, Co-directeur de recherche

Dr. François-Xavier Lacasse, Membre du jury

Dr. Charles Ramassamy , Examinateur externe

Dr. Gaétan Mayer, Représentant du doyen de la FES

February, 2015

Résumé

Les nanoparticules (NPs) de polymère ont montré des résultats prometteurs pour leur utilisation comme système de transport de médicaments pour une libération contrôlée du médicament, ainsi que pour du ciblage. La biodisponibilité des médicaments administrés oralement pourrait être limitée par un processus de sécrétion intestinale, qui pourrait par la suite être concilié par la glycoprotéine P (P-gp). La dispersion de la Famotidine (modèle de médicament) à l'intérieur des nanoparticules (NPs) pegylées a été évaluée afin d'augmenter la biodisponibilité avec du polyéthylène glycol (PEG), qui est connu comme un inhibiteur de P-gp. L'hypothèse de cette étude est que l'encapsulation de la Famotidine (un substrat de P-gp) à l'intérieur des NPs préparées à partir de PEG-g-PLA pourrait inhiber la fonction P-gp. La première partie de cette étude avait pour but de synthétiser quatre copolymères de PEG greffés sur un acide polylactide (PLA) et sur un squelette de polymère (PLA-g-PEG), avec des ratios de 1% et 5% (ratio molaire de PEG vs acide lactique monomère) de soit 750, soit 2000 Da de masse moléculaire. Ces polymères ont été employés afin de préparer des NPs chargés de Famotidine qui possède une faible perméabilité et une solubilité aqueuse relativement basse. Les NPs préparées ont été analysées pour leur principaux paramètres physicochimiques tels que la taille et la distribution de la taille, la charge de surface (Potentiel Zeta), la morphologie, l'efficacité d'encapsulation, le pourcentage résiduel en alcool polyvinylique (PVA) adsorbé à la surface des NPs, les propriétés thermiques, la structure cristalline et la libération du médicament. De même, les formules de NPs ont été testées *in vitro* sur des cellules CaCo-2 afin d'évaluer la perméabilité bidirectionnelle de la Famotidine. Généralement, les NPs préparées à

partir de polymères greffés PLA-g-5%PEG ont montré une augmentation de la perméabilité du médicament, ce par l'inhibition de l'efflux de P-gp de la Famotidine dans le modèle CaCo-2 *in vitro*. Les résultats ont montré une baisse significative de la sécrétion de la Famotidine de la membrane basolatéral à apical lorsque la Famotidine était encapsulée dans des NPs préparées à partir de greffes de 5% PEG de 750 ou 2000 Da, de même que pour d'autres combinaisons de mélanges physiques contenant du PEG5%. La deuxième partie de cette étude est à propos de ces NPs chargées qui démontrent des résultats prometteurs en termes de perméabilité et d'inhibition d'efflux de P-gp, et qui ont été choises pour développer une forme orale solide. La granulation sèche a été employée pour densifier les NPs, afin de développer des comprimés des deux formules sélectionnées de NPs. Les comprimés à base de NPs ont démontré un temps de désintégration rapide (moins d'une minute) et une libération similaire à la Famotidine trouvée sur le marché. Les résultats de l'étude du transport de comprimés à base de NPs étaient cohérents avec les résultats des formules de NPs en termes d'inhibition de P-gp, ce qui explique pourquoi le processus de fabrication du comprimé n'a pas eu d'effet sur les NPs. Mis ensemble, ces résultats montrent que l'encapsulation dans une NP de polymère pegylé pourrait être une stratégie prometteuse pour l'amélioration de la biodisponibilité des substrats de P-gp.

Mots-clés : Poly(ethylene glycol), P-glycoprotéine, Nanoparticules, Perméabilité, CaCo-2, Acide polylactique.

Abstract

Polymeric nanoparticles (NPs) have shown promising results to be used as drug delivery carriers for controlled drug release and for targeting. The bioavailability of orally administrated drugs might be limited by an intestinal absorbed secretion process, which could in turn be mediated by P-glycoprotein (P-gp). The dispersion of Famotidine (drug model) within PEGylated nanoparticles (NPs) was evaluated in order to enhance the bioavailability using polyethylene glycol (PEG), which is known as a P-gp inhibitor. The hypothesis of this study is that the encapsulation of Famotidine into NPs prepared from PEG-g-PLA could inhibit the P-gp function. The first part of the study aimed to synthesize four copolymers of PEG grafted on a polylactide acid (PLA) polymer backbone (PLA-g-PEG) with ratios of 1 % and 5 % (molar ratio of PEG vs lactic acid monomer) of either 750 or 2000 Da molecular weights. These polymers have been used to prepare NPs loaded with Famotidine, which has low permeability and relatively low aqueous solubility. Prepared NPs were analyzed for their main physicochemical parameters such as size and size distribution, surface charge, morphology, encapsulation efficiency, percentage of residual poly(vinyl alcohol) (PVA) adsorbed at the surface of the NPs, thermal properties, crystalline structure and drug release. Also, NP formulations were tested *in vitro* on CaCo-2 monolayer cells in order to assess the bidirectional permeability of Famotidine. Generally speaking, NPs prepared from PLA-g-5%PEG grafted polymers showed improved drug permeability by inhibiting the P-gp efflux of Famotidine in the CaCo-2 *in vitro* model. Results showed a very significant decrease in the secretion of Famotidine from basolateral to apical when Famotidine was encapsulated in NPs prepared from 5 % grafting of either

750 or 2000 Da PEG, as well as in other combinations of physical mixtures containing PEG5%. The second part of the study is about those loaded NPs which showed promising results in terms of permeability and inhibition of P-gp efflux and which were selected to develop a solid oral dosage form. Dry granulation was used to densify NPs in order to develop tablets of the two selected NP formulations. NP based tablets showed a fast disintegration time (less than one minute) and a similar release profile as marketed Famotidine. The transport study of NP based tablets showed consistent results with NP formulations in terms of P-gp inhibition, which explains why the tablet's manufacturing process had no effect on NPs. Our results demonstrated that the presence of hydrophilic polymers (PEG) on the surface of NPs grafted at 5 % PEG, irrespective to molecular weights, provides an effective way to control the interface between NPs and the biological systems (P-gp in this case) as they are designed to interact with. Taken together, these results show that encapsulation in a PEGylated polymeric NP could be a promising strategy to improve the oral bioavailability of P-gp substrates.

Keywords : Poly(ethylene glycol), P-glycoprotein, Nanoparticles, Permeability, CaCo-2, Poly(lactic) acid.

Table of content

List of Tables

List of Figures

Abbreviations

ABC	ATP-Binding Cassette
AFM	Atomic Force Microscope
AGE	Allyl Glycidyl Ether
ANOVA	Analysis of Variance
A˚	Angstrom
AP	Apical
AI	Asymmetric Index
ATP	Adenosine triphosphate
BCS	Biopharmaceutical Classification System
BL	Basolateral
BSA	Bovine serum albumin
ºC	Degree Celsius
CDCl3	Deuteriated chloroform
CO_2	Carbon dioxide
CTB	Cholera toxin B
Da	Dalton
D2O	Deuterium oxide
DCM	DiChloroMethane
DMAP	DiMethylAminoPyrudine
DMF	DiMethylFormamide
DMSO	DiMethyl SulfOxide
DL	Drug Loading
DMEM	Dulbecco's Modified Eagl's Medium

DLS	Dynamic Light Scattering
DSC	Differential scanning calorimetry
EE	Encapsulation efficiency
EPR	Enhanced permeability and retention
EDTA	Ethylene Diamine Tetra Acetic acid
FMT	Famotidine
FBS	Fetal bovine serum
FAE	Follicle-Association Epithelium
FDA	Food Drug Administration
FTIR	Fourier transform infrared spectroscopy
GIT	Gastro Intestinal tract
GPC	Gel permeation chromatography
h	Hour
HBSS	Hanks balanced supplement solution
HDPE	High Density Polyethylene
HCl	Hydrochloric acid
1H NMR	Proton nuclear magnetic resonance
HPLC	High performance liquid chromatography
HPH	High Pressure Homogenizer
IV	Intravenous
kDa	Kilo Dalton
MePEG	Methoxy Poly Ethylene Glycol
Mg	Magnesium
MCC	Micro crystalline cellulose

Mn	Number average molecular weight
MPS	Mononuclear phagocytic system
MTT	3-(4,5-dimethylthiazol-2-yl)-2,5-diphenyltetrazolium bromide
Mw	Weight average molecular weight
NaCl	Sodium chloride
NaOH	Sodium hydroxide
NBD	Nucleotide Binding Domains
NC	Nanocarrier
N/D	Not Detected
NPs	Nanoparticles
NEAA	Non Esstential Amino Acid
O/W	oil in water
PSD	Particle Size Distribution
P_{app}	Apparent permeability coefficient
PAMAM	Poly(amido amine)
PBS	Phosphate buffered saline
PCL	Poly(ε-caprolactone)
PCS	Photon Correlation Spectroscopy
PDI	Polydispersity index
PEG	Poly(ethylene glycol)
PEG-g-PLA	Poly(ethylene glycol)-grafted-poly(D,L-lactide)
PEG1%-g-PLA	Poly(ethylene glycol)1%-grafted-poly(D,L-lactide)
PEG5%-g-PLA	Poly(ethylene glycol)5%-grafted-poly(D,L-lactide)
PK	Pharmacokinetic

PLA	Poly(lactic acid)
PLGA	Poly(lactic-*co*-glycolic acid)
PM	physical Mixtures
PP	Peyer's patches
PPG	Polypropylene Glycol
PS	Polystyrene
PVA	Polyvinyl alcohol
RGD	Arginylglycylaspartic acid
SD	Standard deviation
SDP	Size Distribution Processor
SLN	Solid Lipid Nanoparticle
SLC	Solute Carrier
TEER	Trans epithelial electrical resistance
Tg	Glass transition temperature
TM-AFM	Tapping mode atomic force microscope
TMS	Tetra Methyl Silane
USP	United States Pharmacopeia
UV	Ultraviolet
wt	Weight
XRPD	X-ray Powder Diffraction

To my parents, my wife and my daughters

Remerciements

This work was done at Pharmaceutics technology department, Faculty of Pharmacy, University of Montreal. I would like to express my appreciation to my supervisor, Dr. Patrice Hildgen and co supervisor, Dr. Patrick Gosselin for their continuous support, advice, guidance and being available and willing to help me in the challenges during my study. Also I would like to thanks Dr. Patrice has given me the freedom and reliable basis necessary to advance this project and to develop as an independent researcher. I really value his valuable criticism throughout of my doctoral studies without which it would have been difficult to finish this thesis. I am sincerely grateful to all my co-supervisor, Dr. Patrick Gosselin, for his remarkable support, advices and being available contribution to this work.

Special thanks are due to Jean Michel Rabanel for his technical assistance, valuable discussion and suggestions during my study which I really appreciate. I would like to express my deep thankfulness to all my lab colleagues for discussions, friendship and for creating a pleasant atmosphere during these years.

Finally, I would like to express my gratitude to my parents, my wife, and my daughters for their endless support and love. It is their sacrifice and understanding that allowed me to work hard to finish this thesis.

I also express my gratitude for COREALIS Pharma, BMP innovation and Ministry of Higher Education, Libya for their financial support is gratefully acknowledged.

Contribution des auteurs

Cette thèse se base sur deux articles dont sont soumis. La contribution de chaque auteur est présentée ci-dessous

Chapitre 3: Design of PEG-grafted-PLA nanoparticles as oral permeability enhancer for P-gp substrate drug model Famotidine.

Mohamed Mokhtar*, Patrick Gosselin, Lacasse, François-Xavier and Patrice Hildgen

Tous les travaux expérimentaux ont été faites par Mohamed Mokhtar. Chaque auteur a participé à révision du manuscrit.

Chapitre 4: Tablet Formulation of Famotidine loaded P-gp inhibiting Nanoparticles using PEG-PLA Grafted Polymer.

Mohamed Mokhtar*, Patrick Gosselin, Lacasse, François-Xavier and Patrice Hildgen

Tous les travaux expérimentaux ont été faites par Mohamed Mokhtar. Chaque auteur a participé à révision du manuscrit.

Chapter One

Introduction

1. Introduction

The majority of drugs on the market are formulated for the oral route, most of them aimed at the blood circulation for the systemic action. It is the most convenient and safe administration route, particularly for chronic delivery, but it poses a number of challenges for formulators in terms of bioavailability (fraction of drug actually reaching the circulation) due to degradation by enzymes and harsh pH conditions, low solubility of some drugs and limited absorption by the gastro intestinal tract (GIT) epithelium(1). The GIT (Figure 1.1) is approximately 6 m in length with varying diameters. It consists of the oesophagus, the stomach, the small intestine (the major digestive organ) and large intestine or colon. The luminal surface is not smooth, with deep, circular fold about 1 cm high, villi, mucosal projections about 1 mm long, and microvilli (plasma membrane microprojections), increasing the surface area of absorption to about 200 cm^2. Orally administrated drug molecules must stay for enough time in intestinal lumen and resist harsh gastric and intestinal environments to be efficiently absorbed by intestinal cells via different mechanisms(1-3).

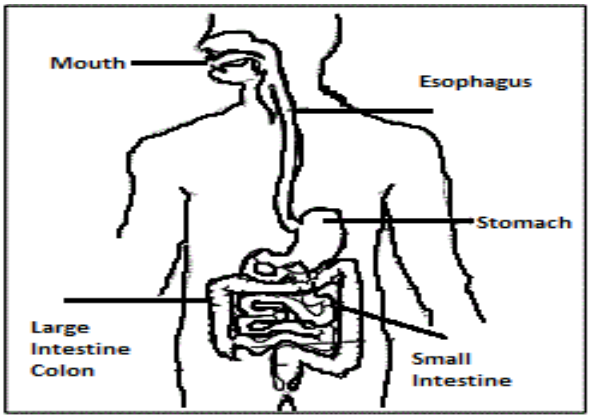

Figure 1.1 Scheme of Gastro-Intestinal-Tract. Adapted from(1).

1.1. Structure and Physiology of GIT

The structure of GIT wall (at the small intestinal level) is comprised of four main histological layers. The first layer, the serosa, is the outer layer of epithelial and supporting connective tissue. The second layer contains two layers of smooth muscle, a thinner outer layer, with longitudinally orientated muscle fibers and a thicker inner layer, with fibers orientated in a circular pattern. The third layer, submucosa is a connective tissue layer consisting of some secretory tissues richly supplied with blood and lymphatic vessels, including the lacteal, a wide lymph capillary at the centre of the villi. The fourth layer, the mucosa, is composed of: the muscularis mucosa, the mucosa, connective tissue and epithelium(1). The intestinal epithelium acts as a physical and physiological barrier to drug absorption. It mainly consists of absorptive enterocytes and mucus producing Goblet cells, endocrine and Paneth cells spread along the epithelium. The GIT epithelium is covered by a layer of mucus. Immuno-competent cells, such as B and T lymphocytes and dendritic cells are located beneath the epithelium(2, 4). The small intestine wall possesses a rich blood network and the GIT blood circulation is nearly a third of cardiac output flow, underlining the importance of exchanges between the GIT lumen and blood circulation. The lymphatic system plays an important part in fat absorption from GIT. The areas of lymphoid tissue close to the epithelial surface called Peyer's patches or follicle-association epithelium (FAE) and serve as immune sampling ports in the intestine. The FAE, separating organized, mucosa associated tissue from the lumen, is composed of enterocytes and M cells. M-cells are found in the follicle-epithelium of Peyer's patches. Microflod M-cells are important in local immune response to pathogens(5) and could

be harness to deliver macromolecules and oral vaccines(6). M cells disorganized brush border at the apical membrane have reduced microvilli and thinner surface mucus. Moreover, M cells have specific surface-adhesion molecules which might be important features for active targeting(1, 2, 4-7).

1.2. Route and Barrier to Drug Absorption

Drugs molecules encounter many barriers in GIT (Figure 1.2) once released from their dosage forms after they have dissolved in the gastrointestinal fluids. Drug molecules must be in solution and not bound to food or other material within GIT, chemically stable to withstand the GIT pH and resist to enzymatic degradation in the lumen. Finally drug molecules need to diffuse across the mucus (unstirred water layer) and across the gastrointestinal membrane, the main cellular barrier in order to reach blood circulation(3). The main drug absorption pathways from the GIT include carrier-mediated transcellular transport, vesicular transport, passive paracellular transport through entrocytes, and lymphatic uptake by M-cells.

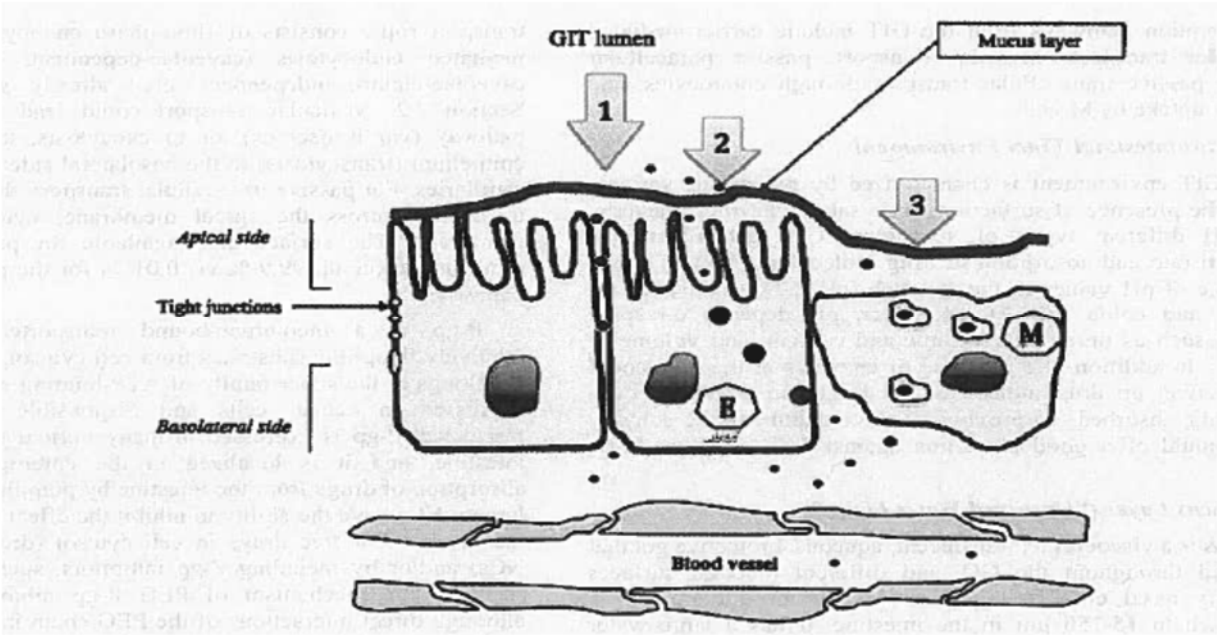

Figure 1.2 Structure of GIT barrier: drug and NC transportation pathways.

on the left,enterocytes, on the right M-cell. A mucus layer is found on the apical side of enterocytes and M-cell.(1) Paracelluar route. (2) Transcelluar route. (3) M-cell phagocytosis. With a permission from (8)

1.2.1. GIT Environment

The GIT environment is characterized by peristalsis, variable pH, and the presence of surfactants (bile salts), enzymes, bacteria, food, and different types of secretions. GIT pH affects the dissolution rate and absorption of drug molecules. The GIT has a wide range of pH values in empty stomach (pH 1.2-3), small intestine (pH 5-7) and colon (pH 6 to 7.5)(9). Moreover, pH depends of some variables such as time of the day, meal volume and volume of secretions. To provide effective treatment, the delivery system should offer a good protection against these enzymes(2, 10).

1.2.2. Mucus Layer (unstirred water layer)

Mucus is a viscoelastic, translucent, aqueous, protective gel that is secreted throughout GIT and different mucosal surfaces (pulmonary, nasal, etc.)(1). Its thickness varies from 50 to 150 μm in the stomach to 15-150 μm in intestine. It has a large water component (≈ 95%) and other constituents, which are responsible for its physical and functional properties, are largely glycoproteins called mucins(11). Mucus acts as a protective layer and a mechanical barrier. It is continually replaced from beneath as it is being removed from GIT surface through acidic, enzymatic breakdown and abrasion (peristaltic movement of food towards the colon). GIT mucus is comprised of two layers, a firmly adherent layer, slowly cleared of an unstirred layer close to the epithelium surface, and luminal mucus layer, a stirred layer, a more rapidly cleared layer(12). It is secreted continuously and digested, so for drugs to be delivered to mucosal surfaces, they need to diffuse through the unstirred mucus layers adhering to cells(1, 12, 13). Below the mucus layer, the cells present a dense of highly diverse glycoproteins and glycolipids, which form the glycocalyx. A glycocalyx (Figure 1.3) found on the apical portion of microvilli within the GIT, especially within the small intestine(3, 5, 7, 13, 14). Mucin glycoproteins are secreted in large quantities by mucosal epithelia, and cell surface mucins are a prominent feature of the apical glycocalyx of all mucosal epithelia**.** It provides additional surface for adsorption and includes enzymes secreted by the absorptive cells that are essential for the final steps of digestion of proteins and sugars(3, 13, 14). The glycocalyx is highly variable from tissue to tissue; for example, the glycocalyx of human intestinal microvilli tips is thick (100–500 nm) in comparison with the glycocalyx of the lateral microvilli surface (30–

60 nm)(5). Both the secreted and adherent mucosal barriers are constantly renewed and could potentially be rapidly adjusted to changes in the environment, for example, in response to microbial infection(5, 13, 14).

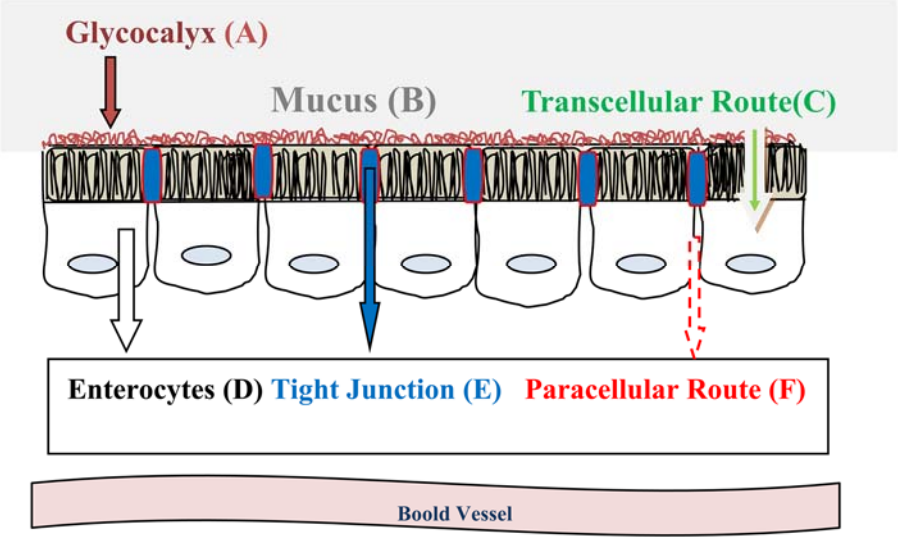

Figure 1.3 Schematic representation of some elements of epithelial cells of GIT: (A)Glycocalyx, (B)Mucus layer, (C)Transcellular Route, (D)Enerocytes, (E)Tigh junction and (F)Paracellular Route. Adapted from(5).

1.2.3. Tight Junctions and Paracellular Route

In the paracellular space, the presence of junctions restricts the passage of large molecules. These include the tight junction, a protein complex that establishes links between adjacent cells through the intercellular space . Two other protein complexes, namely the adherens junctions and desmosomes further tighten cell association, without fusing cell membranes. The apical compartment of the lateral membrane

consists of 3 components: tight junctions, adherent junctions, and desmosomes(9). For desmosomes and adherent junction the adjacent cell membranes are 15 – 20 nm apart, but are in contact at tight junctions, with the intercellular spaces being completely absent. Tight junctions act as gatekeeper paracellular route, regulating drug molecule flux and prevent free movement of molecules in paracellular space. Understanding the barrier function of tight junctions is necessary for developing absorption enhancers to deliver drugs via the paracellular route. Diffusion is regulated by concentration differences and by hydrostatic pressure gradient between the two sides of the epithelium. Tight junctions are main barriers to this type of absorption(15-18).

1.2.4. M-cells

Finally, transportation by Peyer's patches, which contain M-cells found in the Follicle-association epithelium (FAE) at the base of villi, is important in the phagocytosis and endocytosis of NPs and microparticles(5). Peyer's patches are aggregations of lymphoid tissue that are widespread along the intestine and tend to increase in number in the ileum. The physiological role of M-cells is to sample antigens present in the lumen to transport them to immune cells on their basal side. They have high transcytosis activity, but represent less than 1 % of the intestinal mucosa surface. Particles could be taken up by M-cells via specific (active endocytosis) or non-specific (adsorption endocytosis) mechanism(19).

1.2.5. Transcellular Route and Membrane Transporter (Permeability-glycoprotein)

1.2.5.1. Transcellular Route

The transcellular route comprises passive and active transport. For carrier-mediated transcellular transport (active transcellular transport), drugs are moved across membranes by protein transporters present on the apical membrane of enterocytes (generally energy-dependent). The vesicular transport route consists of fluid-phase endocytosis and receptor-mediated endocytosis (caveolae-dependent, clathrin-dependent, caveolae-calthrin-independent, etc.). Vesicular transport could lead to the degradative pathway (via lysosomes), or to exocytosis, transport across the epithelium (transcytosis) to the basolateral side of enterocytes near capillaries(8, 20). For passive transcellular transport, drugs should be able to diffuse across the apical membrane, cytoplasm, and basal membrane. The surface area available for passive transcellular transport makes up 99.9% vs. 0.01 % for the passive paracellular pathway(8).

1.2.5.2. Membrane Transporter P-gp

Recently research has been focus in understanding the role of membrane transporters in drug safety and efficacy. In particular, more than 400 membrane transporters in two major super families ATP-binding cassette (ABC) and solute carrier (SLC) have been characterized and localized to tissues and cellular membrane domains in the human body(21, 22). Membrane transporters are controlling uptake and efflux of crucial compounds such as sugars, amino acids, nucleotides, inorganic ions and drugs(23). Permeability glycoprotein (P-gp) is a plasma membrane glycoprotein of about 170 kDa

that belongs to the superfamily of ATP- binding cassette (ABC) transporters expressed in cancer cells and responsible for chemotherapy resistance(23). P-gp protects cells from cytotoxic compounds and relatively lipophilic substrates by actively transporting them out of the cell against a concentration gradient, thus decreasing intracellular levels below their effective and/or toxic concentrations(23, 24). It is expressed in the apical membrane of many normal tissues such as luminal small intestine, colon, kidney proximal tubules, liver and capillary endothelial cells of the blood brain barrier(23, 24). Membrane transporter expression in the two major sites (the intestine and/or liver) can influence how much of a drug reach the systemic circulation after an oral dose, suggests that factors affecting their function will be determinants of oral drug pharmacokinetics(22-24). It has been demonstrated that the intestinal P-gp localized in the enterocytes, an ATP dependent multidrug efflux pump, can be an active secretion system or an absorption barrier by pumping drugs from the intestinal cells into the lumen(24-27). Numerous studies have demonstrated that P-gp possesses broad substrate specificity and it is involved in the transport of neutral compounds such as digoxin and cyclosporine, negatively charged carboxyl groups such as those found in atorvastatin and fexofenadine, and hydrophilic drugs such as methotrexate(28). The degree of hydrogen bonding and partitioning into the lipid membrane has been determined to be a rate-limiting step for substrate interactions with P-gp(23). There is strong evidence in the literature that P-gp obtains the energy required for transport of drug substrates across the membrane via the hydrolysis of ATP. The mechanistic basis of the transport of substrates by ABC transport proteins has been studied and focused on the characterization of the ATP hydrolysis and transport of a variety of drug-

substrates and understanding how these two activities are coupled(28). A number of innovative approaches have been used to identify the causal events at the nucleotide binding domains (NBDs) that drive conformational changes at the transport-substrate site. It has been proposed by Loo and Clarke that P-gp binding site (Figure 1.4a) to be funnel shaped and narrow at the cytoplasmic side and the central, putative drug-substrate binding region has a diameter of 9–25 Å (also designated as the high affinity site) and approximately 50 A˚ at its widest (low affinity site)(29). Biochemical data and the structures of ABC transporters suggest the presence of a large hydrophobic cavity with remarkable plasticity of this cavity and provide insights into the conformational changes that accompany drug binding(28). It has been proposed that P-gp is composed of two symmetrical halves joined by a linker region and each half with six putative trans-membrane segments and one cytoplasmic nucleotide-binding site (NBD)(30, 31). The cytoplasmic terminus, of each half, contains the sequences for a nucleotide-binding site, responsible for ATP binding and hydrolysis. Both nucleotide binding sites of P-gp are necessary for transport of substrates out of the cell(30).

Figure 1.4 Different mechanism involved in P-gp inhibition and Drug-substrate binding pocket of P-gp. Adapted from(25, 28).

1.3. P-gp Inhibitors

Manipulating membrane transporters level leading to increase or reduce their functions and co-administration with inhibitors are all important tools to alter the ability of membrane transporter to transport substrates (23). Therefore, intestinal absorption of drugs that are secreted by a P-gp-mediated efflux system can be improved by inhibiting the function of P-gp in the intestinal membrane and the oral bioavailability of a wide range of drugs can be increased. NPs have the ability to inhibit the effect of P-gp by

limiting the presence of free drugs in cell cytosol (drugs confined inside NPs) and/or by including P-gp inhibitors, such as PEG, on their surface. Moreover, inhibition of P-gp activity may be an effective way to enhance oral bioavailability and increase anticancer agent efficacy in multi-drug resistant tumors. P-gp inhibitors based on their development duration are classified in three generations. The first generation inhibitors were pharmacological actives such as verapamil, cyclosporin A, quinidine, reserpine and tamoxifen but were of limited use due to their high toxicity profile. Second generation of P-gp inhibitors came into existence to overcome toxicity problem of the first generation. D-isomer of verapamil, that is, dexverapamil, which is less cardiotoxic than verapamil and they were more potent than their parent compounds and also shown less toxicity. Development of third generation of P-gp inhibitors are superior and balanced in performance in relation to activity and toxicity with regard to their earlier counterparts. Third generation P-gp inhibitor are effective at the nanomolar concentration range for example, elacridar, tariquidar and zosuquidar and they are currently being tested(24). Various pharmaceutical excipients both from synthetic and natural sources, belonging to the categories such as surfactants, polymers and lipid excipients have demonstrated ability to inhibit the transport activity of P-gp resulting in enhanced intracellular drug accumulation (24, 28). Directed transport and the mechanisms by which excipients inhibit P-gp activity varies with the excipients types and are currently under investigation. Different mechanisms (Figure 1.4b) are said to be involved in P-gp inhibition for various class of inhibitors. P-gp can be inhibited by: i) blocking drug-binding site(s) either competitively, non-competitively or allosterically; ii) interfering ATP hydrolysis and iii) altering integrity of cell membrane

lipids(24, 28, 32). It was proposed that changes in cellular membrane fluidity may be associated with alterations in P-gp activity and the lipid phase of the membrane plays a crucial role in the multidrug resistance of P-gp(25). Moreover, P-gp drug-binding domains are present in the transmembrane segments of P-gp and P-gp is highly sensitive to the lipid environment(25). Some excipients such PEG, Cremophor El and Tween80 increase cell membrane fluidity, whereas others decrease the fluidity of the cell membrane(33, 34).

1.4. Nanoparticles as Effective Oral Drug Carrier

A significant challenge that most drugs face is their inability to be delivered effectively. Nanotechnology offers a solution to allow for safe, high-dose, specific delivery of pharmaceuticals. Nanotechnology has the potential to transform the pharmaceutical field by offering the ability to encapsulate and strategically deliver drugs while improving their therapeutic index(35, 36). It is becoming evident that nanotechnology prove to b effective in creating new therapies but also in giving old therapies new life. NCs have attracted significant attention due to their promising applications in the fields of drug transport. A major issue in drug delivery is maintaining the stability of nanoparticles in the human body for the effective delivery of a drug to the site of action without clearance by reticuloendothelial (RES). Indeed, significant progress has already been achieved by introducing hydrophilic moieties to the nanoparticle surface, which can inhibit the adsorption of serum proteins and hemocytes, therefore maintaining stable nanoparticle circulation in the blood(35, 36). The following examples (Figure 1.5) have been selected to illustrate the challenge of

drug delivery with different types of NCs. They do not represent an exhaustive compilation of studies produced in this field.

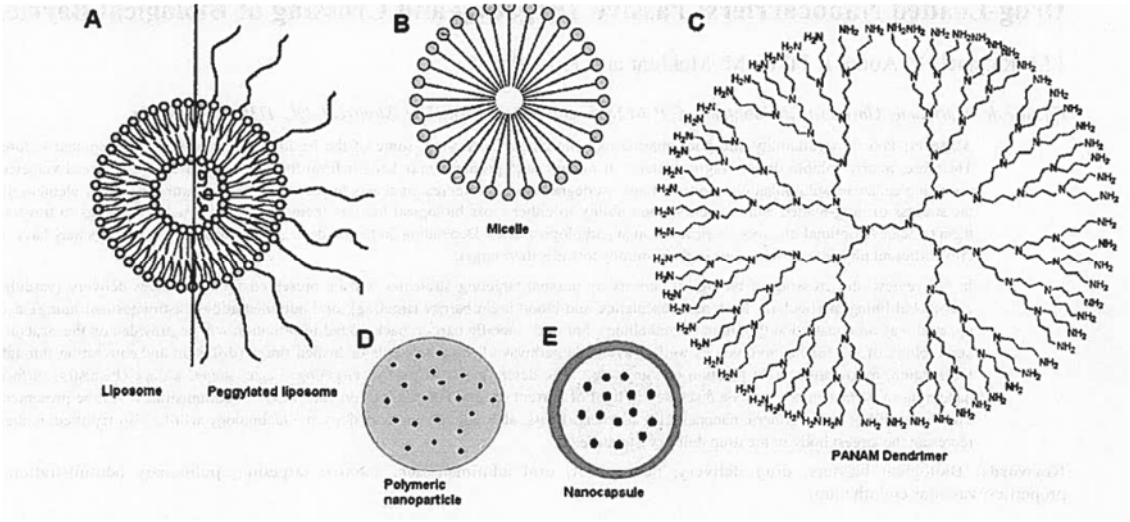

Figure 1.5 Different Types of NCs (A) Micelles, (B) Liposomes, (C) Dendrimers, Poymeric nanoparticles and Nanocapsules With a permission from (8).

1.4.1. Polymeric Nanoparticles

Polymeric NPs are among the most promising strategies to improve oral delivery, because of their stability in the GIT, protection of encapsulated actives and the relative ease with which their physiochemical and drug release characteristics can be modulated(37). A variety of biodegradable and nonbiodegradable polymers have been employed for fabrication of polymeric NPs for oral drug delivery. A large variety of materials can be used to prepare NPs (matrix-structure nanospheres or capsules) and to modify their surfaces. Nanospheres are matrix systems in which the drug is physically

and uniformly dispersed, while nanocapsules are vesicular systems in which the drug is confined to a cavity surrounded by a polymer membrane(11, 38). Synthetic (polyester, acrylates, etc.) and natural materials, such as chitosan, dextran, gelatin, etc., are being used to prepare these NCs. Polymeric NPs are more stable in GIT than other NCs such as liposomes and they can protect encapsulated drug from GIT environment(37, 39, 40). Various polymeric materials enable to modulate the physicochemical characteristics (e.g. zeta potential, hydrophobicity), drug release properties (e.g. delayed, prolonged), and biological behavior (e.g. targeting, bioadhesion, improved cellular uptake) of nanoparticles(37). Nanoparticle surface can be modified by adsorption or chemical grafting of certain molecules such as poloxamers and poly(ethylene glycol) (PEG)(37). Polymeric NPs are distributed more uniformly in the GIT therefore the drug is released and absorbed more uniformly and the risk of local irritation reduced, compared to unique dosage forms(39-41). Insulin has been the focus of research for formulation in effective NCs for oral delivery. Insulin loaded poly(isobutylcyanoacrylate) nanocapsules manifest improved effects on glycemia in a diabetic rat model over oral free Insulin(37, 42). It is noteworthy that the percentage of Insulin dose actually crossing the GIT mucosa is increased but stay low (a few % of bioavailability), requiring higher insulin doses increasing potential toxic effects and underlining the limitations of these approaches(37).

1.4.2. Liposomes and Lipid-Based Nanocarriers

Liposomes are aqueous compartments enclosed by lipid bilayer membranes. Liposomes are concentric bilayered vesicles in which an aqueous volume is entirely

enclosed by a membranous lipid bilayer mainly composed of natural or synthetic phospholipids. Liposomes are formed when thin lipid films or lipid cakes are hydrated and stacks of liquid(39, 40). Liposomes can serve as efficient drug carrier to improve drug bioavailability because of their ability to pass through lipid bilayers and interact with cell membrane(43, 44). Because of liposomes structure, liposomes can be designed for water- and lipid-soluble drugs. Unfortunately, for oral drug delivery, they have limited application because of their instability in the GIT environment(43). Their recent role seems confined to increasing the bioavailability of low-solubility drugs. They appear to accumulate in mucus, prolonging their residence time but limiting their diffusion(43). They have been proposed as vaccination adjuvants and as antigen presentation to M-cells(45). Lipids and phsopholipids in the form of solid lipid nanoparticles (SLN) are an interesting alternative to polymeric matrix NCs for hydrophobic drug and protein encapsulation(43). For instance, camptothecin-loaded SLN coated with poloxamer 188 (200 nm sized particles with zeta potential around -70 mV) display increased bioavailability compared to the oral, soluble drug form(46). Similarly, insulin encapsulated in lectin-modified SLN presents increased bioavailability(47).

1.4.3. Micelles

In an aqueous medium, above a given concentration termed the critical micellar concentration (CMC), surfactants self-assemble into a colloidal dispersion of molecular aggregates called micelles (<50–100 nm)(48). Micelles are composed of a hydrophilic shell (usually PEG) and hydrophobic core(48). Micelles have been studied

as drug delivery systems to improve solubility, absorption and protect drugs molecules(9, 49). Although polymeric micelles have a longer life span than surfactant micelles, there are still some challenges facing their preparation, such as stability, increased drug loading, resistance to dilution in the GIT, and narrow size distribution required(50-53). Micelles have been mainly studied to improve the drug solubilisation of highly hydrophobic drugs, such as taxanes, for oral chemotherapy(49, 54). There are no clear indication that they can cross the mucosal epithelium other than in the form of isolated copolymers(9, 48).

1.4.4. Hydrogel Nanocarrier

Hydrogels are polymeric networks with three-dimensional configuration capable of absorbing high amounts of water or biological fluids(55). Hydrogel nanoparticles have gained considerable attention as one of the most promising NC owing to their unique potentials via combining the characteristics of a hydrogel system with a nanoparticle(55, 56). NC delivery systems, hydrogel nanospheres, fabricated from poly(methacrylic acid) (PMAA) and PEG, and loaded with the chemotherapeutic agent bleomycin, have disclosed an improved effect because of their mucoadhesive properties and P-gp inhibition(57). Negatively-charged, 700nm sized NCs of alginate and chitosan encapsulating insulin were prepared and results indicate a decrease of glycemia about 40 % in diabetic rats(56, 58). 400nm sized alginate and dextran sulphate NCs encapsulating insulin increased GIT uptake (13 % bioavailability) and

decreased glycemia in a diabetic rat model. This superior uptake comparison to free insulin seems to be linked to uptake of NCs by small intestine epithelial cells(58).

1.4.5. Dendrimers

A dendrimer is generally described as a macromolecule, which is characterized by its highly branched 3D structure that provides a high degree of surface functionality and versatility. Due to their multivalent and monodisperse character, dendrimers have attracted wide interest in the field of chemistry and biology, especially in applications like drug delivery, gene therapy and chemotherapy(59, 60). Dendrimers have hydrophilic exteriors and hydrophilic interiors, which are responsible for its unimolecular micellar nature. They form covalent as well as non-covalent complexes with drug molecules and hydrophobes, which are responsible for its solubilisation behaviour(59-61). Dendrimers have a distinctive small size and could serve as solubilizing agents for hydrophobic drugs(59). Poly(amido amino) (PAMAM) dendrimers have been reported to improve the intestinal absorption of poorly soluble drugs (propranolol) but appeared less efficient with macromolecular drugs (insulin)(60, 62). Moreover, the dendrimer dose should be kept low to reduce toxicity(62, 63). In vitro, PAMAM toxicity was diminished by surface modification with lauroyl chloride while their permeation through CaCo-2 cell monolayer was increased(62).

1.5. NanoCarrier Translocation and Drug Bioavailability

A nanocarrier (NC) is nanomaterial being used as a transport module for another substance, such as a drug. Nanocarriers for drug delivery have become key vehicles for

the storage and delivery of drugs. Various nanocarriers including liposomes, polymers, micelles and dendrimers have been developed and explored for drug delivery(64). Drug bioavailability refers to the rate and extent at which the active drug reaches the systemic circulation. For most drugs, their pharmacological activity can be directly related to bioavailability(65). As consequence of GIT morphology and physiology, drugs must overcome GIT barriers to be absorbed efficaciously: conditions prevailing in GIT lumen favoring degradation, the barrier mucus layer and, finally, transport across the epithelium themselves toward the blood or lymphatic circulation. NC role could be limited to protection against degradation and/or enhancing drug solubilisation. In this scenario, intact NCs are confined to the GIT lumen, but contribute to increased bioavailability by releasing drugs near the epithelium, acting as permeability enhancer, favoring adhesion and penetration of mucus layer, and/or contributing to the opening of tight junctions. On the other hand, drug encapsulation could involve NCs translocation, along with the drug load, across the epithelium(66). It could even involve a role for the orally administrated NCs in drug distribution in the systemic circulation. Indeed intact NCs introduced in the blood circulation could provide the advantages of protection from metabolism, long circulation (if PEGylated), targeting and improved pharmacokinetic. While most studies have focused on blood drug levels or pharmacodynamic effects, few have followed the fate of NCs(51). However, in animal experiments, several types of NCs, administrated by oral route, have been found in blood or organs, but in general, they are poorly taken up, the order of magnitude being a few percentage of the initial dose (67). There are also stability issues, as polymeric NPs are more likely to be discerned in blood compared to

liposomes or micelles that are most likely to undergo dissociation and degradation in the GIT lumen or during translocation across the epithelium. For most of the drugs administered as oral solid dosage forms, except in case of controlled release formulations and disintegration occur rapidly. In these cases, the rate limiting processes in the absorption of dosage forms are (a) dissolution rate and (b) rate of drug permeation through the biological membrane(65). Dissolution is the rate determining step for hydrophobic, poorly water soluble drugs. In case of hydrophilic drugs with high aqueous solubilities, dissolution is rapid and the rate determining step in the absorption is often the rate of permeation through the biological membrane. Drug instability during absorption can affect its bioavailability(65). Two major stability problems resulting in poor bioavailability of an orally administered drug are degradation of the drug into inactive form, and interaction with one or more components of the dosage form or those present in the GIT to form a complex that is poorly soluble or is unabsorbable.(65)

1.6. Optimizing Nanocarrier Physiochemical Properties for Oral Delivery

1.6.1. Increased Drug Dissolution, Absorption, and Protection from Degradation

NCs could offer protection to drug molecules, and could also decrease the amount of drug needed for therapeutic action, thus reducing drug side effects. This could be

particularly significant for peptide and protein delivery, such as insulin for instance. Unprotected drugs, when introduced into the GIT, might not achieve the expected pharmacological effect because of many factors, such as drug stability in GIT fluid, incomplete absorption and permeability issues. Particles in nano-scale could improve bioavailability by increasing drug absorption by augmenting dissolution rate, due to favorable surface/volume ratios and favorable physical drug states (crystalline, amorphous or dispersed molecularly) in NCs for release dissolution(10, 19, 68-70). Lastly, NCs stability is variable, and some are more sensitive than others (micelles, liposomes) to the GIT environment (acidity, bile salts, lipids, etc.).

1.6.2. Mucus Adhesion and Penetrating Properties

1.6.2.1. Mucoadhesive Nanocarrier

Increasing the residence time of drug loaded NCs in small intestine might result in greater absorption of the drug and/or of the carrier itself. Adhesion to mucus has been proposed to extent NC residence time. For instance, mucoadhesion has been documented for NC surface modification with chitosan, the cationic charges of the polymer interacting with the negatively charged mucus(71). The creation of disulphate bonds on mucus glycoproteins with NC surface derived from thiols have been proposed as a mucoadhesion strategy(72). Broomberg et al. studied mucoadhesive ionic micelles, composed of the copolymer Pluronic® poly(acrylic acid), for oral delivery(73). The mucoadhesive properties of the copolymer linked to ionic interaction between mucin and carboxyl groups on the polymer, and the entanglement of Pluronic (PPG-PEG-PPG block) with the mucin network. Mucoadhesion is size dependent, with

maximum adhesion at around 100 nm(74). Examination of the behavior of NCs with different surfaces, i.e., PLA-PEG NPs (200 nm, zeta potential -24 mV), PS NPs (200 nm, +1 mV), and chitosan NPs (30 nm, +17 mV) revealed the effects of mucus adhesion (via interactions of hydrophobic surface with hydrophilic domains of mucus gylcoproteins) on NC uptake *in vitro*(75). pH-responsive NPs (250 nm diameter) of chitosan and poly(glutamic acid) encapsulating a modified insulin were prepared. It was found that the drug carrier was retained in the GIT, while modified insulin showed an increase in absorption into systemic circulation, a result consistent with the mucoadhesion properties of chitosan NCs(76). Mucoadhesion increases the residence time. On the other hand, bounding to mucin fibers are subjected to natural and continuous clearance of the mucus layer (stirred layer) with as a consequence a maximum residence of about 4-6 h(12).

1.6.2.2. Mucus-Penetrating Nanocarriers

Penetration of mucus is limited by gel porosity and interactions between NC surfaces and gel components. Conflicting data on charges required to avoid ionic interactions with mucus resulted in an attempt to develop neutral hydrophilic surface modifications(12). PEG a hydrophilic polymer, has been used to coat NPs. PEG (2kDa) minimizes interactions with anionic-charged hydrogel, allowing faster transport(77). PEGylated 100 nm sized particles show slower transport and diffusion than 200 or 500 nm sized particles through the mucus layer. This could be explained by the existence of large pores in gel, allowing large NPs to be transported, while smaller ones enter the more densely packed gel (a process similar to size exclusion

chromatography). It could also be explained by differences in the PEG layer structure in smaller NCs, with a higher radius of curvature, permitting direct interaction between the NC surface and mucus compare to larger NC(78). Indeed lowering PEG coverage to 40 % and increasing PEG length to 10 KDa, decrease NC diffusion in the mucus layer(12). PEG effect on further translocation across the epithelium by different pathways remains to be clarified(67, 75, 79).

1.6.3. Translocation Across Tight Junctions

In normal physiological conditions, translocation of NCs through tight junctions is severely limited by their relative small surface area and tightness. In fact, NC passage is dependent on junction opening. NCs made of chitosan or with chitosan on surface (and also co-administration with free chitosan) have displayed the ability to transiently open tight junctions between epithelial cells, facilitating the transport of drug molecules(16, 18). Other permeability enhancers such as synthetic peptides (Occludin) and fatty acids (Tween) have been proposed, but all of them have intrinsic toxicity and indiscriminately open the junctions to all kinds of GIT contents(15, 37).

1.6.4. Translocation Across Enterocytes

NC translocation across enterocytes can occur by transcytosis, consisting of three steps, i.e., uptake of the NC at the apical side, intracellular trafficking toward the basolateral side and exocytosis (67). Size and surface properties are the main

determinants of transport efficacy and pathway chosen by NCs. Particle size, a critical characteristic of NCs, has a direct effect on cellular uptake. It has been well-accepted in research that small sized particles could be taken up by enterocytes and M-cells, enterocytes having a maximum uptake of 50-100 nm sized particles, while M-cells can engulf particles up to the mcirometer range(5, 67, 80). Peyer's patches have up to 200-fold higher uptake of PLGA NCs than non-patch tissues(68, 81). 100 nm sized NCs diffuse in the submucosal layers while large size particles (micrometer range) are predominantly localized in epithelial lining of tissue(80). Moreover, Peyer's patch uptake predominates over enterocytes uptake, even if the former represents only about 1 % of the intestinal mucosal surface(80). The presence of hydrophilic polymers on the surface of NPs might increase transport through mucosal surface, although conflicting results have been reported(82). The adsorption of hydrophilic block-co-polymers (poloxamer) onto polystyrene NCs markedly reduces uptake in the small intestine(67). For instance, 300-nm sized PLGA particles were found to migrate from the GIT into different tissues and organs, especially the liver(83). When modified on the surface with PEG and chitosan, they migrated from the GIT into peritoneal macrophage(84). These results are consistent with the importance of polymeric NC stability as well as surface modification to cross the GIT epithelium. Endocytosis pathways depend on surface properties. PLGA particles, or chitosan NCs, for instance, are predominantly endocytosed via clathrin-dependent pathways(51). In contrast, it has been demonstrated that the bioavailability of paclitaxel loaded in lipid nanocapsules (from 25 to 135 nm) is improved across CaCo-2 cell monolayers because of this type of NC capacity to improve transport, predominantly via caveolae-dependent pathways(85,

86). Non-specific adhesion properties might improve NC localization and transport. Lectins are saccharide-binding membrane glycoproteins, which can bind reversibly to sugars either in free form or supported on other membranes. They might adhere to the GIT surface to improve absorption and permeability(87). Lectin binding was found to be favored at neutral pH and reduced under acidic pH. Tomato lectin has been reported to increase bioadhesive and conjugate with mucus gel. Surface modification with covalent attachment of tomato lectin molecules indicated widespread uptake of PS NP by enterocytes rather than by Peyer's patchs(67). Lectin conjugation with the NP surface improved NP transport across the intestinal mucosa by increasing interaction with mucus or epithelial cells(87, 88). Gliadin, another mucoadhesive agent, was conjugated with NPs carrying amoxicillin. These NPs were more effective for local treatment of Helicobacter pylori than conventional GIT therapy(89).

1.6.5. Translocation Across M-cells

The ability of M-cells to transport different materials by transcytosis (either phagocytosis or endocytosis) have made them a good target to deliver vaccines and drugs(90). Moreover, steric hindrance by mucus layer is lowered as the layer over M-cells is thinner than over enterocytes. M-cells in the intestine might be targeted for mucosal vaccination to transport antigens to induce mucosal immunity(6). PLA particles (in the 200 nm range), traced by fluorescence, showed initial accumulation in mucus and then moved to M-cells (in 15 min). Further examination disclosed NPs in immune cells in sub epithelial tissue, confirming barrier crossing(91). In summary,

optimal NC size seems to be below 1 μm with maximal uptake between 100 nm and 200 nm.

1.7. Poly (Ethylene Glycol) (PEG) Used as P-gp Inhibitor

Poly(ethylene glycol) (PEG) is water soluble, uncharged, having very low order of toxicity (up to 10 mg/kg body-weight), and non-immunogenic(92). It is a commonly used pharmaceutical excipient as coating agent, plasticizing agent, stabilizer for emulsion and to enhance the solubility of drugs(92). Presently PEG is one of the most popular material to modify particulate surfaces in order to avoid recognition by cells of the mononuclear phagocyte system (MPS) and inhibit P-gp efflux(8, 35, 93). The incorporation of PEG onto the NC surface (absorbed or covalently linked) increases the NC half life in the systemic circulation and this effect is related to decrease opsonization(94, 95). PEG decreases protein interaction with NC surfaces, modifies PK and biodistribution(96), and decrease NC cellular uptake(97). Hydrophilic and flexible PEG chains act via a steric repulsion effect, rendering protein binding unfavorable and that repulsion effect depends on chain length, optimal surface density, and optimal chain configuration(96). 2 to 5 kDa seems to be the minimum length for the stealth effect and are able to reduce the absorption of opsonins and other serum proteins(8, 93, 95). Optimal protein resistance has been reported in PLA polymeric NPs with 5% w/w PEG content and PEG density for optimal conformation and efficacy translates into an inter-chain distance of around 1.5 nm on polyester NP

surfaces(93). PEG layer density which cover NCs should reach a density where PEG chains are forced to configure a mushroom/brush configuration (Figure 1.6), however without leaving uncovered hydrophobic or charged surface where opsonins can bind(35, 44). The efficacy result of PEG 'brush' to alter the biodistribution of biodegradable nanoparticles was composed of poly (lactic-co-glycolic acid) (PLGA) or of poly (lactic acid) (PLA) as core was demonstrated(10, 12, 93). However other configurations have been tested, the linear PEG (usually methoxy-PEG) is the standard to be used. Generally, linear PEGs are more effective than branched PEGs of equivalent size, as shown by a decrease in opsonization and macrophage uptake(98). A complex relationship of PEG chain length, carrier size (determining surface availability for PEG anchorage), and weight ratio between PEG and hydrophobic component of the carrier (e.g, PLA-PEG particles) influences the final surface properties of NCs. It was demonstrated that a free PEG, a pharmaceutical excipients, is capable of inhibiting efflux transporter (e.g., P-gp and/or MRP activity) activity in Caco-2 cell monolayer and such PEG-induced inhibition of efflux transporter activity is most likely related to changes in the microenvironment of P-gp in Caco-2 cell membranes(99). It was reported that PEG capability to inhibit the P-gp transporter function in CaCo-2 monolayer cells and in vitro model of intestinal mucosa might likely be due to changes in membrane fluidity of P-gp in CaCo-2 monolayer cells(25, 33, 100). Although the mechanism of PEG for P-gp inhibition is unclear, direct interactions of the PEG chain with substrate binding site of P-gp pump and alter phospholipids membrane fluidity have been also proposed (22, 23, 100-103). Some concerns about the importance of the microenvironment of P-gp expressed in CaCo-2 model were raised. For instance,

would it be the same environment as intestinal mucosal cells in vivo and whether P-gp in these cells react in similar way to PEG? In the case where the lipid composition of membrane in the human intestinal mucosa differs from CaCo-2 cells, it is possible that the effects of PEG on P-gp activity *in vitro* may be different from those observed *in vivo* in animal and/or human(100). Therefore, further studies (e.g., gut perfusion studies, pharmacokinetic studies in animal models) should be conducted to establish a possible *in vitro/in vivo* correlation. Besides mucus penetration, PEG addition to the PLA NP surface has been reported to enhance particle stability in biological fluids, preventing protein and enzymes absorption(104).

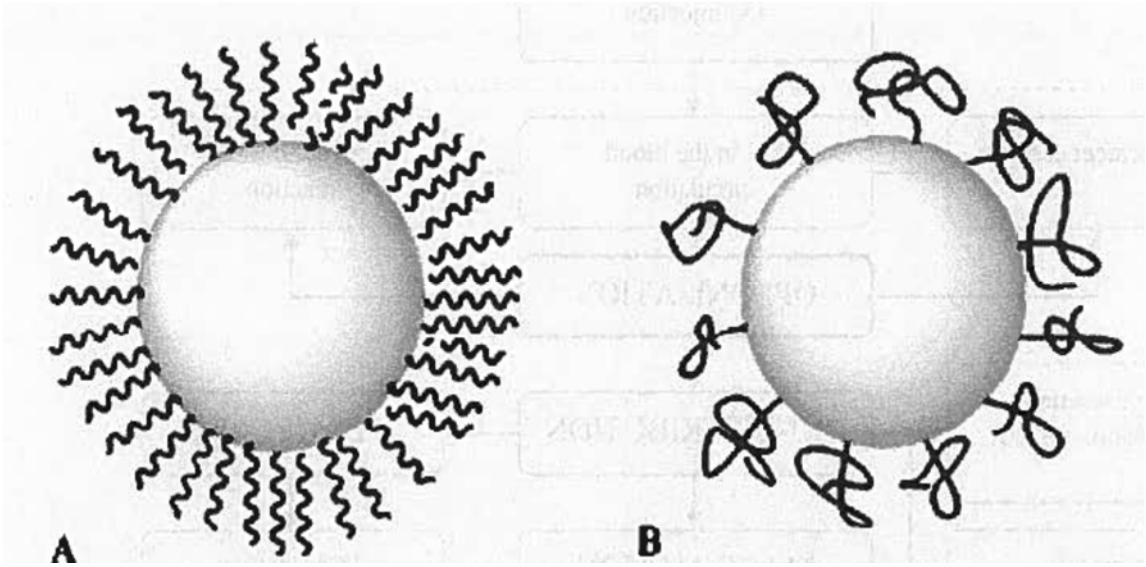

Figure 1.6 PEG NCs coverage. (A) Brush configuration and (B) Mushroom configuration. With a permission from (8).

1.8. Targeting

The main purpose in the development of nanocarriers for drug delivery application is certainly drug targeting to the desired site of action and controllable biodistribution into the body. Orally administered targeted nanoparticles have a large number of potential biomedical applications and display several putative advantages for oral drug delivery, such as the protection of fragile drugs or modification of drug pharmacokinetics. Nanoparticles have advantages, such as small size, high surface area, and modification using functional groups for high capacity or selectivity. Nanoparticles have emerged as potential drug delivery systems and are used for targeting drug to particular organs/tissues via the peroral route of administration(105-107). It could be drug or drug carrier targeting and the ability of the drug to accumulate in the organ or tissue selectively and quantitatively, independent of the site and method of its administration. Therefore, drug concentration at the site(s) of action should be high, while its concentration in other non-targeted organs and tissues should be below certain minimal levels thus minimizing any negative side-reactions and maximizing therapeutic index(19, 105, 106). Some ligand such as lectin and proteins that bind sugars reversibly and are involved in many cell recognition and adhesion processes. Nanoparticles with peptidic ligands are especially worthy of notice because they can be used for specific targeting in the gastrointestinal (GI) tract. The optimization of particle size and surface properties and targeting by ligand grafting have been shown to enhance nanoparticle transport across the intestinal epithelium. Different grafting strategies for non-peptidic ligands, e.g., peptidomimetics, lectin mimetics, sugars and vitamins, that are stable in the gastrointestinal tract. Some ligand such as lectin and proteins that bind sugars reversibly and are involved in many cell recognition and

adhesion processes. Tomato lectin-conjugated NP resist the digestion process and increase the bioadhesive and endocytic potential of latex particles. Ligand density on the particle surface is somehow difficult to reproduce and must be optimized to allow cellular uptake in order to achieve optimal therapeutic efficacy. Lectin insulin liposomes (190 nm) modified with a hydrophobic anchor, N-glut-PE, promoted the oral absorption of insulin due to the site-specific combination of the GI cell membrane and vitamin B12-coated dextran NP (150-300 nm) improved the cellular uptake of absorptive enterocytes. Despite promising results with agents that increase specific receptor-mediated endocytosis, insufficient quantities of insulin loaded particles are absorbed through the intestinal epithelium. Therefore, targeted drug has advantages over conventional drug delivery system such as the drug quantity required to achieve a therapeutic effect may be greatly reduced, as well as the cost of therapy. This challenging goal can be obtained exploiting natural passive targeting that always occurs into the body or altering this process by a modification of the nanocarriers in order to achieve the so-called active targeting(105, 106).

1.8.1. Passive Targeting

Passive targeting refers to the accumulation of drug or drug carrier system at a particular site whose explanation may be attributed to physicochemical or pharmacological factors of disease. Passive targeting is based on NCs size and surface

properties, namely, surface charge, degree of hydrophobicity and non-specific adhesion, which direct them towards particular organs, across biological barrier, such as specialized epithelia, or enter the cell cytoplasm(8, 106). For GIT intestinal mucosa, passive targeting could be done through enterocytes to deliver proteins and peptides or through M-cells to delivery vaccine and it generally depends on the type approach that determined the specific parameters required to design NC delivery system(19, 50, 69, 108). M-cells have been targeted to deliver vaccine or drugs due to M-cell ability to transcytosis and transport of different materials. NCs and a ligand such as cholera toxin B (CTB) could be used in vaccine targeting to M-cells membrane and PEGylated PLGA nanoparticles displaying RGD-peptide also was used to target M cells for oral vaccination(6, 7, 90). NCs functionalized with lectins have been used to target possibly over expressed sugar residues on the surface of some cells such as epithelial improve NPs transport across intestinal mucosa by increasing interaction with mucus or epithelial cells(87, 88, 90). Gladin nanoparticles, muco-adhesive agent, were found more effective to use for local treatment of H.pylori by carrying amoxicillin than conventional therapy(109). It is reported that bioavailability of paclitaxel loaded in lipid nanocapsules was improved across CaCo-2 cell monolayer because of NC capacity to improve paclitaxel transport across intestinal barrier(85, 86, 110).

1.8.2. Active Targeting

Active targeting includes specific modification of drug or drug carrier systems with active agents having selective affinity to recognize and interact with specific cell, tissue or organ in the body(105, 106). A number of possibilities to obtain the decoration and the most commons are alteration of the surface charge, adsorption to the ligands on the surface or direct attachment of a specific biomolecules(105, 106). Grafting ligands (biorecognition molecules) onto the nanoparticles refers to active targeting and aims to increase specific cell uptake. The ligands must be linked on the surface in the form of decorating moieties and this ligands may be active molecules (proteins, peptides, monoclonal antibody, or any other moiety)(111). Nanoparticles bearing these ligands are recognised by cell surface receptors and this leads to receptor-mediated endocytosis(105, 106). Doxorubicin-loaded PLGA-b-PEG nanocarriers targeted with folate were used as folate receptor is over expressed in a wide variety of human tumors(112).

1.9. Oral Dosage Form

The oral route of drug administration is the most convenient for patients. Solid oral dosage forms are the preferred route for many drugs and are still the most widely used formulations for new and existing formulations(1). The tablet one of the many forms that an oral drug can take such as syrups, elixirs, suspensions and emulsions(1). Of all pharmaceutical preparations, tablet is one of the most commonly used oral solid dosage forms to deliver the drug for therapy, because of its convenience in terms of self

administration, compactness and ease in manufacturing(113). A wide range and diversity of ingredients are often included in tablet formulations. A tablet comprises a mixture of active substances and excipients, usually in powder form, pressed or compacted from a powder into a solid dose. A pharmaceutical dosage form typically consists of active pharmaceutical ingredient and excipients(113). The excipients usually play an important role in manufacturing, stability and performance(92). The excipients are added to aid the formulation stability, manufacture, facilitate the preparation, patient acceptability and drug delivery. Some properties of final dosage form, such as bioavailability and stability, are dependent on the excipients chosen, concentrations and interactions with each other and the active ingredients (65). The commonly used excipients such as diluents, binders, glidants (flow aids) and lubricants to ensure efficient tabletting. A binder is added to help hold the tablet together and give it strength. A wide variety of binders may be used such as lactose, dibasic calcium phosphate and corn (maize) starch. Some binders, such as starch and cellulose, are also excellent disintegrants. Diluents are used to increase dosage form volume or weight, and as such they can also be referred to as fillers. Some diluents, such as microcrystalline cellulose (MCC), can also be considered as dry binders since they improve the compactibility or tabletability of the compression mix. Tablets need to be strong enough to resist the stresses of packaging, shipping and handling. The hardness of tablets is the principle measure of mechanical strength. A disintegrate is also needed to aid tablet dispersion once swallowed, releasing the drug for absorption. Lubricants prevent ingredients from clumping together and from sticking to the tablet punches filling machine. Lubricants also ensure that tablet formation and ejection can

occur with low friction between the solid and die wall, as well as between granules, which helps in uniform filling of the die. Common minerals like talc or silica, and fats, e.g. vegetable stearin, magnesium stearate or stearic acid are the most frequently used lubricants in tablets. In the tablet manufacturing process, it is important that all ingredients be fairly dry, powdered or granular, uniform in particle size, and freely flowing. Mixed particle sized powders segregate during manufacturing operations due to different densities, which can result in tablets with poor drug content uniformity but granulation should prevent this.

1.9.1. Direct Compression

Direct compression (DC) is the tableting of a blend of ingredients without a preliminary granulation or agglomeration process as shown in Figure 1.7(1, 114-117). To perform DC, powder blend can be mixed well, do not require granulation and can be compressed into tablets through DC. The powder blend has to flow to ensure a consistent tablet weight, it has to compress and compact into tablets and the resulting tablets have to stay stable over time to maintain safety and efficacy(114). When a adequately homogenous mix of the components cannot be obtained with simple blending processes, the ingredients must be granulated prior to compression to assure an even distribution of the active compound in the final tablet. Figure 1.7 showed whether wet granulation and dry granulation, two basic techniques are used to granulate powders for compression into a tablet(1, 118).

1.9.2. Wet Granulation

Wet granulation is a process for size enlargement, where small primary particles are joined together using agitation and a liquid binder(119). Wet granulation is a process of using a liquid binder to lightly agglomerate the powder mixture(1, 120). The amount of liquid has to be properly controlled, as over-wetting will cause the granules to be too hard and under-wetting will cause them to be too soft and friable. Aqueous solutions have the advantage of being safer to deal with than solvent-based systems but may not be suitable for drugs which are degraded by hydrolysis(118). Low shear wet granulation processes use very simple mixing equipment, and can take a considerable time to achieve a uniformly mixed state. High shear wet granulation processes use equipment that mixes the powder and liquid at a very fast rate, and thus speeds up the manufacturing process. Fluid bed granulation is a multiple-step wet granulation process performed in the same vessel to pre-heat, granulate, and dry the powders(1, 118-120).

1.9.3. Dry Granulation

Generally, for thermal or moisture sensitive substance, dry granulation process is preferably used to prepare granules and to densify the powder blend, for proper flow and compressibility properties(118). The dry granulation process involves the

compaction and densification of powders, using a roller compactor or tablet press that is employed as a slugging tool for powders that may not have a sufficiently uniform stream in the die cavity(118). Dry granulation consists in compacting powder to form a slug with a heavy duty, rotary tablet press or a solid strip, using a roller compactor and then reducing its size by milling or screening to achieve a desired granule(116, 117, 121). Dry granulation requires drugs or excipients with cohesive properties, and a dry binder may need to be added to the formulation to facilitate the formation of granules. Dry granulation does not require solvents, which is advantage over wet granulation and would be preferable especially for drugs, which are moisture or heat sensitive(25, 99, 100, 122).

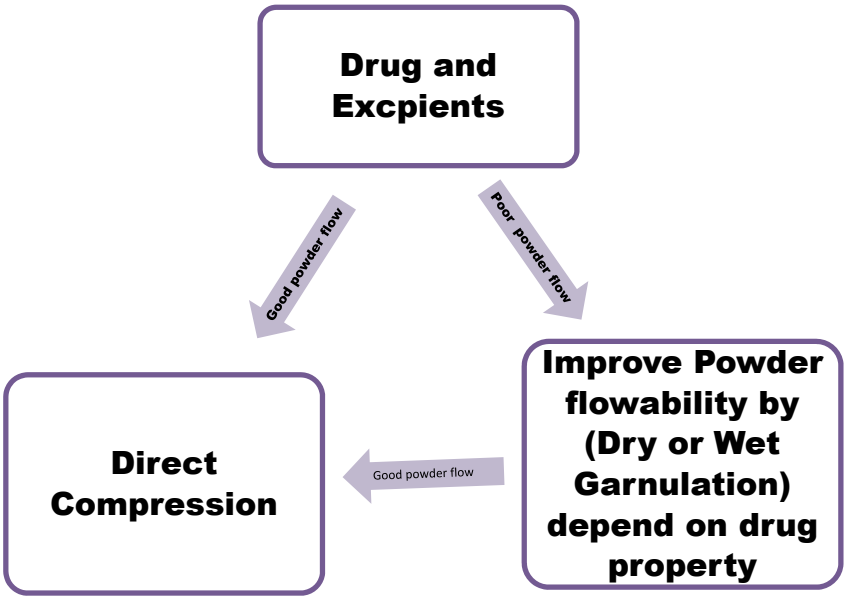

Figure 1.7 Powder blend flow properties and different techniques for compression into tablet. Adapted from(113).

Chapter Two

Hypothesis and Objectives

2. Hypothesis and Objectives of the study

2.1. Hypothesis

Generally the objective of drug delivery is to design a sophisticated system that could deliver the drug molecules at the desired site of action and minimize the side effects(35, 123). Degradable polymers such as Poly(lactic acid) (PLA), Poly(amido amine) (PAMAM) and Poly(ε-caprolactone) (PCL) have been used to design and develop microcarriers and nanocarriers(11, 38, 124, 125). Bioavailability of oral drugs can be influenced by many factors such as solubility, permeability, metabolism and transporter glycoprotein (P-gp). Famotidine is a hydrophilic since the octanol/water coefficient is log P = -0.64. Moreover, Famotidine has a ionisable quanidin basic group pKa = 8.44 (Figure 2.1)and it has log D (-3.4) which is very hydrophilic at working pH (7.4). Famotidine water solubility is 1g/l and this solubility and ionisable properties are part of poor bioavailability. Famotidine was selected as drug model for this study because of Famotidine is P-gp substrate and its bioavailability is influenced by P-gp efflux(23, 126, 127). Some studies recently demonstrated that PEG, a pharmaceutical excipient, is capable to inhibit P-gp efflux and there is close association between P-gp and cell membrane(24, 33, 100, 122, 128). A relation between PEG and P-gp inhibition has been shown by Ashiru-Oredope et.al, and Huger et.al (24, 128). Indeed, because PEG contains many oxyethylene groups, it is reasonable to believe that PEG might alter the activity of P-gp by a nonspecific mechanism involving changes in membrane fluidity(100). The proposed mechanism of PEG assumes that it has the ability to alter the membrane fluidity of polar head group regions due to interruption of hydrophobic

environment in which P-gp acts(129). Moreover it is suggested by Hugger *et al* (2002) that increasing the concentration of PEG could cause a significant decrease in fluidity of polar head group regions of membrane(130). It has also been proposed that PEG-induced P-gp inhibition by the steric hindrance effect of PEG chains that may interfere with interaction of P-gp substrate and P-gp binding site(130). *The hypothesis of this study is based on using NPs prepared from grafted PLA-g-PEG polymer could improve oral permeability of drugs via P-gp inhibition(130-132).* This grafted polymer is composed of hydrophilic segment PEG grafted on PLA hydrophobic backbone and both parts are FDA approved polymers.

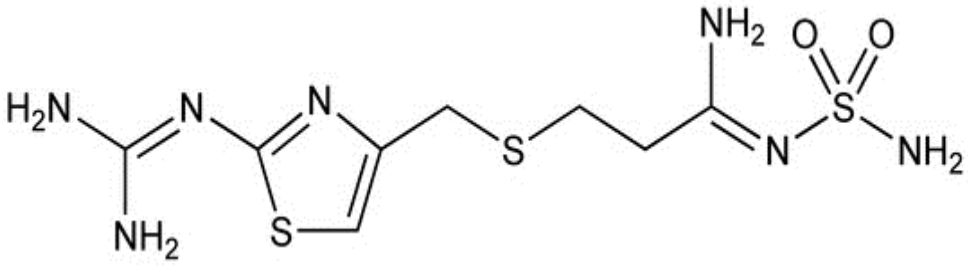

Figure 2.1 Famotidine Structure

2.2. The objectives of the study

The general objective of this research is to design a nanocarrier from PLA-g-PEG copolymer capable to inhibit P-gp efflux of drugs across CaCo-2 cell monolayers (pump drug back from basolateral side to apical side).

Therefore, the specific objectives of this research are that:

1) PLA-g-PEG will be synthesized with two PEG molecular weights and two grafting ratios.
2) NPs will be prepared from PLA-g-PEG polymers. Beside the inhibition function of PEG on P-gp, drugs which are P-gp substrate will be encapsulated in NPs to protect from harsh environment as the model drugs chosen will be given orally.
3) Loaded NPs prepared from different PLA-g-PEG polymers will be tested for their bidirectional permeability across CaCo-2 cell monolayers in order to evaluate the effect of PEG on P-gp efflux.
4) Loaded NPs with promising CaCo-2 results will be selected to develop an oral dosage formulation (tablet).
5) Tablets prepared from selected NPs formulations will be tested for their bidirectional permeability across CaCo-2 cell monolayers in order to evaluate whether the effect of PEG on P-gp efflux influenced by tablet compressing.

In order to meet those objectives, the following experiments were performed:

i. Polymer synthesis based on two PEG molecular weights (750 Da and 2000 Da)and grafting ratios (1% and 5%) based on the method used in our lab(133) :-

1. PLA-g-1%PEG750Da

2. PLA-g-1%PEG2000Da

3. PLA-g-5%PEG750Da

4. PLA-g-5%PEG2000Da

ii. Characterization of synthesized polymers by GPC, NMR, FTIR, grafting efficiency calculation and DSC.

iii. NP preparation by emulsion-solvent evaporation method (high pressure homogenizer) from four grafted polymers to encapsulate Famotidine as a model drug.

iv. Characterization of prepared nanoparticles for particle size and size distribution, PVA, surface charge, morphology, efficiency encapsulation, FTIR, DSC, XRPD, drug release and cytotoxicity.

v. CaCo-2 cell monolayers *in vitro* model bidirectional permeability evaluation of prepared NPs loaded with Famotidine

vi. NPs powder characterization as per bulk and tapped density, powder flow and compressibility.

vii. Formulation and process development of selected NPs with promising results from CaCo-2 oral solid tablet.

    1. F1 NPs PLA-g-5%PEG2000Da
    2. F2 NPs PLA-g-5%PEG750Da

viii. Tablet physical characterization such as DSC, XRPD, particle size and size distribution tablet weight, thickness, hardness, disintegration, drug stability and drug release carried out for:-

    1. PLA-g-5%PEG750Da NPs based formulation
    2. PLA-g-5%PEG2000Da NPs based formulation
    3. Commercial Famotidine formulation (Control)

ix. *In vitro* permeability evaluation of NPs based and commercial tablet formulations across CaCo-2 cell monolayers in bidirectional sides

References

1. Aulton, M.E., Aulton's pharmaceutics : the design and manufacture of medicines. 3rd ed. 2007, Edinburgh ; New York: Churchill Livingstone.
2. Mudie, D.M., G.L. Amidon, and G.E. Amidon, Physiological Parameters for Oral Delivery and in Vitro Testing. Molecular Pharmaceutics, 2010. 7(5): p. 1388-1405.
3. O'Neill, M.J., et al., Intestinal delivery of non-viral gene therapeutics: physiological barriers and preclinical models. Drug Discovery Today, 2011. 16(5-6): p. 203-218.
4. Schneeman, B.O., Gastrointestinal physiology and functions. British Journal of Nutrition,, 2002. 88: p. S159-S163.
5. Monjed, S., P. Gilles, and F. Elias, Particle uptake by Peyer's patches: a pathway for drug and vaccine delivery. Expert Opinion on Drug Delivery, 2004. 1(1): p. 141-163.
6. Marie, G., et al., PEGylated PLGA-based nanoparticles targeting M cells for oral vaccination. Journal of Controlled Released, 2007. 120: p. 195-204.
7. Frey, A., et al., Role of the glycocalyx in regulating access of microparticles to apical plasma membranes of intestinal epithelial cells: implications for microbial attachment and oral vaccine targeting. The Journal of Experimental Medicine, 1996. 184(3): p. 1045-1059.
8. M. Rabanel, J., et al., Drug-Loaded Nanocarriers: Passive Targeting and Crossing of Biological Barriers. Current Medicinal Chemistry, 2012. 19(19): p. 3070-3102.
9. Gaucher, G.v., et al., Polymeric micelles for oral drug delivery. European Journal of Pharmaceutics and Biopharmaceutics, 2010. 76(2): p. 147-158.

10. Laroui, H., et al., Nanomedicine in GI. American Journal of Physiology - Gastrointestinal and Liver Physiology, 2011. 300(3): p. G371-G383.

11. Hunter, A.C., et al., Polymeric particulate technologies for oral drug delivery and targeting: a pathophysiological perspective. Nanomedicine: Nanotechnology, Biology and Medicine, 2012. 8, Supplement 1(0): p. S5-S20.

12. Lai, S.K., Y.-Y. Wang, and J. Hanes, Mucus-penetrating nanoparticles for drug and gene delivery to mucosal tissues. Advanced Drug Delivery Reviews, 2009. 61(2): p. 158-171.

13. Cone, R.A., Barrier properties of mucus. Advanced Drug Delivery Reviews, 2009. 61(2): p. 75-85.

14. Linden, S.K., et al., Mucins in the mucosal barrier to infection. 2008. 1(3): p. 183-197.

15. Kondoh, M. and K. Yagi, Progress in absorption enhancers based on tight junction. Expert Opinion on Drug Delivery, 2007. 4(3): p. 275-286.

16. M, G.B., Breaking through the tight junction barrier. Journal of Cell Biology, 1993December 15. 123(6): p. 1631-1633.

17. Hayashi, M. and M. Tomita, Mechanistic analysis for drug permeation through intestinal membrane. Drug Metabolism and Pharmacokinetics, 2007. 22(2): p. 67-77.

18. Matsuhisa, K., et al., Tight junction modulator and drug delivery. Expert Opinion on Drug Delivery, 2009. 6(5): p. 509-515.

19. Lambkin, I. and C. Pinilla, Targeting approaches to oral drug delivery. Expert Opinion on Biological Therapy, 2002. 2(1): p. 67-73.

20. Salama, N.N., N.D. Eddington, and A. Fasano, Tight junction modulation and its relationship to drug delivery. Advanced Drug Delivery Reviews

Challenges in Pediatric Drug Delivery: the Case of Vaccines, 2006. 58(1): p. 15-28.

21. Hediger, M.A., et al., The ABCs of solute carriers: physiological, pathological and therapeutic implications of human membrane transport proteins - Introduction. Pflugers Archiv-European Journal of Physiology, 2004. 447(5): p. 465-468.

22. Giacomini, K.M., et al., Membrane transporters in drug development. 2010. 9(3): p. 215-236.

23. Estudante, M., et al., Intestinal drug transporters: An overview. Advanced Drug Delivery Reviews, 2013. 65(10): p. 1340-1356.

24. Akhtar, N., et al., The emerging role of P-glycoprotein inhibitors in drug delivery: a patent review. Expert Opinion on Therapeutic Patents, 2011. 21(4): p. 561-576.

25. Ferté, J., Analysis of the tangled relationships between P-glycoprotein-mediated multidrug resistance and the lipid phase of the cell membrane. European Journal of Biochemistry, 2000. 267(2): p. 277-294.

26. Collnot , E.-M., et al., Mechanism of Inhibition of P-Glycoprotein Mediated Efflux by Vitamin E TPGS: Influence on ATPase Activity and Membrane Fluidity. Molecular Pharmaceutics, 2007. 4(3): p. 465-474.

27. Shen, Q., et al., Modulation of intestinal P-glycoprotein function by polyethylene glycols and their derivatives by in vitro transport and in situ absorption studies. International Journal of Pharmaceutics, 2006. 313(1-2): p. 49-56.

28. Ambudkar, S.V., I.-W. Kim, and Z.E. Sauna, The power of the pump: Mechanisms of action of P-glycoprotein (ABCB1). European Journal of Pharmaceutical Sciences, 2006. 27(5): p. 392-400.

29. Loo, T.W. and D.M. Clarke, Do drug substrates enter the common drug-binding pocket of P-glycoprotein through "gates"? Biochemical and Biophysical Research Communications, 2005. 329(2): p. 419-422.

30. Ambudkar, S.V., et al., Biochemical, cellular, and pharmacological aspects of the multidrug transporter. Annual Review of Pharmacology and Toxicology, 1999. 39: p. 361-398.

31. Higgins, C.F. and K.J. Linton, The ATP switch model for ABC transporters. Nature Structural & Molecular Biology, 2004. 11(10): p. 918-926.

32. Stouch, T.R. and O. Gudmundsson, Progress in understanding the structure-activity relationships of P-glycoprotein. Advanced Drug Delivery Reviews, 2002. 54(3): p. 315-328.

33. Hugger, E.D., K.L. Audus, and R.T. Borchardt, Effects of poly(ethylene glycol) on efflux transporter activity in Caco-2 cell monolayers. Journal of Pharmaceutical Sciences, 2002. 91(9): p. 1980-1990.

34. Li, M., et al., Excipients enhance intestinal absorption of ganciclovir by P-gp inhibition: Assessed in vitro by everted gut sac and in situ by improved intestinal perfusion. International Journal of Pharmaceutics, 2011. 403(1-2): p. 37-45.

35. Vonarbourg, A., et al., Parameters influencing the stealthiness of colloidal drug delivery systems. Biomaterials, 2006. 27(24): p. 4356-4373.

36. Morachis, J.M., E.A. Mahmoud, and A. Almutairi, Physical and Chemical Strategies for Therapeutic Delivery by Using Polymeric Nanoparticles. Pharmacological Reviews, 2012. 64(3): p. 505-519.

37. Rieux, A.d., et al., Nanoparticles as potential oral delivery systems of proteins and vaccines: A mechanistic approach. Journal of Controlled Release, 2006. 116(1): p. 1-27.

38. Soppimath, K.S., et al., Biodegradable polymeric nanoparticles as drug delivery devices. Journal of Controlled Release, 2001. 70(1-2): p. 1-20.

39. Rawat, M., et al., Nanocarriers: Promising Vehicle for Bioactive Drugs. Biological and Pharmaceutical Bulletin, 2006. 29(9): p. 1790-1798.

40. Zhang, L., et al., Nanocarriers for oral drug delivery. Journal of Drug Targeting, 2013. 21(6): p. 515-527.

41. Mora-Huertas, C.E., H. Fessi, and A. Elaissari, Polymer-based nanocapsules for drug delivery. International Journal of Pharmaceutics, 2010. 385(12): p. 113-142.

42. Damgé, C., et al., Nanocapsules as carriers for oral peptide delivery. Journal of Controlled Release, 1990. 13(2-3): p. 233-239.

43. Fricker, G., et al., Phospholipids and Lipid-Based Formulations in Oral Drug Delivery. Pharmaceutical Research, 2010. 27(8): p. 1469-1486.

44. Moghimi, S.M., A.C. Hunter, and J.C. Murray, Long-Circulating and Target-Specific Nanoparticles: Theory to Practice. Pharmacological Reviews 2001 53 (2): p. 283-318

45. Jain, S., et al., Nanocarriers for Transmucosal Vaccine Delivery. Current Nanoscience, 2011. 7(2): p. 160-177.

46. Yang, S.C., et al., Body distribution of camptothecin solid lipid nanoparticles after oral administration. Pharmaceutical Research, 1999. 16(5): p. 751-757.

47. Zhang, N., et al., Lectin-modified solid lipid nanoparticles as carriers for oral administration of insulin. International Journal of Pharmaceutics, 2006. 327(1-2): p. 153-159.

48. Mathot, F., et al., Intestinal uptake and biodistribution of novel polymeric micelles after oral administration. Journal of Controlled Release, 2006. 111(1-2): p. 47-55.

49. Bromberg, L., Polymeric micelles in oral chemotherapy. Journal of Controlled Release, 2008. 128(2): p. 99-112.

50. Devalapally, H., A. Chakilam, and M.M. Amiji, Role of nanotechnology in pharmaceutical product development. Journal of Pharmaceutical Sciences, 2007. 96(10): p. 2547-2565.

51. Plapied, L., et al., Fate of polymeric nanocarriers for oral drug delivery. Current Opinion in Colloid & Interface Science, 2011. 16(3): p. 228-237.

52. Blanchette, J., N. Kavimandan, and N.A. Peppas, Principles of transmucosal delivery of therapeutic agents. Biomedecine & Pharmacotherapy, 2004. 58(3): p. 142-151.

53. Kim, S., et al., Overcoming the barriers in micellar drug delivery: loading efficiency, in vivo stability, and micelle-cell interaction. Expert Opinion on Drug Delivery, 2010. 7(1): p. 49-62.

54. Gaucher, G.v., R.H. Marchessault, and J.-C. Leroux, Polyester-based micelles and nanoparticles for the parenteral delivery of taxanes. Journal of Controlled Release, 2010. 143(1): p. 2-12.

55. Hamidi, M., A. Azadi, and P. Rafiei, Hydrogel nanoparticles in drug delivery. Advanced Drug Delivery Reviews, 2008. 60(15): p. 1638-1649.

56. Sarmento, B., et al., Alginate/Chitosan Nanoparticles are Effective for Oral Insulin Delivery. Pharmaceutical Research, 2007. 24(12): p. 2198-2206.

57. Blanchette, J. and N.A. Peppas, Cellular evaluation of oral chemotherapy carriers. Journal of Biomedical Materials Research Part A, 2005. 72A(4): p. 381-388.

58. Woitiski, C.B., et al., Pharmacological effect of orally delivered insulin facilitated by multilayered stable nanoparticles. European Journal of Pharmaceutical Sciences, 2010. 41(3-4): p. 556-563.

59. Jain, N.K. and U. Gupta, Application of dendrimer-drug complexation in the enhancement of drug solubility and bioavailability. Expert Opinion on Drug Metabolism & Toxicology, 2008. 4(8): p. 1035-1052.

60. Mignani, S., et al., Expand classical drug administration ways by emerging routes using dendrimer drug delivery systems: A concise overview. Advanced Drug Delivery Reviews, 2013. 65(10): p. 1316-1330.

61. Al-Jamal, K.T., C. Ramaswamy, and A.T. Florence, Supramolecular structures from dendrons and dendrimers. Advanced Drug Delivery Reviews Dendrimers: a Versatile Targeting Platform, 2005. 57(15): p. 2238-2270.

62. Gajbhiye, V., et al., Dendrimeric Nanoarchitectures Mediated Transdermal and Oral Delivery of Bioactives. Indian Journal of Pharmaceutical Sciences, 2008. 70(4): p. 431-439.

63. Jevprasesphant, R., et al., Engineering of Dendrimer Surfaces to Enhance Transepithelial Transport and Reduce Cytotoxicity. Pharmaceutical Research, 2003. 20(10): p. 1543-1550.

64. Qian, W.Y., et al., pH-sensitive strontium carbonate nanoparticles as new anticancer vehicles for controlled etoposide release. International Journal of Nanomedicine, 2012. 7: p. 5781-5792.

65. Panakanti, R. and A.S. Narang, Impact of Excipient Interactions on Drug Bioavailability from Solid Dosage Forms. Pharmaceutical Research, 2012. 29(10): p. 2639-2659.

66. Florence, A., The Oral Absorption of Micro- and Nanoparticulates: Neither Exceptional Nor Unusual. Pharmaceutical Research, 1997. 14(3): p. 259-266.

67. Florence, A.T., et al., Factors Affecting the Oral Uptake and Translocation of Polystyrene Nanoparticles: Histological and Analytical Evidence. Journal of Drug Targeting, 1995. 3(1): p. 65-70.

68. Li, S.-D. and L. Huang, Pharmacokinetics and Biodistribution of Nanoparticles. Molecular Pharmaceutics, 2008. 5(4): p. 496-504.

69. Mozafari, M.R., et al., Role of nanocarrier systems in cancer nanotherapy. Journal of Liposome Research, 2009. 19(4): p. 310-321.

70. Kesisoglou, F., S. Panmai, and Y.H. Wu, Nanosizing - Oral formulation development and biopharmaceutical evaluation. Advanced Drug Delivery Reviews, 2007. 59(7): p. 631-644.

71. Bravo-Osuna, I., et al., Mucoadhesion mechanism of chitosan and thiolated chitosan-poly(isobutyl cyanoacrylate) core-shell nanoparticles. Biomaterials, 2007. 28(13): p. 2233-2243.

72. Bernkop-Schnurch, A., et al., Thiomers: Preparation and in vitro evaluation of a mucoadhesive nanoparticulate drug delivery system. International Journal of Pharmaceutics, 2006. 317(1): p. 76-81.

73. Bromberg, L., et al., Bioadhesive properties and rheology of polyether-modified poly(acrylic acid) hydrogels. International Journal of Pharmaceutics, 2004. 282(1-2): p. 45-60.

74. Lamprecht, A., U. Schafer, and C.-M. Lehr, Size-Dependent Bioadhesion of Micro- and Nanoparticulate Carriers to the Inflamed Colonic Mucosa. Pharmaceutical Research, 2001. 18(6): p. 788-793.

75. Behrens, I., et al., Comparative Uptake Studies of Bioadhesive and Non-Bioadhesive Nanoparticles in Human Intestinal Cell Lines and Rats: The Effect of Mucus on Particle Adsorption and Transport. Pharmaceutical Research, 2002. 19(8): p. 1185-1193.

76. Sonaje, K., et al., Biodistribution, pharmacodynamics and pharmacokinetics of insulin analogues in a rat model: Oral delivery using pH-Responsive nanoparticles vs. subcutaneous injection. Biomaterials, 2010. 31(26): p. 6849-6858.

77. Lai, S.K., et al., Rapid transport of large polymeric nanoparticles in fresh undiluted human mucus. Proceedings of the National Academy of Sciences, 2007. 104(5): p. 1482-1487.

78. Wong, C., et al., Multistage nanoparticle delivery system for deep penetration into tumor tissue. Proceedings of the National Academy of Sciences, 2011. 108(6): p. 2426-2431.

79. Jung, T., et al., Biodegradable nanoparticles for oral delivery of peptides: is there a role for polymers to affect mucosal uptake? European Journal of Pharmaceutics and Biopharmaceutics, 2000. 50(1): p. 147-160.

80. Rieux, A.d., et al., Transport of nanoparticles across an in vitro model of the human intestinal follicle associated epithelium. European Journal of Pharmaceutical Sciences, 2005. 25(4-5): p. 455-465.

81. Desai, M., et al., Gastrointestinal Uptake of Biodegradable Microparticles: Effect of Particle Size. Pharmaceutical Research, 1996. 13(12): p. 1838-1845.

82. Vila, A., et al., Transport of PLA-PEG particles across the nasal mucosa: effect of particle size and PEG coating density. Journal of Controlled Release, 2004. 98(2): p. 231-244.

83. Semete, B., et al., In vivo evaluation of the biodistribution and safety of PLGA nanoparticles as drug delivery systems. Nanomedicine: Nanotechnology, Biology and Medicine, 2010. 6(5): p. 662-671.

84. Semete, B., et al., In vivo uptake and acute immune response to orally administered chitosan and PEG coated PLGA nanoparticles. Toxicology and Applied Pharmacology, 2010. 249(2): p. 158-165.

85. Peltier, S., et al., Enhanced Oral Paclitaxel Bioavailability After Administration of Paclitaxel-Loaded Lipid Nanocapsules. Pharmaceutical Research, 2006. 23(6): p. 1243-1250.

86. Roger, E., et al., Lipid nanocarriers improve paclitaxel transport throughout human intestinal epithelial cells by using vesicle-mediated transcytosis. Journal of Controlled Release, 2009. 140(2): p. 174-181.

87. Yin, Y., et al., Preparation and evaluation of lectin-conjugated PLGA nanoparticles for oral delivery of thymopentin. Journal of Controlled Release, 2006. 116(3): p. 337-345.

88. Irache, J.M., et al., Bioadhesion of Lectin-Latex Conjugates to Rat Intestinal Mucosa, in Pharmaceutical Research. 1996, Springer Netherlands. p. 1716-1719.

89. Umamaheshwari, S.R., 1 and Narendra Kumar Jain1, Anti–Helicobacter Pylori Effect of Mucoadhesive Nanoparticles Bearing Amoxicillin in Experimental Gerbils Model. Aaps Pharmscitech, 2004. 5(2): p. 9.

90. Clark, M.A., M.A. Jepson, and B.H. Hirst, Exploiting M cells for drug and vaccine delivery. Advanced Drug Delivery Reviews, 2001. 50(1-2): p. 81-106.

91. Primard, C., et al., Traffic of poly(lactic acid) nanoparticulate vaccine vehicle from intestinal mucus to sub-epithelial immune competent cells. Biomaterials, 2010. 31(23): p. 6060-6068.

92. Rowe, R.C., P.J. Sheskey, and M.E. Quinn, Handbook of pharmaceutical excipients. 2009, Pharmaceutical Press ;American Pharmacists association: London ; Chicago, Washington,DC.

93. Gref, R., et al., Stealth corona-core nanoparticles surface modified by polyethylene glycol (PEG): influences of the corona (PEG chain length and surface density) and of the core composition on phagocytic uptake and plasma protein adsorption. Colloids and Surfaces B: Biointerfaces, 2000. 18(3-4): p. 301-313.

94. Bazile, D., et al., Stealth Me.PEG-PLA nanoparticles avoid uptake by the mononuclear phagocytes system. Journal of Pharmaceutical Sciences, 1995. 84(4): p. 493-498.

95. Mosqueira, V., et al., Biodistribution of Long-Circulating PEG-Grafted Nanocapsules in Mice: Effects of PEG Chain Length and Density. Pharmaceutical Research, 2001. 18(10): p. 1411-1419.

96. Owens , D.E. and N.A. Peppas, Opsonization, biodistribution, and pharmacokinetics of polymeric nanoparticles. International Journal of Pharmaceutics, 2006. 307(1): p. 93-102.

97. Sant, S., S. Poulin, and P. Hildgen, Effect of polymer architecture on surface properties, plasma protein adsorption, and cellular interactions of pegylated nanoparticles. Journal of Biomedical Materials Research Part A, 2008. 87A(4): p. 885-895.

98. Lacasse, F.X., et al., Influence of Surface Properties at Biodegradable Microsphere Surfaces: Effects on Plasma Protein Adsorption and Phagocytosis. Pharmaceutical Research, 1998. 15(2): p. 312-317.

99. Brendan M. Johnson, William N. Charman, and C.J.H. Porter, An In Vitro Examination of the Impact of Polyethylene Glycol 400, Pluronic P85, and Vitamin E d-a-Tocopheryl Polyethylene Glycol 1000 Succinate on PGlycoprotein Efflux and Enterocyte-Based Metabolism in Excised Rat Intestine. AAPS Pharmscitech, 2002. 4(4): p. 13.

100. Hugger, E.D., et al., A comparison of commonly used polyethoxylated pharmaceutical excipients on their ability to inhibit P-glycoprotein activity in vitro. Journal of Pharmaceutical Sciences, 2002. 91(9): p. 1991-2002.

101. del Amo, E.M., A. Heikkinen, and M. Jukka, In vitro-in vivo correlation in p-glycoprotein mediated transport in intestinal absorption. European Journal of Pharmaceutical Sciences, 2009. 36(2-3): p. 200-211.

102. McDevitt, C.A. and R. Callaghan, How can we best use structural information on P-glycoprotein to design inhibitors? Pharmacology & Therapeutics, 2007. 113(2): p. 429-441.

103. Srivalli, K.M.R. and P.K. Lakshmi, Overview of P-glycoprotein inhibitors: a rational outlook. Brazilian Journal of Pharmaceutical Sciences, 2012. 48(3): p. 353-367.

104. Tobio , M., et al., The role of PEG on the stability in digestive fluids and in vivo fate of PEG-PLA nanoparticles following oral administration. Colloids and Surfaces B: Biointerfaces, 2000. 18(3-4): p. 315-323.

105. Wang, M. and M. Thanou, Targeting nanoparticles to cancer. Pharmacological Research

Towards clinical applications of nanoscale medicines, 2010. 62(2): p. 90-99.

106. Locatelli, E. and M. Comes Franchini, Biodegradable PLGA-b-PEG polymeric nanoparticles: synthesis, properties, and nanomedical applications as drug delivery system. Journal of Nanoparticle Research C7 - 1316, 2012. 14(12): p. 1-17.

107. Gupta, S., et al., Oral delivery of therapeutic proteins and peptides: a review on recent developments. Drug Delivery, 2013. 20(6): p. 237-246.

108. Hussain, N., V. Jaitley, and A.T. Florence, Recent advances in the understanding of uptake of microparticulates across the gastrointestinal lymphatics. Advanced Drug Delivery Reviews Transport and absorption of Drugs Via the Lymphatic System, 2001. 50(1-2): p. 107-142.

109. Giuseppe Del Giudice, A.C., John L. Telford, Cesare Montecucco, and Rino Rappuoli, The Design of Vaccines against Heliobacter Pylori and their Development. 2001. Vol. 19: p. 523-563.

110. Venkatraman, S.S., et al., Micelle-like nanoparticles of PLA-PEG-PLA triblock copolymer as chemotherapeutic carrier. International Journal of Pharmaceutics, 2005. 298(1): p. 219-232.

111. Barua, S. and S. Mitragotri, Challenges associated with penetration of nanoparticles across cell and tissue barriers: A review of current status and future prospects. Nano Today, 2014. 9(2): p. 223-243.

112. Zhao, H. and L.Y.L. Yung, Selectivity of folate conjugated polymer micelles against different tumor cells. International Journal of Pharmaceutics, 2008. 349(1-2): p. 256-268.

113. Teng, Y., Z. Qiu, and H. Wen, Systematical approach of formulation and process development using roller compaction. European Journal of Pharmaceutics and Biopharmaceutics, 2009. 73(2): p. 219-229.

114. Thoorens, G., et al., Microcrystalline cellulose, a direct compression binder in a quality by design environment. International Journal of Pharmaceutics, 2014. 473(1-2): p. 64-72.

115. Abdelbary, A., A.H. Elshafeey, and G. Zidan, Comparative effects of different cellulosic-based directly compressed orodispersable tablets on oral bioavailability of famotidine. Carbohydrate Polymers, 2009. 77(4): p. 799-806.

116. Parrott, E.L., Densification of powders by concavo-convex roller compactor. Journal of Pharmaceutical Sciences, 1981. 70(3): p. 288-291.

117. Kleinebudde, P., Roll compaction/dry granulation: pharmaceutical applications. European Journal of Pharmaceutics and Biopharmaceutics, 2004. 58(2): p. 317-326.

118. Loh, Z.H., et al., Spray granulation for drug formulation. Expert Opinion on Drug Delivery, 2011. 8(12): p. 1645-1661.

119. Hansuld, E.M. and L. Briens, A review of monitoring methods for pharmaceutical wet granulation. International Journal of Pharmaceutics, 2014. 472(1-2): p. 192-201.

120. Faure, A., P. York, and R.C. Rowe, Process control and scale-up of pharmaceutical wet granulation processes: a review. European Journal of Pharmaceutics and Biopharmaceutics, 2001. 52(3): p. 269-277.

121. Sepassi, S., et al., Effect of polymer molecular weight on the production of drug nanoparticles. Journal of Pharmaceutical Sciences, 2007. 96(10): p. 2655-2666.

122. Ashiru-Oredope, D.A.I., et al., The effect of polyoxyethylene polymers on the transport of ranitidine in Caco-2 cell monolayers. International Journal of Pharmaceutics, 2011. 409(1-2): p. 164-168.

123. Govender, T., et al., PLGA nanoparticles prepared by nanoprecipitation: drug loading and release studies of a water soluble drug. Journal of Controlled Release, 1999. 57(2): p. 171-185.

124. Umesh Gupta, H.B.A.a.N.K.J., Polypropylene Imine Dendrimer Mediated Solubility Enhancement: Effect of pH and Functional Groups of Hydrophobes. J Pharm Pharmaceut Sci, 2007. 10(3): p. 358-367.

125. Dong, Y. and S.S. Feng, Poly(D,L-lactide-co-glycolide) (PLGA) nanoparticles prepared by high pressure homogenization for paclitaxel chemotherapy. International Journal of Pharmaceutics, 2007. 342(1-2): p. 208-214.

126. Dahan, A. and G.L. Amidon, Segmental Dependent Transport of Low Permeability Compounds along the Small Intestine Due to P-Glycoprotein: The Role of Efflux Transport in the Oral Absorption of BCS Class III Drugs. Molecular Pharmaceutics, 2008. 6(1): p. 19-28.

127. Thakker, K.L.a.D.R., Saturable Transport of H2-Antagonists Ranitidine and Famotidine Across Caco-2 Cell Monolayers. Journal of Pharmaceutical Sciences, 1999. 88(7): p. 680-687.

128. Dudeja, P.K., et al., Reversal of Multidrug-Resistance Phenotype by Surfactants: Relationship to Membrane Lipid Fluidity. Archives of Biochemistry and Biophysics, 1995. 319(1): p. 309-315.

129. Liu, Y. and G.N.C. Chiu, Dual-Functionalized PAMAM Dendrimers with Improved P-Glycoprotein Inhibition and Tight Junction Modulating Effect. Biomacromolecules, 2013. 14(12): p. 4226-4235.

130. Nadeau, V., et al., Synthesis of new versatile functionalized polyesters for biomedical applications. Polymer, 2005. 46(25): p. 11263-11272.

131. Essa, S., J.M. Rabanel, and P. Hildgen, Effect of polyethylene glycol (PEG) chain organization on the physicochemical properties of poly(d, l-lactide) (PLA) based nanoparticles. European Journal of Pharmaceutics and Biopharmaceutics, 2010. 75(2): p. 96-106.

132. Shilpa, S., N. Ve´ronique, and P. Hildgen, Effect of porosity on the release kinetics of propafenone-loaded PEG-g-PLA nanoparticles. Journal of Controlled Release, 2005. 107: p. 203-214.

133. J-M. Rabanel1, V.A., and P. Hildgen1, Impact of Polymer Physico-chemical Properties on PEG-grafted-PLA Nanoparticles Structure. CRS annual meeting, 2012. 2012 CRS 37th annual meeting.

Experimental Works

Chapter Three. Design of PEG-grafted-PLA nanoparticles as oral permeability enhancer for P-gp substrate drug model Famotidine

Mohamed Mokhtar[1], Patrick Gosselin[2], Lacasse François-Xavier[1]

and Patrice Hildgen*[1]

[1] Faculté de pharmacie, Université de Montréal, Montréal, QC, H3C 3J7, Canada;

[2] Corealis Pharma Inc, Laval, QC, H7V 4A6, Canada

Submitted to Journal of Microencapsulation on Janaury,3th, 2015 (Manuscript Number: TMNC-2015-0002)

Keywords: Caco-2, Famotidine, Nanoparticles, Permeability, P-gp , PLA, PEG

Résumé :

La biodisponibilité des médicaments administrés par voie orale peut être limitée par les processus intestinaux médiés par les glycoprotéines-P (P-gp). Le polyéthylène glycol (PEG) est connu comme étant un inhibiteur des P-gp. La dispersion de famotidine (substrat des P-gp) encapsulée dans des nanoparticules pegylées (NPs) a été utilisée afin d'augmenter sa biodisponibilité. Le but de ce projet est d'évaluer l'utilisation

potentielle des NPs préparées à partir des fonctions PLA-g-PEG en étudiant la perméabilité *in vitro* avec le test cellulaire Caco-2. Des PLA-g-PEG qui sont des PEG greffés sur l'acide polylactique de 750 et 2000 Da (PLA) ont été synthétisés avec 1% et 5% (ratio molaire de PEG vs monomère d'acide lactique). Ces polymères ont été utilisés pour préparer des nanoparticules de famotidine et testées in vitro avec le test Caco-2. Une baisse significative de la sécrétion de famotidine a été observée du côté basolatéral vers l'apical lorsque des nanoparticules de famotidine de PEG5%-g-PLA ont été utilisées. Ces nanoparticules semblent être une alternative promettante pour améliorer la biodisponibilité orale des substrats de P-gp.

3.1. Abstract

Bioavailability of oral drugs may be limited by an intestinal secretion process mediated by P-glycoprotein (P-gp). Polyethylene glycol (PEG) is known as P-gp inhibitor. Dispersion of Famotidine (P-gp substrate) within pegylated nanoparticles (NPs) was used to enhance its bioavailability. In this work, our goal was to evaluate the potential use of NPs prepared from PLA-g-PEG on P-gp function by studying *in vitro* permeability across CaCo-2 cells. PEG grafted on a polylactide acid (PLA) backbone (PLA-g-PEG) were synthesized with 1 % and 5 % (molar ratio of PEG vs lactic acid monomer) of 750 and 2000 Da. These polymers were used to prepare Famotidine loaded NPs and tested *in vitro* on CaCo-2 cells. Significant decrease in secretion of Famotidine from Basolateral-to-Apical was observed when Famotidine was encapsulated in NPs prepared from PLA-g-5%PEG. NPs prepared from PLA-g-5%PEG could be a promising strategy to improve oral bioavailability of P-gp substrate.

Keywords: Caco-2, Famotidine, Nanoparticles, Permeability, P-gp , PLA, PEG

3.2. Introduction

In order to be absorbed via the oral route, drug molecules must dissolve into gastrointestinal fluids, resist to enzymatic degradation and not bind to food. Moreover, drug molecules need to diffuse across the gastrointestinal membrane to reach the systemic circulation, either by entering epithelial cells from the apical

(luminal) side and exiting from the basolateral side (transcellular transport) or by passing through the intercellular space (paracellular transport). Small molecule transporters act as biochemical barriers to transcellular transport while the tight junctions of the epithelium act as a physical barriers to paracellular transport (Aulton, 2007). Amongst transport proteins is P-glycoprotein (P-gp), a glycoprotein of about 170 kDa also called apical efflux transporter (Akhtar, et al., 2011, Estudante, et al., 2013). P-gp is part of the super family of ATP-binding cassette (ABC) transporters involved in the transport of various substrates across extra- and intracellular membranes. P-gp is expressed in various normal tissues including liver, kidney, adrenal glands, brain, testis and the intestinal brush border membranes (Akhtar, et al., 2011, Estudante, et al., 2013). P-gp is also expressed in tumor cells and responsible for the efflux of chemotherapeutic agents from multidrug-resistant (MDR) cancer cells. In the GI tract, P-gp acts as absorption barrier by lowering intracellular drug concentration, by secreting drugs from the cytosol of intestinal cells to the intestinal lumen and by reducing permeability and bioavailability, thus having a profound impact on the pharmacokinetics of several drugs (Akhtar, et al., 2011). Therefore the oral bioavailability of drugs that are P-gp substrates could be improved by inhibiting the P-gp efflux function within the intestinal membrane (Dahan, et al., 2008, Shen, et al., 2006).

Some pharmaceutical excipients can inhibit the secreting function of P-gp in the intestinal membrane and therefore improve the oral bioavailability of P-gp substrate drugs (Ashiru-Oredope, et al., 2011, Hugger, et al., 2002). Polyethylene glycol (PEG)

is uncharged, hydrophilic and soluble in many organic solvents. PEG is commonly used as an excipient in pharmaceutical formulations and available commercially in molecular weights ranging from 200 to 8000 Da (Rowe, et al., 2009). For instance, PEG 6000 Da has been used to increase aqueous solubility or dissolution of some drugs by solid dispersion technique (Essa, et al., 2010). Moreover, PEG has been shown to enhance bioavailability of some drugs by inhibiting P-gp efflux (Hugger, et al., 2002). Indeed, PEGs within a range of 300 to 4000 Da have been used to improve oral permeability of P-gp substrate drugs (M. Rabanel, et al., 2012). Some studies showed that P-gp is highly sensitive to the lipid environment of cell membranes and that increased concentrations of PEG alter membrane fluidity probably through interactions between oxyethylene groups and the phospholipid polar headgroups (Ashiru-Oredope, et al., 2011, Collnot, 2007, Hugger, et al., 2002, Hugger, et al., 2002, Iqbal, et al., 2010).

Nanosized formulations have been shown efficient at enhancing drug absorption and bioavailability of several drugs (Hunter, et al., 2012, Lenhardt, et al., 2008, Mittal, et al., 2007, Sepassi, et al., 2007). Nanoparticles (NPs) are drug carriers with a size varying from 10 to 1000 nm in which the drug is either physically or molecularly uniformly dispersed. Nanocapsules are vesicular systems in which the drug is confined to a cavity surrounded by a unique polymer membrane (Merisko-Liversidge, et al., 2003, Panoyan, et al., 2003). In recent years, biodegradable NPs have been increasingly tested in pharmaceutical research as promising drug delivery systems (Li, et al., 2008). Nanoformulation may contribute to improving drug adsorption in several ways such as preventing premature degradation of the drug in hostile

gastrointestinal environment, contributing to target drugs to specific parts of the gastrointestinal tract and allowing the delivery of poorly soluble drugs (Bala, et al., 2004, Bhardwaj, et al., 2005, Mittal, et al., 2007). Indeed, improvement of passage through biological barriers by nanocarriers administered orally has been reported for several encapsulated drugs (M. Rabanel, et al., 2012). PEGylated drug carriers have initially been developed to prevent rapid elimination by mononuclear phagocyte system and increase systemic circulation time to optimise drug delivery (Owens , et al., 2006). However, PEGylated drug carriers can also be of benefit to oral delivery by improving penetration through the mucus barrier covering the epithelium, favouring interaction with epithelial cell membranes, decreasing interaction with food and, as discussed earlier, decreasing P-gp activity (Mert, et al., 2012). Famotidine, a H2-receptor antagonist, inhibits gastric acid secretion and heals gastric and duodenal ulcers. After oral administration, the onset of the antisecretory effect occurred within one hour; the maximum effect was dose-dependent, occurring within one to three hours. Famotidine has been chosen as model drug because of its relatively low and variable oral bioavailability apparently due to its relatively low aqueous solubility and efflux transport by P-gp (Kiho Lee, 2002). Encapsulation of this drug in PEGylated nanocarriers could therefore be a promising approach. The objective of this paper is thus to develop and evaluate the effect of nano-encapsulation of Famotidine in PEG-grafted poly(lactic acid) (PLA-*g*-PEG) NPs on P-gp efflux and permeability through Caco-2 cell monolayers.

3.3. Materials and methods

3.3.1. Materials

Pharmaceutical grade famotidine was obtained from Corealis Pharma Inc, (Laval, QC, Canada). Organic solvents were purchased from Laboratoire MAT (Montréal, QC, Canada) while other chemicals were from Sigma-Aldrich (St-Louis, MI, USA). All solvents were HPLC grade and used without further purification. All materials for cell culture were purchased from Invitrogen (Burlington, ON, Canada).

3.3.2. Polymer synthesis

Polymers of PEG randomly grafted on poly(D,L-lactide) were synthesised as previously (Essa, et al., 2010, Nadeau, et al., 2005, Shilpa, et al., 2005). PEG grafting was performed at density ratios of 1% and 5% (mol/mol of lactic acid). In brief, a polyester-*co*-ether copolymer of D, L-lactide (21.5 g, 99 mmol or 95 mmol) and allyl glycidyl ether (AGE) (0.343 g, 2 mmol or 10 mmol) was first synthesised by ring-opening polymerisation using tetraphenyl tin as catalyst (1:10 000 molar ratio with regard to lactide) under argon. The reaction was maintained at 180 °C for 6 h. The copolymer thus obtained was dissolved in acetone and precipitated in water. After polymer drying under vacuum, the allyl pendant groups were oxidised to hydroxyl groups by hydroboration with an equimolar quantity of borane in tetrahydrofuran.

The reaction was carried out for 2 h at 0 °C followed by oxidation in presence of hydrogen peroxide under alkaline condition (1 N NaOH). The pendant hydroxyl groups were further oxidised to carboxylic acid groups by Jones reagent under stirring for 3 h at 0°C, then converted to acyl chloride by adding thionyl chloride (1:1000 molar equivalents) under stirring at ambient temperature for 2 h. Methoxy poly(ethylene glycol) (mPEG) (2000 or 750 g/mol) was grafted onto the PLA copolymer backbone by reacting the hydroxyl groups of MPEG with the pendant acyl chlorides in presence of pyridine and 4-dimethylaminopyridine (DMAP). Subsequently, the polymer was purified by successive washings with 1 N HCl and precipitation in water from acetone. The final polymer was dried under vacuum (900 mbar) before storage at -20 °C.

3.3.3. Polymer characterisation

3.3.3.1. Nuclear magnetic resonance (NMR)

Samples of each polymer (10 to 20 mg) were dissolved in $CDCl_3$ and ^{1}H-NMR spectra were recorded using a Brucker ARX 400 spectrometer (Bruker, Germany). Chemical shift (d) was measured in ppm using tetramethylsilane (TMS) as internal reference.

3.3.3.2. Gel permeation chromatography (GPC)

The number average (Mn) and the weight average (Mw) molecular weights of the synthesised polymers were determined by GPC. GPC was performed using a Waters chromatography system (Waters, USA) equipped with a refractive index detector and a Phenogel 5-µm column (Phenomenex). Polystyrene standards (400, 200, 90, 50, 30, 20, 4, and 2 kDa) were used for calibration with chloroform as mobile phase at a flow rate of 0.6 mL/min. Polymer was dissolved in of chloroform at 2.5 mg/mL. Polydispersity index (PDI) was calculated using the Mw/Mn ratio from GPC data.

3.3.3.3. Grafting efficiency

The number and weight percentages (w/w %) of PEG units present in a copolymer chain were calculated based on ^{1}H NMR spectra, GPC data, lactic acid molecular weight and PEG molecular weight. Poly(D,L-lactide)-graft-PEG (PLA-*g*-PEG) is a random branched copolymer with a structure shown in Figure 3.1, where x is the number of lactic acid moieties and y the number of grafted PEG chains. Equation 1 describes the calculation of the molar fraction of PEG (p) from the x and y values obtained by ^{1}H NMR.

$$p = \frac{y}{x+y} \quad \text{(Equation 1)}$$

The molecular weight of the graft copolymer (m_p) is the sum of all lactic acid units

and grafted PEG branches (Equation 2)

$$m_p = 72x + m_g \cdot y \quad \text{(Equation 2)}$$

Where 72 is the molecular weight of a lactic acid monomer and m_g the molecular weight of a grafted PEG moiety.

Extracting *x* from Equation 1 yields: $x = \frac{1-p}{p} y$ (Equation 3)

Substituting x in (Equation 2) and expressing for y yields:

$$y = \frac{mp \cdot p}{72(1-p)+p \cdot m_g} \quad \text{(Equation 4)}$$

$$y = \frac{m_p}{72\left(\frac{1-p}{p}\right) + m_g}$$

Where *p* is obtained by ^{1}H-NMR, m_p is measured by GPC (J-M. Rabanel1, 2012) and m_g is approximated to the M_n of a PEG chain considering that the grafting connecting group (AGE) has a minor impact on M_n of PEG.

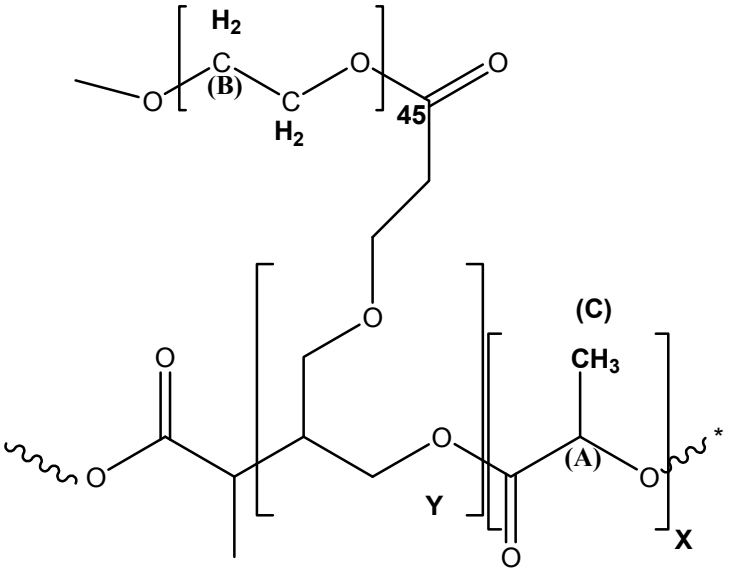

Figure 3.1 Structure of PLA-*g*-PEG polymer

3.3.3.4. Fourier transform infrared spectroscopy

Fourier transform infrared (FTIR) spectroscopy was used to characterise the functional groups of PLA and PEG from PLA-*g*-PEG polymers and NPs. The spectra of PLA-*g*-PEG polymers with four different compositions, of PEG and of PLA were recorded using a Nicolet spectrometer (Nicolet iS10, Madison, WI). All spectra were recorded at ambient temperature at a resolution of 2 cm^{-1} and 64 scans per measurement to obtain an adequate signal-to-noise ratio. The IR spectra were recorded in transmission mode from dry powders of the polymers, which were spread on a sample holder stage and scanned from 4000 cm^{-1} to 400 cm^{-1}.

3.3.3.5. Differential scanning calorimetry (DSC)

Thermal characterisation was carried out using a TA Universal Analysis Q20 instrument (TA instruments, DE, USA). Polymers, NPs, physical mixtures of Famotidine and blank NPs as well as two polymorphs of Famotidine were characterised. Physical mixtures were prepared by triturating Famotidine and blank NPs at a similar weight ratio as for Famotidine-loaded NPs. Samples of approximately 5 mg were sealed in flat bottom aluminium pans with lids. Samples

were analysed in triplicate from -35 to 200 °C at a heating rate of 10 °C/min under nitrogen flow (50 mL/min). Indium was used as the calibration standard.

3.3.4. NP preparation

3.3.4.1. Emulsion-solvent evaporation

NPs were prepared by an (oil/water) emulsion-solvent evaporation method. Famotidine (110 mg) and the polymer (1090 mg) were dissolved in 12 mL of a 1:1 mixture of dichloromethane (DCM) and dimethylformamide (DMF) and emulsified in 100 mL of a 0.5% (w/v) polyvinyl alcohol (PVA) solution using a high-pressure homogeniser Emulsiflex C30 (Avestin, ON, Canada) at a pressure of 10,000 psi for 3 min. DCM and DMF were then evaporated under reduced pressure with constant stirring for 3 h. NP suspensions were centrifuged at 18,500 g (Sorval Evolution RC, USA) for 1 h, the NPs collected and reprocessed four times. The NPs were then lyophilised (Lyph-Lock 4.5, Labconco, USA) to obtain dry NPs and stored at -20 °C until further use. Blank NPs were prepared in a similar manner.

3.3.4.2. Nanoprecipitation

The nanoprecipitation technique was used to prepare PLA-*g*-PEG and PLA blank NPs. The resulting NPs are PVA-free and were prepared for size and zeta potential comparison purposes. An organic phase was prepared by dissolving 200 mg of polymer in 10 mL of acetone. The polymeric solution was added dropwise to 20 mL of milliQ water with magnetic stirring at room temperature. The dispersing phase, water, was chosen as a liquid in which the polymer is insoluble (the non-solvent, NS). The freshly formed NPs were stirred overnight in order to let the solvent diffuse out of the NPs. The NPs were then lyophilised to obtain dry NPs and stored at -20 °C until further use.

3.3.5. NPs characterisation

3.3.5.1. Particle size

Freeze-dried NPs were resuspended in Milli-Q water (0.01% w/v) and sonicated for 3 min prior to measurement so as to break aggregates. The size and size distribution of blank, Famotidine-loaded as well as PLA NPs were measured by dynamic light scattering (DLS) using a ZetaSizer Nanoseries ZS instrument (Malvern instrument, Worcester, UK). Mean particle diameter was calculated by differential size distribution processor (SDP) intensity analysis. Three measurements consisting each of three runs particle size analysis were performed at 25 °C.

3.3.5.2. Surface charge (zeta potential)

Surface charge of blank and Famotidine-loaded NPs was measured in triplicate using a Zeta Sizer Nanoseries ZS instrument (Malvern instrument, Worcester, UK). NPs were suspended in 10 mM aqueous sodium chloride and measurements were carried out at 25 °C. The mean value and standard deviation were calculated from the triplicates.

3.3.5.3. Determination of residual PVA

The amount of residual PVA was determined using a colorimetric method based on the formation of a complex between two adjacent hydroxyl groups of PVA and an iodine molecule (Sahoo, et al., 2002). Briefly, 2 mg of lyophilised NPs were treated with 2 mL of 0.5 M NaOH for 15 min at 60 °C. Each sample was neutralised with 900 μL of 1 N HCl and the volume was adjusted to 5 mL with distilled water. To each sample, 3 mL of a 0.65 M solution of boric acid, 0.5 mL of a solution of I_2/KI (0.05 M/0.15 M) and 1.5 mL of distilled water were added. The samples were incubated for 15 min at room temperature and absorbance was measured at 690 nm using a Biochrom Ltd spectrophotometer (Cambridge, UK). The amount of PVA was calculated using calibration curve of PVA prepared under the same conditions.

3.3.5.4. Particle morphology

Size, shape and surface morphology of NPs were studied using a Nanoscope IIIa Dimension 3100 atomic force microscope (Digital Instruments, CA, USA). NP suspensions in Milli-Q water (0.01% w/v) were deposited on freshly cleaved mica, air dried and analysed. Images were obtained in tapping mode using an etched silicon probe (TESP7) with tip radius of 5 to 10 nm, spring constant of 20-100 N/m and resonance frequency of 200-500 kHz. Cantilever length was 125 μm. A set-point ratio (-i.e., ratio of oscillation amplitude after engagement to oscillation amplitude in free air) between 0.5 and 0.7 (moderate tapping mode) was used for all topographic and phase images unless otherwise stated.

3.3.5.5. Encapsulation efficiency and drug loading

Encapsulation efficiency of Famotidine in NPs was determined by high-performance liquid chromatogrphy (HPLC). Briefly, 10 mL of 1N aqueous NaOH was added to 10 mg of NPs and stirred for 30 min. The samples were analysed using a Shimadzu HPLC system (Kyoto, Japan) with SPD-20A UV/vis detector and a Hyperclone 5 μm packing 130 Å pore size BDS C18 column (Phenomenex, CA, USA). A mixture of phosphate buffered solution at pH 6.0 and methanol (10/90 v/v) was used as the mobile phase at a flow rate of 1 mL/min. Famotidine was detected at 267 nm at a retention time of 7.5 min. Analyses were performed in triplicate. Encapsulation

efficiency (EE) was calculated as the percentage of drug entrapped in NPs compared to the initial amount of drug added to the solvent during NP preparation using Equation 5:

Equation 5

$$EE\% = \frac{\text{Amount of drug entrapped in NPs}}{\text{Initial amount of drug added}} \text{x}100$$

Drug loading (DL) of NPs was calculated as the percentage of drug entrapped in NPs compared to the total weight of NPs using Equation 6:

Equation 6

$$DL\% = \frac{Amount\ of\ drug\ entrapped\ in\ NPs}{Total\ amount\ of\ NPs}\ X\ 100$$

3.3.5.6. X-Ray powder diffraction (XRPD)

The crystal structure of the NPs was studied by XRPD using a Bruker X-ray diffractometer model D2 phaser (Karlsrushe, Germany) with a CuKα radiation source (ɦλ=1.59 A°) operating at 30 kV and 10 mA and with a LynxEye detector with 2.49239° angular opening. The opening slit, scatter plate and detector windows were 0.6 mm, 1.0 mm and 3 mm, respectively. The measurements were made over a range from 4 to 40° 2θ with increments of 0.02° at a scanning speed of 3.4º per min. The samples were analysed using a low volume sample holder. Famotidine forms (A and

B), Famotidine-loaded NPs and physical mixtures of Famotidine and blank NPs were analysed.

3.3.5.7. Drug release

The dialysis diffusion technique was used to evaluate *in vitro* Famotidine release from different NPs formulations. Briefly, known amounts of NPs were suspended in 3 mL of buffered saline medium at pH 7.4 and placed into cellulose ester dialysis bags (6-8 kDa cut-off, Spectra-Por 1 membrane, Spectrum laboratories, USA). The dialysis bags were placed in 50-mL screw cap tubes containing 10 mL of phosphate buffered saline (PBS) medium at pH 7.4 (external volume) and incubated at 37 °C with shaking at 150 rpm using a horizontal water bath shaker (Orbit Shaker Bath, Labline, USA). The medium (10 mL) was sampled at predetermined time intervals to quantify Famotidine and replaced with 10 mL of fresh buffered saline medium. The HPLC method described earlier (see encapsulation efficiency and drug loading section) was used to quantify Famotidine released from the NPs.

3.3.5.8. Cytotoxicity

Caco-2 cells were seeded in 96well microplates (100 µL of a 500,000 cells/mL suspension in culture medium) and incubated at 37 °C with 5% CO_2 for 24 h. The Caco-2 cells were added to each well except for one control row containing medium only. Suspensions of pure Famotidine, Famotidine-loaded NPs and blank NPs were prepared at concentrations ranging from 0.04 to 10 mg/mL prepared under sterile environment. A fixed amount of test solutions (10 µL) was added to cells (n=4 per test solution). One row of cells was not treated and served as control. The microplate was centrifuged at 600 rpm for 30 seconds to ensure bring the liquid phase at the bottom of the wells. The medium was removed and the cells washed with 150 µL cold PBS (4°C). The cold PBS was then replaced with 100 µL of fresh medium. A colorimetric assay was used for the assessment of cell proliferation. Briefly, 10 µL of MTT solution (5 mg/mL thiazolyl blue tetrazolium in PBS pH 7.4) was added to each wells and the plate incubated for 4 h at 37 °C. An acidic isopropanol solution (40 mL of Isopropanol, 5 mL 1N HCL and 5 mL Triton X-100, 50 µL) was then added to each well. The plate was covered with aluminium foil and slowly agitated for 12 h. The microplates were read using the Magellan 4 software at a wavelength of 570 nm and reference wavelength of 690 nm. Calculation of cell viability was done according to Equation 7:

Equation 7

$$\text{Cell proliferation (\%)} = \frac{\textbf{Absorbance of medium with sample} - \textbf{Absorbance of medium without cells}}{\textbf{Absorbance of medium with cells} - \textbf{Absorbance of medium without cells}}$$

3.3.5.9. *In vitro* permeability evaluation by bidirectional Caco-2 cells monolayer

3.3.5.9.1. Culture of Caco-2 cells

The Caco-2 ATCC cell line (American Type Culture Collection, Manassas, VA, USA) was cultured in Dulbecco's modified eagle's medium (DMEM) supplemented with 10% Fetal Bovine Serum, 1% non-essential amino acids, 0.25 µg/mL Amphotericin B and 100 U/mL Penicillin/Streptomycin (Gibco, USA). The cells were grown and maintained in tissue culture flasks and incubated at 37 °C under a 5 % CO_2 and 90 % relative humidity atmosphere (Sanyo CO_2 incubator, USA).

3.3.5.9.2. Caco-2 cells monolayer

The Caco-2 cells were grown until reaching 90% confluence. Using trypsin-EDTA (Ethylene Diamine Tetra acetic Acid), the cells were detached from the culture flask and seeded at a density of 60,000 cells/cm^2 on Transwells™ (Costar, NY, USA) with polycarbonate membranes (12 mm i.d., 3.0 µm pore size). Culture medium (DMEM) was changed in both the apical and basolateral compartments on the day after seeding and every successive day (Apical volume: 0.5 mL, Basolateral volume: 1.5 mL). Caco-2 cells monolayer were used 21-28 days post-seeding. The integrity of the cell monolayer during the growth phase was monitored by taking trans epithelial

electrical resistance (TEER) readings using an EVOM™ epithelial tissue volt-ohm-meter with an Endohm-12 electrode (Millipore Corp. USA). The resistance of the monolayer was determined by subtracting the total resistance (membrane support and cell monolayer) from the membrane support resistance. Cells monolayers with TEER values greater than 300 W/cm^2 were used in transport experiments.

3.3.5.9.3. Transport experiments

Cells monolayers were pre-incubated for 30 min at 37 ºC in Hank's balanced salt solution (HBSS). Basolateral-to-apical and apical-to-basolateral transport experiments were performed by respectively adding 1.5 and 0.4 mL of solutions containing 80 μg/mL Famotidine. Transport studies were carried out for five test groups, namely pure Famotidine, Famotidine-loaded PLA-*g*-PEG NPs (four formulations were tested), physical mixtures of Famotidine and blank NPs, physical mixtures of Famotidine and PEG (two molecular weights were tested, PEG750Da and PEG2000Da) and Famotidine-loaded PLA NPs. Transport studies were carried out in triplicate for each formulation. The HPLC method described in the section entitled "encapsulation efficiency and drug loading" was used to quantify Famotidine in the basolateral and apical compartments over 4 h. From the results, the apparent permeability coefficients in both directions as well as the asymmetry index of the transport were calculated. The apparent permeability coefficient is determined from

the amount of Famotidine diffused with time. P_{app} is calculated according to Equation (8):

Equation 8

$$P_{app}\ (cm\ s^{-1}) = (dQ/dt)\ (1/(AC_0))$$

Where *dQ/dt* is the rate of permeation in centimetre per second, C_0 is the initial concentration of Famotidine in the donor cell (either the basal or apical compartment) and *A* is the area of the monolayer. The asymmetry index allows identifying potential P-gp substrates. This efflux ratio was obtained by dividing P_{app} value in the basolateral-to-apical direction by the corresponding value in the apical-to-basolateral direction. A ratio greater than 1.0 indicates the predominance of secretory transport and suggests the presence of an efflux transporter such as P-gp.

3.3.6. Data analysis

All experiments were conducted at least in triplicate (n=3) and results were expressed as mean ± standard deviation unless otherwise noted. Statistical significance was evaluated by one-way analysis of variance (ANOVA) using SigmaStat software version 3.1. The effect of PEG on the P-gp efflux of Famotidine compared to pure Famotidine was evaluated from the transport study data using ANOVA followed by the Holm-Sidak test. The statistical significance was set as $p < 0.05$, with a confidence level of 95%.

3.4. Results and discussion

3.4.1. Polymer synthesis and characterisation

3.4.1.1. NMR

A typical ^{1}H NMR spectrum was obtained for the PLA homopolymer, with a characteristic peak at 5.2 ppm corresponding to the tertiary PLA proton (m, –CH) and another peak at 1.5 ppm corresponding to the pendant methyl group of the PLA chain (m, $–CH_3$). Moreover, the integration ratio of both peaks was 3:1, which is also characteristic of the PLA homopolymer (Nadeau, et al., 2005, Shilpa, et al., 2005). Likewise, typical spectra were obtained the for PLA-*g*-PEG polymers with a peak at 5.2 ppm for the tertiary PLA proton (m, –CH), a peak at 3.6 ppm for the protons of the repeating units of the PEG chain (m, $OCH_2–CH_2O$), a minor peak at 4.3 ppm for the protons connecting the PEG graft to the PLA backbone (m, $CH_2–OCO$) and a peak at 1.5 ppm for the pendant methyl group of the PLA chain (m, $–CH_3$).

3.4.1.2. GPC

PLA-*g*-PEG graft polymers were synthesised by ring-opening polymerisation. Gel permeation chromatography was used to measure the Mw and Mn of the graft polymers. In this study, two types of PEG (750 and 2000 Da) were grafted at two PEG vs. lactic acid ratios (1 and 5%) in order to evaluate the impact of PEG on the P-gp efflux. PEG molecular weight of 750Da or 2000Da were chosen for optimal biocompatibility. PEG with high molecular weight become too big to be eliminated. PEG with lower molecular weight than 750Da is not enough to increase the hydrophilicity of the NPs surface. Table 3.1 shows GPC results for the different PLA-*g*-PEG polymer compositions as well as for the PLA polymer used in this study. The Mw of the grafted PLA-*g*-PEG polymers varies from 6000 to 21 137 Da while Mn is from 3100 to 17 330 Da. PLA-1%PEG750 is the shortest polymer while PLA-g-5%PEG2000 is the largest, in agreement with the PEG molecular weights and grafting ratios used. Polydispersity index (PDI) values were calculated by dividing Mw by Mn. PDI was higher for graft polymers with 1% PEG compared to polymers with 5% PEG. PLA-*g*-5%PEG2000 had the smallest PDI value at 1.22 while PLA-g-1%PEG750 had the highest at 1.93. The presence of unreacted mPEG or PLA species may explain the large PDI in case of PLA-*g*-1%PEG750.

3.4.1.3. Grafting efficiency

Grafting efficiency of PEG to PLA backbone was calculated by comparing the intensity ratio of the ^{1}H-NMR PEG peak at 4.3 ppm to that of the PLA peak at 5.16 ppm (% mol PEG to mol of lactic acid monomer). Comparison of the expected grafting

percentage of PEG to the actual grafting percentage (Table 3.1) shows that PEG2000 grafting was complete at both percentages while PEG750 grafting was incomplete (0.4% and 1% instead of the theoretical 1% and 5.7% values, respectively). It is remarkable that PEG 750 Da grafting was lower than theoretical one, whereas PEG Da 2000 grafting higher than the expected. The best results obtained of PEG 2000 Da compare to PEG 750 Da, it may be explained by the reactivity of different PEG (2000Da and 750 Da) with pendant carboxylic compare to ended carboxylic group. Mechanistic study could demonstrate the following hypothesis, PEG750Da reacts with lactic carboxylic group at the end of polymer backbone while PEG 2000 Da reacts more with pendant group. Based on the results, the actual grafting of PLA-*g*-5%PEG750 is close to 1% and the polymer will therefore be compared to PLA-*g*-1%PEG2000 in studies examining the effect of the PEG molecular weight on properties of the NPs. Moreover, Table 3.1 also indicates the PEG content of the graft polymers on a weight basis. Generally, the PLA-*g*-PEG2000 polymers had higher PEG content than the PLA-*g*-PEG750. For instance, PLA-*g*-5%PEG2000 contains 66% w/w PEG per polymer chains compared to 8.6% for PLA-g-5%PEG750 (J-M. Rabanel1, 2012).

Polymer Composition	Mw (Da)	Mn (Da)	PDI	Actual grafting (%)	PEG per polymer chain (%)	PEG melting point (°C)	PLA Glass transition temperature (°C)
PLA	46 400	32 040	1.44	N/D	N/D	N/D	50.24 ± 0.73
PLA-g-1%PEG750Da	6000	3100	1.93	0.4	4.4	N/D	--
PLA-g-1%PEG2000Da	17 697	11 340	1.56	1.1	24.1	50.68 ± 0.13	*
PLA-g-5%PEG750Da	16 621	12 905	1.29	0.9	8.6	N/D	29.68 ± 1.87
PLA-g-5%PEG2000Da	21 137	17 330	1.22	5.7	66.2	53.42 ± 0.39	*

* Tg and PEG melting point at same temperature, -- Tg not detected , N/D Not detected , n=(3)

Table 3.1 Molecular weight, PDI, grafting percentage and thermal properties (n=3) of polymers evaluated during this study.

3.4.1.4. Fourier transform infrared FTIR

FTIR scans were done for pure PLA, pure PEG and the four graft polymers. The FTIR scan of pure PLA (Figure3. 2) exhibits characteristic absorption bands corresponding to asymmetric and symmetric stretching of C-H at 2998 and 2944 cm^{-1} and of CH_3 at 1451 cm^{-1}, respectively. The PLA C-O stretching bands from -CH-O- and -O-C=O also appeared at 1182 cm^{-1}, 1083 cm^{-1} and 1747 cm^{-1} (Choi, et al., 2013, Elmowafy, et al., 2008). The FTIR scan of pure PEG 2000 (Figure 3.2) showed an absorption band at 2883 cm^{-1} which is attributed to the aliphatic C-H stretching band of PEG (Choi, et al., 2013, Elmowafy, et al., 2008). The characteristic and major stretch bands of PLA and PEG at 1747 cm^{-1} and at 2880 cm^{-1}, respectively, were used as reference when comparing to the spectra of PLA-*g*-PEG polymers. FTIR scans of the four synthesised

polymers (Figure3. 2) showed that both characteristic PLA and PEG peaks were detected. Moreover, Figure 3. 2 presents an absorption band at 3300 cm^{-1} in case of PLA-g-5%PEG, which is attributed to the O-H stretching band of PEG. The FTIR results confirmed the presence of both PEG and PLA in the graft polymers, which is in agreement with the ^{1}H NMR results.

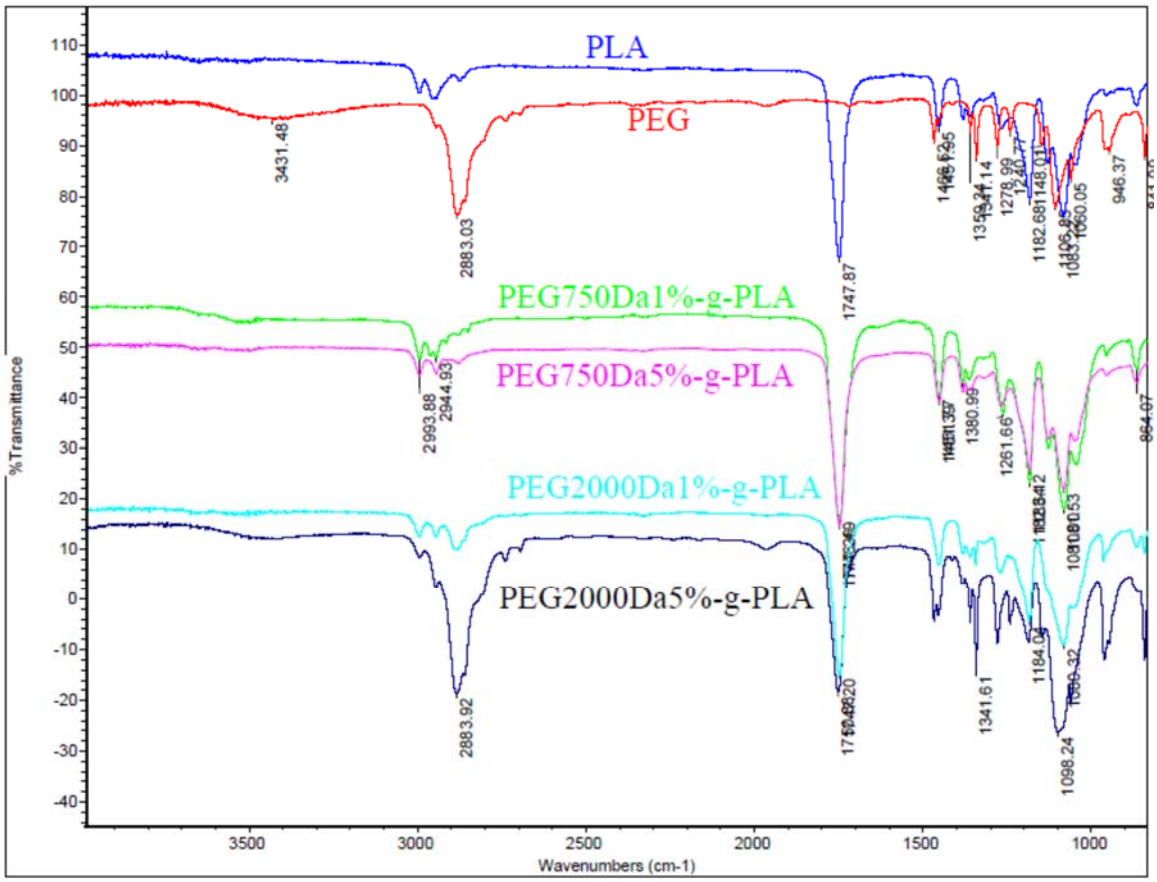

Figure 3.2 FTIR Spectra of PLA, PEG and different PLA-*g*-PEG polymers

3.4.1.5. DSC

In case of PLA-*g*-5%PEG750, the PLA glass transition temperature (Tg) can be detected at 29.68°C while for PLA-*g*-1%PEG750 no Tg was detected (Table 1). For both PLA-*g*-PEG2000 polymers, the PLA Tg could not be measured due to the interference with PEG melting. The reported melting point of PEG 2000 at 52°C (Rowe, et al., 2009) was used to characterise the PLA-*g*-PEG2000 polymers. Table 3.1 shows presence of the PEG peak at 50.68°C for PLA-*g*-1%PEG2000 and at 53.42°C for PLA-*g*-5%PEG2000. Unassigned transitions at -1.77°C and -0.09°C were observed for the first and second heating runs of PLA-*g*-1%PEG750 and PLA-*g*-1%PEG2000, respectively. Since the signals are not attributable to the Tg of PLA or PEG, they might be due to dimer of end PLA grafted PEG yield synthesis.

3.4.2. NPs characterisation

3.4.2.1. Particle size

Famotidine-loaded and blank NPs were prepared from four PLA-*g*-PEG polymers by the emulsion solvent evaporation method. For comparison purposes, Famotidine-loaded and blank NPs were also prepared from PLA polymer. The mean size of NPs can be influenced by parameters such as surfactant concentration (PVA in this case), polymer molecular weight and homogenisation pressure (Lamprecht, et al., 2000,

Sahoo, et al., 2002). DLS, also called photon correlation spectroscopy PCS, is a rapid and accurate method often used to determine the mean size, the size distribution and the polydispersity index (PI) of NPs (Gaumet, et al., 2008). The diameter obtained by DLS is a value that pertains to how particles diffuse within a fluid and corresponds to a hydrodynamic diameter. The diameter obtained by this technique is the diameter of a sphere having the same translational diffusion coefficient as the measured particle Particle size and size distribution obtained by DLS for different NP formulations are shown in Table 3.2. Drug-loaded PLA-*g*-1%PEG750 NPs were the smallest with a mean particle size of 156 nm, followed by PLA-g-1%PEG2000 NPs at 180 nm. PLA-*g*-5%PEG750 NPs had a mean particle size of 192 nm while PLA-g-5%PEG2000 were the largest with a mean size of 211 nm. Even though drug-loaded NPs were prepared under similar conditions, a significant difference in particle size (p=0.004) was observed among the different formulations. The differences in size may be due to the varying PEG grafting densities and molecular weights of the polymers used to prepare the NPs. Indeed, NPs prepared from PLA-*g*-5%PEG2000 had the largest diameter, which might be a consequence of the highest PEG grafting density affecting the surface of the NPs surface, the higher molecular weight, and an increased polymeric solution viscosity, as previously reported (Gorner, et al., 1999, Lamprecht, et al., 2000). Table 3.2 shows that the particle size of blank NPs prepared from PLA-g-5%PEG were significantly smaller ($p\leq$0.001) than their drug-loaded counterparts, probably due to volume occupied by the drug (Lamprecht, et al., 2000). NPs presented a unimodal and homogeneous size distribution with relatively low PI values ranging from 0.026 to 0.139 (Table 3.2) (Patravale, et al., 2004). NPs prepared

from PLA-*g*-1%PEG750 were the most polydisperse due to the fact that the PLA-*g*-1%PEG750 polymer had lowest molecular weight, lowest grafting efficiency and itself had the largest polymer PDI. Furthermore, the presence of NPs consisting of ungrafted and grafted polymers might have also contributed to dispersity. Drug-loaded NPs prepared from PLA had a mean particle size of 166 nm and PI of 0.135. The difference in polymer composition between PLA and the graft polymers (PLA-*g*-PEG) brought about differences in the resulting NPs.

Composition		Average Particle size (nm) ±SD	PI ±SD	D L (%)	Tg (°C)	Famotidine melting point (°C)
Blank NPs	PEG750Da1%-g-PLA	154 ± 1.21			41.80 ± 0.37	
Loaded NPs		156 ± 2.75	0.139 ± 0.02	2.8 ± 0.08	47.00 ± 0.00	186.32 ± 0.45
Blank NPs	PEG2000Da1%-g-PLA	174 ± 0.66			40.70 ± 2.90	
Loaded NPs		180 ± 6.09	0.095 ±0.01	0.8 ± 0.06	45.00 ± 0.13	190.11 ± 0.24
Blank NPs	PEG750Da5%-g-PLA	149 ± 2.26			41.93 ± 0.12	
Loaded NPs		192 ± 0.58	0.026 ±0.09	2.2 ± 0.03	43.00 ± 0.61	183.67 ± 5.06
Blank NPs	PEG2000Da5%-g-PLA	161 ± 1.6			47.30 ± 0.60	
Loaded NPs		211 ± 2.44	0.056 ± 0.02	1.5 ± 0.04	48.02 ± 2.00	184.73 ± 6.99
Blank NPs	PLA	140 ± 1.2				
Loaded NPs	PLA	166 ± 0.5		0.5 ± 0.01	50.00±0.13	185.19 ± 0.17
SD=Standard Deviation, PI=Polydispersity, DL= Drug Loading, Tg = Glass transition temperature						

Table 3.2 Particle size, PI, drug loading, and thermal properties Famotidine and different NPs (n=3)

3.4.2.2. Surface charge

The surface charge is an important indicator of NPs' stability and predictor of *in vivo* fate (Mittal, et al., 2007). A method widely used to measure surface charge is zeta potential (Soppimath, et al., 2001). The zeta potential of NPs can take positive or negative values depending on the composition of NPs. Both PVA used as surfactant and the PEG grafts of the PLA-*g*-PEG polymers could have an impact on the zeta potential of the present NPs. PVA was used during NP preparation to prevent coalescence of emulsion droplets. In order to examine the distinct contributions of PVA and PEG to zeta potential, PLA-*g*-PEG and PLA NPs were prepared from two methods (either emulsion evaporation in presence of PVA or nanoprecipitation in absence of PVA) and studied. Drug-loaded NPs prepared by emulsion solvent evaporation method were also studied. Drug-loaded NPs could not be prepared by nanoprecipitation because Famotidine was insoluble in the solvent used to prepare the NPs (acetone). As shown in Table 3.3, PLA-*g*-PEG NPs prepared by nanoprecipitation (without PVA) had zeta potential values ranging from -24.4 to -46.7 mV compared to -45.2 mV for PLA NPs, consistent with results from others (Gref, et al., 1999, Tobio, et al., 1998). The presence PEG at the surface of the NPs significantly brought the zeta potential of the NPs prepared from PLA-*g*-PEG polymers closer to neutrality compared to NPs. The effect is attributed to PEG shifting the shear plane away from the NP surface. Similar observations were previously reported (Hawley, et al., 1997). The results in Table 3 show that the highest zeta potential value was obtained for the PLA-*g*-5%PEG2000 NPs (highest PEG content) while the lowest value was obtained for PLA-*g*-1%PEG750 (lowest PEG content), further suggesting a correlation between zeta potential and PEG-to-PLA ratio. The zeta potential results obtained for drug-

loaded and blank NPs prepared by the emulsion evaporation method in presence of 0.5% PVA are reported in Table 3. The zeta potential values ranged from -4.6 to -9.9 mV for the drug-loaded NPs and were between -4.2 to -6.3 mV for the corresponding blank NPs, in agreement with the results reported for similar polymers (Sant, et al., 2008). The drug-loaded PLA-*g*-1%PEG750 NPs had a low PVA residual content (8.4% w/w) and presented the lowest zeta potential value at -9.9mV while the drug-loaded PLA-*g*-5%PEG750 NPs had the highest PVA residual content (15.3% w/w) and presented the highest zeta potential value at -4.6 mV, suggesting a correlation between zeta potential PVA association to NPs (Vila, et al., 2004, Yoncheva, et al., 2005). In case of the blank NPs, no clear relationship between residual PVA content and zeta potential value could be seen. The presence of residual PVA at the surface of PLA NPs prepared by emulsion evaporation brought the zeta potential of the NPs closer to neutrality (-5.4 mV) compared to PLA NPs prepared by nanoprecipitation in absence of PVA (-45.2 mV). Overall, the zeta potential results obtained for NPs prepared by the two methods indicate an important contribution of PVA to zeta potential.

Composition		PVA (w/w %)	Zeta potential (mV)	
			emulsion solvent evaporation method	Nanoprecipitation method
		Average ± SD	Average ± SD	Average ± SD
Blank NPs	PLA-g-1%PEG750Da	10.13 ± 0.33	-6.3 ± 0.5	-46.7 ± 0.8
Loaded NPs		8.4 ± 0.13	-9.9 ± 1.4	
Blank NPs	PLA-g-1%PEG2000Da	9.05 ± 0.47	-4.2 ± 0.0	-30 ± 1.0
Loaded NPs		12.3 ± 1.13	-4.8 ± 0.2	
Blank NPs	PLA-g-5%PEG750Da	11.18 ± 1.39	-5.1 ± 0.2	-30.2 ± 1.4
Loaded NPs		15.3 ± 2.23	-4.6 ± 0.4	
Blank NPs	PLA-g-5%PEG2000Da	15.51 ± 2.89	-4.5 ± 0.2	-24.5 ± 0.2
Loaded NPs		14.6 ± 1.34	-7.7 ± 1.0	
Blank NPs	PLA	10.01 ± 0.92	-5.4 ± 0.1	-45.3 ± 0.8
Loaded NPs	PLA	9.07 ± 1.83	-15.2 ± 1.1	

Table 3.3 Residual PVA content of NPs prepared by emulsion evaporation as well as zeta potential of blank and drug-loaded NPs prepared by emulsion evaporation or nanoprecipitation Methods (n=3)

3.4.2.3. Residual PVA determination

PVA was used as emulsifier during NP preparation as it forms an interconnected network on the PLA polymer surface capable of stabilizing the emulsion. However, PVA remains associated with the NPs despite repeated washings (Sahoo, et al., 2002), thus potentially affecting properties such as particle size, zeta potential, release

kinetics, etc. (Sahoo, et al., 2002). As reported in Table 3.3, 8.4 to 15.3% w/w residual PVA remained at the surface of all drug-loaded formulations, despite four washings. It has been reported that the solvents used during NP preparation influence the quantity of PVA adsorbed at the polymer-organic solvent/water interface. The amount of residual PVA associated to NPs increases with increased miscibility between the organic solvent and water since partitioning of PVA into the polymeric phase is then favoured (Sahoo, et al., 2002). Such phenomenon could explain the relatively higher residual PVA content associated to our NPs compared to other NPs previously prepared in our lab using DCM only (Shilpa, et al., 2005). DMF is more miscible in water than DCM and could indeed bring higher amounts of residual PVA to associate with NPs (Sahoo, et al., 2002).

3.4.2.4. Particle morphology

The NPs were studied by Atomic Force Microscope (AFM). Tapping mode AFM is a versatile technique to study sample surface at the nanoscale (phase image) as well as topography (height image) of soft materials such as polymers. The AFM images revealed that the NPs were spherical in shape and agglomerated. AFM also served as a second method to confirm the NP sizes obtained by DLS. The height image reproduced in Figure 3.3 shows a representative population of NPs with spherical shape and sizes ranging from 120 nm to 130 nm at the resolution of 5 nm to 10 nm.

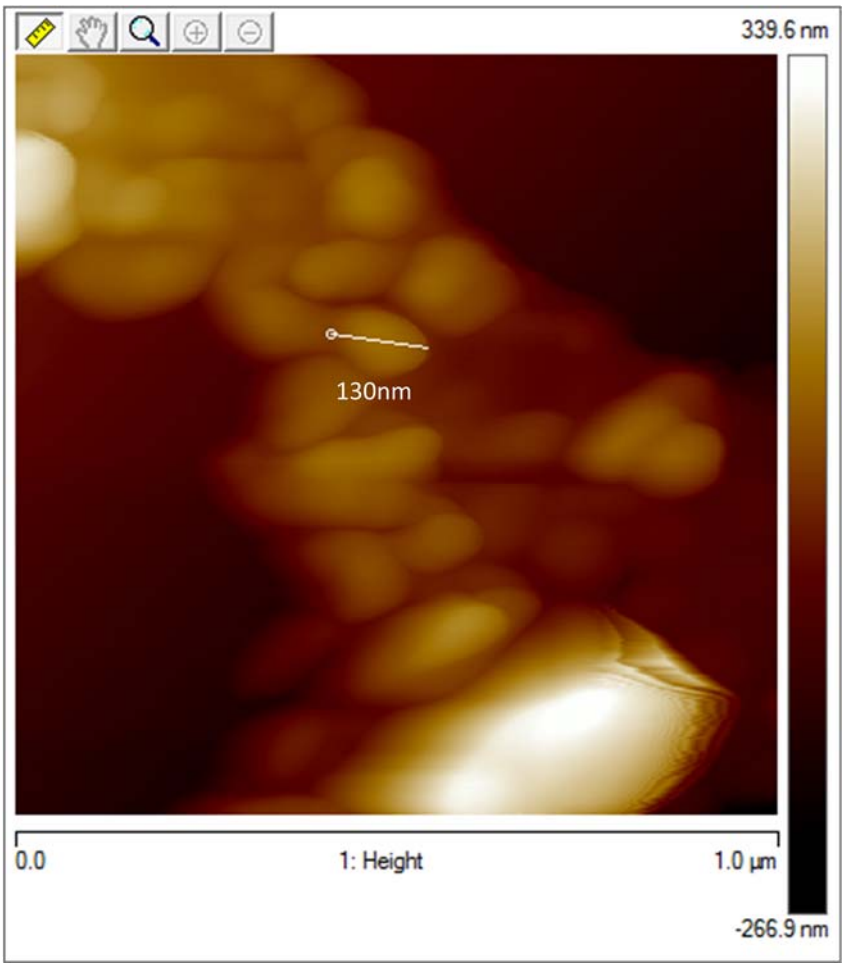

Figure 3.3 Tapping mode AFM image (topography) of NPs (PLA-g-5%PEG2000Da), scan size 1µmx1µm

3.4.2.5. Encapsulation efficiency and drug loading

Encapsulation efficiency and drug loading of Famotidine varied for the four NP batches produced and were fairly low at 7 to 22% and 0.8 to 2.8%, respectively (Table 3.2). Encapsulation efficiency was found to be in the following order for the four polymers: PLA-g-1%PEG750 > PLA-g-5%PEG750 > PLA-*g*-5%PEG2000 > PLA-g-1%PEG2000. In general, NPs prepared with PEG2000 had a lower drug loading

compared to NPs prepared from PEG750 ($p \leq 0.001$). Many factors can influence encapsulation efficiency and drug loading such as the nature of drug to be encapsulated and the size of the particles. Famotidine is rather hydrophilic and may have rapidly partitioned into the external aqueous phase during NP preparation, thereby decreasing its entrapment into the NPs during polymer deposition (Govender, et al., 1999). Encapsulation efficiencies of NPs prepared using an o/w method have previously been shown to depend on the partition of the drug between the internal and external phases as well as on the nature of the entrapping material (Mittal, et al., 2007, Redhead, et al., 2001). In addition, drug loading may be influenced by the size of the NPs, as NPs have a high surface area compared to their volume. Because of the small volume of NPs, a high proportion of drug molecules will be incorporated near or at the surface of NPs and readily released during NPs preparation and washing steps (Mittal, et al., 2007, Redhead, et al., 2001). Furthermore, it has been suggested that the PEG chains of graft polymers such as PLA-g-PEG are located toward the NPs' surface, which also might not favour high Famotidine loading (J-M. Rabanel1, 2012).

3.4.2.6. FTIR

Several characteristic absorption bands of Famotidine form B (3504, 3398, 1530, 1275 and 1142 cm^{-1}) were previously observed in NPs by FTIR spectroscopy(Elmowafy, et al., 2008, Lin, et al., 2006, Ramachandran, et al., 2011). Here, the characteristic peak at 3504 cm^{-1} for the amino group of Famotidine was used as a reference to follow

Famotidine loaded in NPs. The amine (NH) band at 3504 cm^{-1} was not detected in the four Famotidine-loaded NP formulations produced.

3.4.2.7. DSC

The crystal state of Famotidine was characterised by DSC during and after NP preparation. Famotidine has two polymorphic crystal forms (A and B) with melting points at 171.43 and 164.4 °C, respectively. Form B is the metastable, kinetically-favoured form and was used as starting material for this study (Hassouna, et al., 2011)., In a control experiment, Famotidine was crystallised from a mixture of DCM and DMF and analysed by DSC. The melting peak at 163.13 °C corresponded to Famotidine form B and indicated that no change due to the DCM:DMF solvent couple used was to be expected during the process of the NPs. The DSC results obtained for the Famotidine-loaded NPs prepared from PLA-*g*-1%PEG750 and PLA-g-1%PEG2000 indicate sharp melting of Famotidine with peaks at 186.32 and 190.11 °C, respectively (Table 3.2 and Figure 3.4). Similar results were obtained for Famotidine-loaded NPs prepared from both PLA-g-5%PEG polymers as well as PLA (Table 3.2). After encapsulation a shift of melting point to higher temperature was observed in accordance to the presence of a crystalline form however no polymorphic form at this temperature has been described in the literature. A possible explanation is an interaction between the drug molecules and the polymer yielding a complex. The Tgs detected for blank NP formulations of PLA-*g*-1%PEG750, PLA-*g*-1%PEG2000 and

PLA-*g*-5%PEG750 were 41.8, 40.7 and 41.93 °C, respectively (Table 3.2). The Tg of PLA-g-5%PEG2000 NPs was higher at 48.02 °C. The DSC scans obtained for Famotidine-loaded NP formulations were comparable to those of the blank NPs, except for NPs prepared from PLA-*g*-1%PEG750. In the later case, a 6-°C Tg shift to higher temperatures ($p \leq 0.001$) was observed in presence of Famotidine. The Tg shift to higher temperature might be due to Famotidine restricting the mobility of the polymer molecules. Indeed, NPs prepared from PLA-*g*-1%PEG750 had the highest drug loading (2.8% w/w) amongst all four NP formulations.

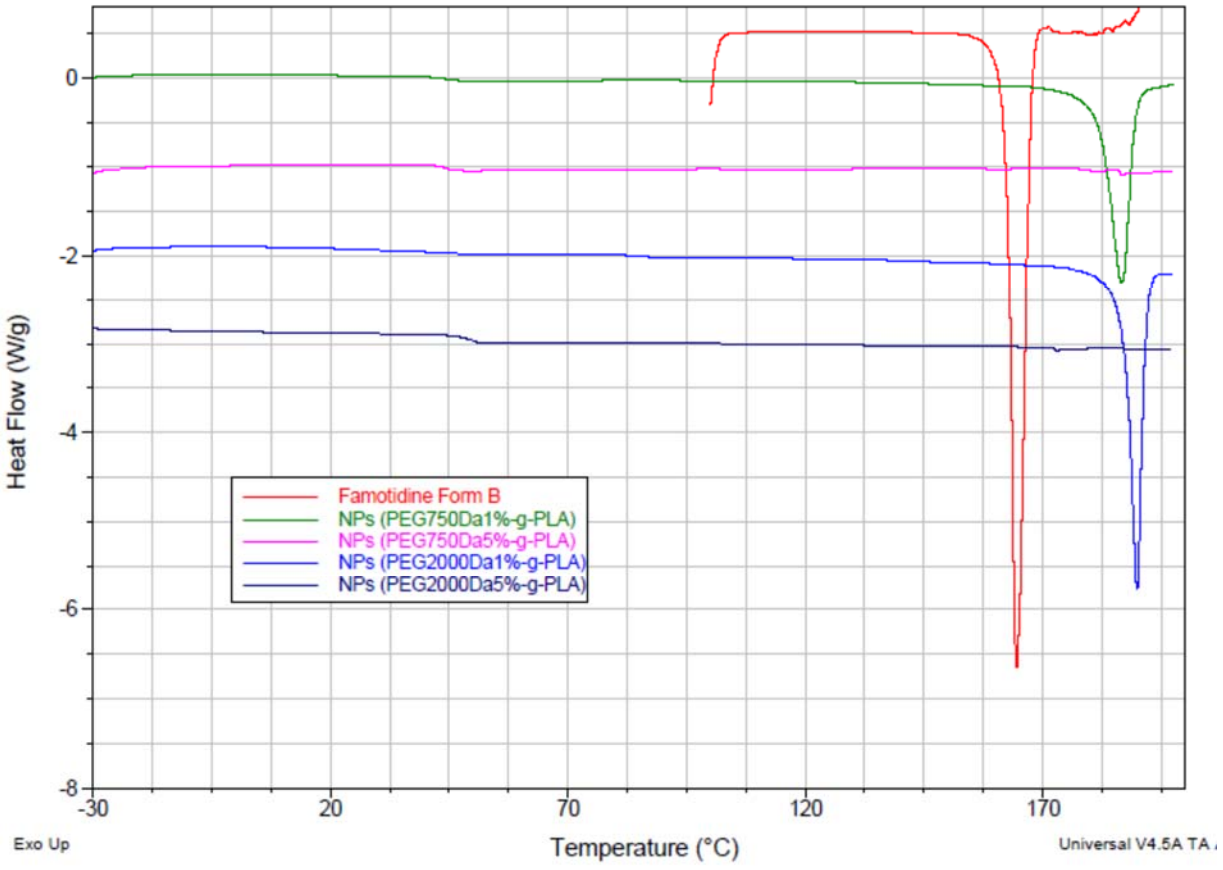

Figure 3.4 Thermogram of Famotidine and four loaded NPs formulations

3.4.2.8. XRPD

XRPD was used to identify the crystal structure of materials, notably to detect Famotidine crystal peaks after encapsulation in NPs. The starting material Famotidine form B possesses distinct major characteristic peaks at 5.96, 11.5, 15.7, 17.5, 19.5, 20.5, 22.5 and 24.5° 2Θ (Ferenczy, et al., 2000). Figure 3.5 showed the characteristic diffractogram of Famotidine crystal B. XRPD confirmed that the pure Famotidine used in this study was crystalline, since it showed sharp, distinct peaks. Famotidine crystallised from a 1:1 mixture of DCM and DMF was again used as control to evaluate the potential impact of the NP formation process on Famotidine crystallinity. Compared to the starting material, the major peaks of Famotidine crystallised from DCM and DMF were preserved, with some peak inversions at lower intensities. The XRPD scans of Famotidine-loaded NPs showed two pattern types that varied with grafting ratio more than with PEG length. In case of NPs prepared from PLA grafted at 1% PEG, a peak at 8.50° 2Θ was detected (Figure 5) instead of 5.94° for Famotidine form B. Moreover, other peaks at 11.5, 15.7, 19.5, 20.5, 22.5 and 24.5° corresponding to Famotidine (B) were detected. In case of NPs prepared from PLA grafted at 5% PEG, Famotidine exhibited two minor peaks at 21.50° and 23.50° 2Θ (Figure 5), suggesting a change in Famotidine's state from crystal to amorphous or to nanocrystal below the XRPD limit of detection (Jiang, et al., 2012, Liu, et al., 2011, Morakul, et al., , Sahoo, et al., 2011). Such absence and/or reduction of Famotidine peaks for NPs

with 5% grafting density could indicate the presence of PEG at high density at the NPs' surface(Yu, 2001).

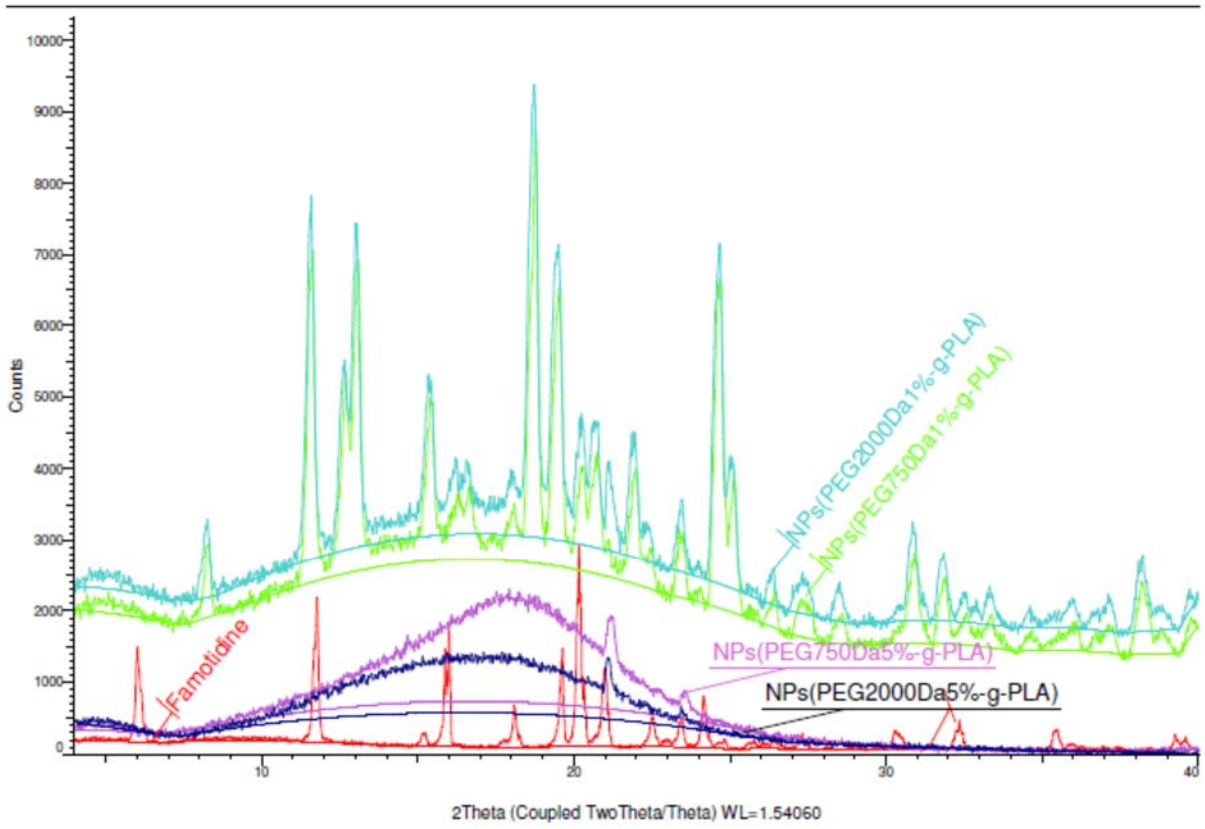

Figure 3.5 X- Ray diffractograms of Famotidine and four loaded NPs formulations

3.4.3. Drug release

The purpose of studying release kinetics from different NPs formulations is to observe the effect of polymer composition (PEG molecular weight, grafting density, residual PVA) and particle size on Famotidine release profiles. Figure 3.6 shows the percentage of Famotidine released *in vitro* from NPs prepared from the different PLA-*g*-PEG

polymers as well as from PLA. In all cases, nearly all Famotidine was released within four hours. The release profiles of Famotidine were comparable among all NP formulations, except for PLA-*g*-1%PEG750 NPs at the 5 min sampling time when a significantly higher release of Famotidine was observed (p=0.034). The higher initial release compared to other NP formulations may be attributed to the higher drug loading of this formulation. All release profile of Famotidine from NPs showed a biphasic release behaviour, as reported by others (Avgoustakis, et al., 2002). The first phase lasted up to 30 min and accounted for the release of 50 to 60 % of Famotidine. It was followed by a slower release phase from 30 min to 4 h.

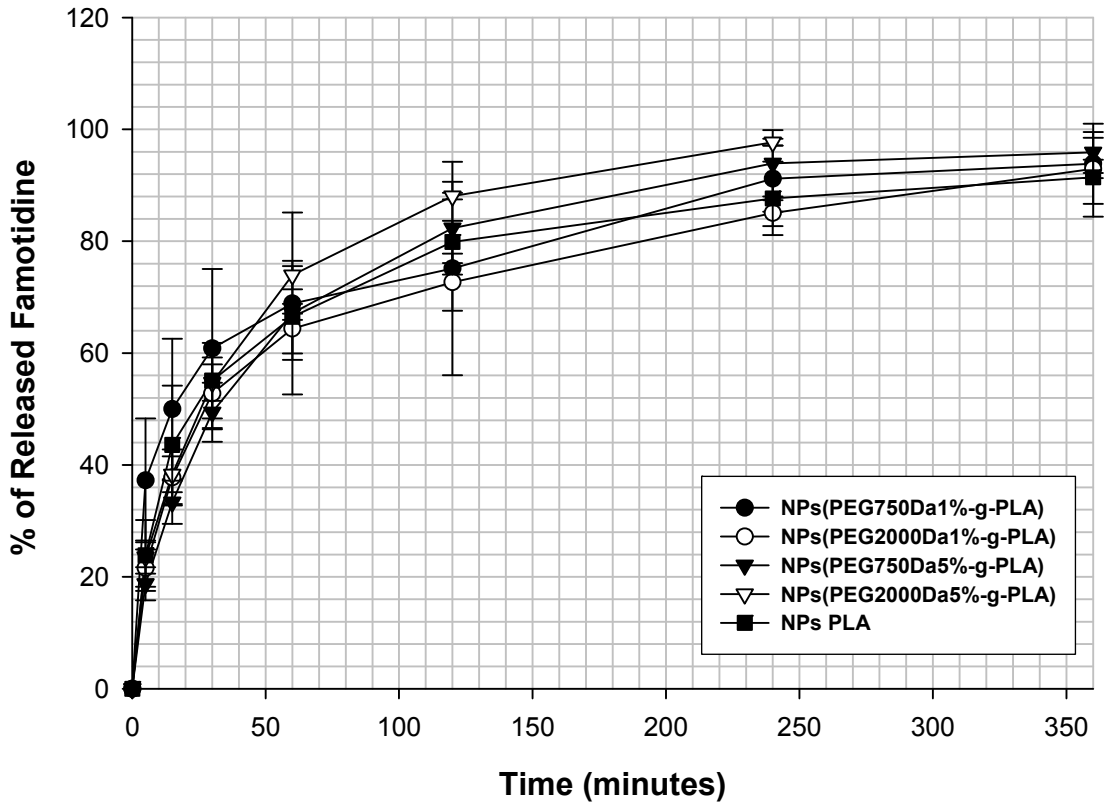

Figure 3.6 Percentage of Released Famotidine from different loaded NPs formulations (n=3)

The release of Famotidine from all NP formulations was fast, which might be due to the hydrophilic nature of Famotidine (Baseer, et al., 2013, Shoaib, et al., 2010). Famotidine release profiles showed no significant influence of graft polymer molecular weight, PEG molecular weight, PEG grafting ratios particle size and PVA.

3.4.4. Cytotoxicity

Cell growth is determined by counting viable cells after staining with a vital dye. Trypan blue staining is a simple way to evaluate cell membrane integrity (and thus infer on cell proliferation or death). PLA is a well-known biodegradable and biocompatible polymer and PEG is regarded as having a very low order of toxicity; toxicity of the graft polymers was therefore expected to be low (Rowe, et al., 2009). Results showed that, after 24 h of contact with the NPs, cell viability ranged from 100% to 60%at the concentrations tested (0.31, 0.63, 1.25, 2.5, 5 and 10 mg/mL). When in contact with pure Famotidine for 24 h, cell viability ranged from 100% to 80% at the various concentrations tested (0.04, 0.08, 0.17, 0.34, 3.5 and 7.6 mg/mL). As its concentration encapsulated in NPs, Famotidine exhibited no toxic effect during the transport studies.

3.4.5. Transport experiments

Caco-2 cells (a human adenocarcinoma cell line) were used as a well-established and reliable model to evaluate intestinal drug absorption, drug permeability and substrate activity on efflux transport proteins such as P-gp (Artursson, et al., 2012, Pranav Shah, 2006). The transport experiments were conducted to evaluate permeability of Famotidine and to examine the potential effects of polymer composition (PEG molecular weight, grafting density, residual PVA) and NP size on P-gp efflux of encapsulated Famotidine across Caco-2 cells *in vitro*. Different Famotidine-loaded NP formulations, physical mixtures (PMs) of Famotidine and blank NPs (at concentrations corresponding to drug-loaded NP formulations) as well as PMs of Famotidine with PEG 2000 Da and PEG 750 Da were tested. Pure Famotidine and drug-loaded PLA NPs (no PEG) were used as control to evaluate the effect of PEG on P-gp efflux of Famotidine. Transport experiments were performed in triplicate using Famotidine at 80 ug/mL applied either on the apical or basal side of the model. In the model, the upper surface of the cells represents the apical (mucosal) side while the lower surface represents the basolateral (serosal) side. P-gp inhibitors such as PEG act on the mucosal side and their *in vitro* effect will be seen in the upper part of the Caco-2 model. The formulations most effective at inhibiting P-gp efflux of Famotidine will decrease or inhibit the basolateral-to-apical Famotidine transport. The asymmetry index, namely the ratio of secretory (basolateral-to-apical) to absorptive (apical-to-

basolateral) transport, reflects the overall effect of P-gp. Figure 3.7 and Table3.4 show that pure Famotidine had an asymmetric index value of 1.01 which means the secretory action of P-gp (basolateral-to-apical) compensates for the absorption of Famotidine (apical-to-basal) (Rozehnal, et al., 2012). As indicated in Table 3.4, NPs of PLA-*g*-5%PEG2000 had the lowest asymmetry index (0.007), followed by NPs prepared from PLA-*g*-5%PEG750 (0.01) and PLA-g-1%PEG750 (0.58), suggesting that P-gp efflux inhibition of Famotidine can be attributed to PEG content. Asymmetry index results were related more to actually grafting, in case of PLA-g-5%PEG2000 which had 5% actually grafting compared with PLA-g-5%PEG750 which had 1% actual grafting. Indeed, as PEG content increased the inhibition effect increased, which is consistent with the general hypothesis of the study (Hugger, et al., 2003, Iqbal, et al., 2010, Kin-Kai, et al., 2002, Shen, et al., 2006).

Formulations & Combinations	AP-BL Papp (cm/s x10^{-06}) ± SD	BL-AP Papp (cm/s x10^{-06}) ± SD	AI ± SD
Pure Famotidine	10.45 ± 0.62	10.51 ± 0.9	1.01± 0.11
PLA-g-1%PEG750Da+2.8%FMT	55.34 ± 13.69	30.93 ± 2.26	0.58±0.11
PLA-g-5%PEG750Da+2.2%FMT	45.12 ± 12.9	0.67 ± 0.16	0.01±0.00
PLA-g-1%PEG2000Da+0.8%FMT	N/D	0.77 ± 0.29	***
PLA-g-5%PEG2000Da+1.5%FMT	19.10 ± 8.38	0.13 ± 0.01	0.007±0.0
PM (Blank NPs PLA-g-1%PEG750Da&FMT)	N/D	0.30 ± 0.08	***
PM (Blank NPs PLA-g-5%PEG750Da&FMT)	38.76 ± 31.7	6.23 ± 5.43	0.16±0.01
PM (Blank NPS PLA-g-1%PEG2000Da&FMT)	11.75 ± 6.79	0.3 ± 0.08	0.025±00
PM (Blank NPs PLA-g-5%PEG2000Da&FMT)	84.43 ± 6.8	22.51 ± 1.82	0.27±00
PM(PEG750Da&FMT)	53.25 ± 11.02	5.48 ± 0.1	0.11±0.02
PM(PEG2000Da&FMT)	40.02 ± 21.08	0	***

*** (AI) was not calculated, N/D: Not detected

Table 3.4 Results of bidirectional transport of different NP formulations and PMs of Famotidine across Caco-2 cell monolayer (n=3)

No results were obtained from bidirectional experiments in case of Famotidine-loaded PLA NPs. It can be noticed from the asymmetry index results that increased P-gp inhibition is obtained for formulations and mixtures containing 5 mol% PEG, resulting in good absorptive transport. This is consistent with other findings (Hugger, et al., 2002, Hugger, et al., 2003). It has been reported by some authors that NPs absorbed via transcellular transport enter cells by endocytic processes at the cell apical side and, after intracellular trafficking, exit by exocytic processes at the basolateral side (M. Rabanel, et al., 2012, Monjed, et al., 2004, Rieux, et al., 2006). Surface properties,

hydrophobicity and surface charge dictate the behaviour of NPs *in vitro* and *in vivo*. In this study, the presence of the hydrophilic polymer PEG at the surface of the NPs provides an effective way of controlling the interface between NPs and biological systems (P-gp in this case) which they are designed to interact with.

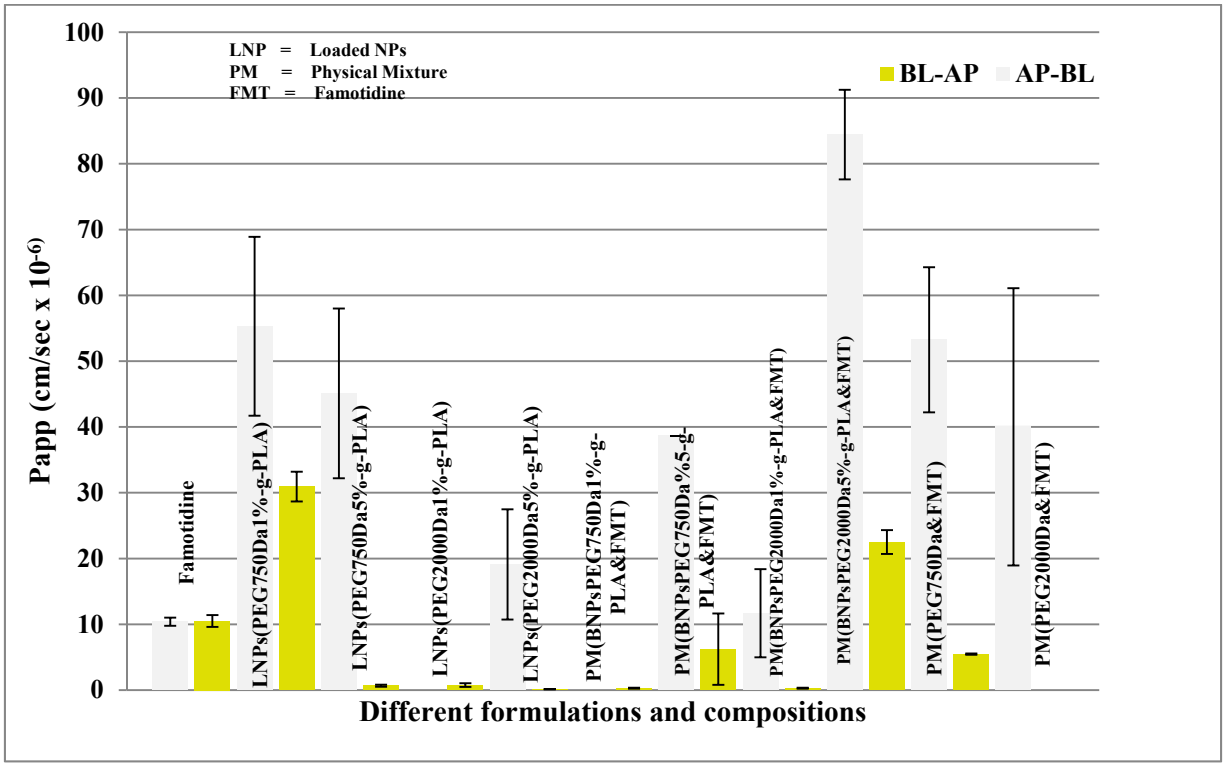

Figure 3.7 Bidirectional transport study of Famotidine across Caco-2 from different NPs formulations and (PM) combinations (n=3)

3.5. Conclusion

PLA-*g*-PEG polymers with different grafting ratios were synthesised and PEG molecular weights. The final molecular weight of the graft polymers was consistent with the PEG length and grafting ratio used. PLA-*g*-1%PEG1 polymers were more

polydisperse than PLA-*g*-5%PEG polymers, which might be due to the presence of ungrafted PEG in the former case. The grafting of PEG to PLA was confirmed by ^{1}H NMR and FTIR. The PLA Tg was detected only for PLA-g-5%PEG750while PEG melting was detected for both PLA-g-PEG2000 polymers, confirming the grafting of PEG. Together, the ^{1}H-NMR, GPC, FTIR and DSC results indicate that PLA-*g*-PEG polymers with different PEG molecular weights and grafting ratios were successively synthesised. Different NP formulations were thus prepared from those polymers. The NPs were prepared with mean particle sizes ranging between 156 and 211nm, as confirmed by DLS and AFM. The NPs had a unimodal size distribution with PI values ranging from 0.026 to 0.139. The zeta potential of the NPs ranged between -4.6 and -9.9 mV. Based on FTIR, DSC and XRPD results, Famotidine exists in crystal form when loaded in PLA-*g*-1%PEG NPs while they are in amorphous state when loaded in PLA-*g*-5%PEG NPs. Famotidine release from NPs showed a biphasic release behaviour. Similar Famotidine release kinetics were obtained for all NP formulations, except for PLA-g-1%PEG750 for which a burst was observed. Transport studies across Caco-2 membranes showed that Famotidine-loaded NPs prepared from both PLA-g-5%PEG polymers were able to inhibit the P-gp efflux of Famotidine. Therefore, NPs prepared from PLA-g-5%PEG are proposed as promising solid oral formulations to improve oral bioavailability of P-gp substrate drugs.

3.6. References

N. Akhtar, A. Ahad, R. K. Khar, M. Jaggi, M. Aqil, Z. Iqbal, F. J. Ahmad and S. Talegaonkar. The emerging role of P-glycoprotein inhibitors in drug delivery: a patent review. Expert Opinion on Therapeutic Patents, 2011;21:561-576

P. Artursson, K. Palm and K. Luthman. Caco-2 monolayers in experimental and theoretical predictions of drug transport. Advanced Drug Delivery Review, 2012;64, Supplement:280-289

D. A. I. Ashiru-Oredope, N. Patel, B. Forbes, R. Patel and A. W. Basit. The effect of polyoxyethylene polymers on the transport of ranitidine in Caco-2 cell monolayers. International Journal of Pharmaceutics, 2011;409:164-168

K. Avgoustakis, A. Beletsi, Z. Panagi, P. Klepetsanis, A. G. Karydas and D. S. Ithakissios. PLGA-mPEG nanoparticles of cisplatin: in vitro nanoparticle degradation, in vitro drug release and in vivo drug residence in blood properties. Journal of Controlled Release, 2002;79:123-135

I. Bala, S. Hariharan and M. Kumar. PLGA nanoparticles in drug delivery: The state of the art. Critical Reviews in Therapeutic Drug Carrier Systems, 2004;21:387-422

A. B. Baseer, Abdul), F. H. Hassan, Fouzia), S. H. Hassan, Syed Muhammad Fareed), S. J. Jabeen, Sabahat), F. I. Israr, Fozia), G. M. Murtaza, Ghulam) and N. H. Haque, Naheed). Physico-chemical comparison of famotidine tablets prepared via dry granulation and direct compression techniques. Pakistan Journal of Pharmaceutical Sciences, 2013;26:439-443

V. Bhardwaj, S. Hariharan, I. Bala, A. Lamprecht, N. Kumar, R. Panchagnula and M. Kumar. Pharmaceutical Aspects of Polymeric Nanoparticles for Oral Drug Delivery. Journal of Biomedical Nanotechnology, 2005;1:235-258

K.-m. Choi, M.-C. Choi, D.-H. Han, T.-S. Park and C.-S. Ha. Plasticization of poly(lactic acid) (PLA) through chemical grafting of poly(ethylene glycol) (PEG) via in situ reactive blending. European Polymer Journal, 2013;49:2356-2364

E.-M. e. a. Collnot. Mechanism of Inhibition of P-Glycoprotein Mediated Efflux by Vitamin E TPGS: Influence on ATPase Activity and Membrane Fluidity. Molecular Pharmaceutics

Mol. Pharmaceutics, 2007;4:465-474

A. Dahan and G. L. Amidon. Segmental Dependent Transport of Low Permeability Compounds along the Small Intestine Due to P-Glycoprotein: The Role of Efflux Transport in the Oral Absorption of BCS Class III Drugs. Molecular Pharmaceutics, 2008;6:19-28

E. Elmowafy, G. Awad, S. Mansour and A. El-Shamy. Release Mechanisms Behind Polysaccharides-Based Famotidine Controlled Release Matrix Tablets. Aaps Pharmscitech, 2008;9:1230-1239

S. Essa, J. M. Rabanel and P. Hildgen. Effect of polyethylene glycol (PEG) chain organization on the physicochemical properties of poly(d, l-lactide) (PLA) based nanoparticles. European Journal of Pharmaceutics and Biopharmaceutics, 2010;75:96-106

M. Estudante, J. G. Morais, G. a. Soveral and L. Z. Benet. Intestinal drug transporters: An overview. Advanced Drug Delivery Reviews, 2013;65:1340-1356

G. G. Ferenczy, L. Parkanyi, J. G. Angyan, A. Kalman and B. Hegedus. Crystal and electronic structure of two polymorphic modifications of famotidine. An experimental and theoretical study. Journal of Molecular Structure: (Theochem), 2000;503:73-79

M. Gaumet, A. Vargas, R. Gurny and F. Delie. Nanoparticles for drug delivery: The need for precision in reporting particle size parameters. European Journal of Pharmaceutics and Biopharmaceutics, 2008;69:1-9

T. Gorner, R. Gref, D. Michenot, F. Sommer, M. N. Tran and E. Dellacherie. Lidocaine-loaded biodegradable nanospheres. I. Optimization of the drug incorporation into the polymer matrix. Journal of Controlled Release, 1999;57:259-268

T. Govender, S. Stolnik, M. C. Garnett, L. Illum and S. S. Davis. PLGA nanoparticles prepared by nanoprecipitation: drug loading and release studies of a water soluble drug. Journal of Controlled Release, 1999;57:171-185

R. Gref, G. Miralles and É. Dellacherie. Polyoxyethylene-coated nanospheres: effect of coating on zeta potential and phagocytosis. Polymer International, 1999;48:251-256

F. Hassouna, J.-M. Raquez, F. d. r. Addiego, P. Dubois, V. r. Toniazzo and D. Ruch. New approach on the development of plasticized polylactide (PLA): Grafting of

poly(ethylene glycol) (PEG) via reactive extrusion. European Polymer Journal, 2011;47:2134-2144

A. Hawley, L. Illum and S. Davis. Preparation of Biodegradable, Surface Engineered PLGA Nanospheres with Enhanced Lymphatic Drainage and Lymph Node Uptake. Pharmaceutical Research, 1997;14:657-661

E. D. Hugger, K. L. Audus and R. T. Borchardt. Effects of poly(ethylene glycol) on efflux transporter activity in Caco-2 cell monolayers. Journal of Pharmaceutical Sciences, 2002;91:1980-1990

E. D. Hugger, C. J. Cole, T. J. Raub, P. S. Burton and R. T. Borchardt. Automated analysis of polyethylene glycol-induced inhibition of P-glycoprotein activity in vitro. Journal of Pharmaceutical Sciences, 2003;92:21-26

E. D. Hugger, B. L. Novak, P. S. Burton, K. L. Audus and R. T. Borchardt. A comparison of commonly used polyethoxylated pharmaceutical excipients on their ability to inhibit P-glycoprotein activity in vitro. Journal of Pharmaceutical Sciences, 2002;91:1991-2002

A. C. Hunter, J. Elsom, P. P. Wibroe and S. M. Moghimi. Polymeric particulate technologies for oral drug delivery and targeting: a pathophysiological perspective. Nanomedicine: Nanotechnology, Biology and Medicine, 2012;8, Supplement 1:S5-S20

J. Iqbal, J. Hombach, B. Matuszczak and A. Bernkop-Schnurch. Design and in vitro evaluation of a novel polymeric P-glycoprotein (P-gp) inhibitor. Journal of Controlled Release, 2010;147:62-69

T. Jiang, N. Han, B. Zhao, Y. Xie and S. Wang. Enhanced dissolution rate and oral bioavailability of simvastatin nanocrystal prepared by sonoprecipitation. Drug Development and Industrial Pharmacy, 2012;38:1230-1239

V. A. J-M. Rabanel1, and P. Hildgen1. Impact of Polymer Physico-chemical Properties on PEG-grafted-PLA Nanoparticles Structure. CRS annual meeting, 2012;2012 CRS 37th annual meeting:

C. N. Kiho Lee, Kim L. R. Brouwer, and Dhiren R, Thanker. Secretory Transport of Rantidine and Famotidine across CaCo-2 cell Monolayers. The Journal of Pharmacology and Experimental Therapeutics, 2002;303:574-580

H. Kin-Kai, D. H. Giesing, G. H. Hurst and US6451815. Aventis Pharmaceuticals, Inc. Method of enhancing bioavailability of fexofenadine and its derivatives. US6451815, 2002;

A. Lamprecht, N. Ubrich, M. Hombreiro Perez, C.-M. Lehr, M. Hoffman and P. Maincent. Influences of process parameters on nanoparticle preparation performed by a double emulsion pressure homogenization technique. International Journal of Pharmaceutics, 2000;196:177-182

S.-D. Li and L. Huang. Pharmacokinetics and Biodistribution of Nanoparticles. Molecular Pharmaceutics, 2008;5:496-504

S.-Y. Lin, W.-T. Cheng and S.-L. Wang. Thermodynamic and kinetic characterization of polymorphic transformation of famotidine during grinding. International Journal of Pharmaceutics, 2006;318:86-91

P. Liu, X. Rong, J. Laru, B. van Veen, J. Kiesvaara, J. Hirvonen, T. Laaksonen and L. Peltonen. Nanosuspensions of poorly soluble drugs: Preparation and development by wet milling. International Journal of Pharmaceutics, 2011;411:215-222

J. M. Rabanel, V. Aoun, I. Elkin, M. Mokhtar and P. Hildgen. Drug-Loaded Nanocarriers: Passive Targeting and Crossing of Biological Barriers. Current Medicinal Chemistry, 2012;19:3070-3102

E. Merisko-Liversidge, G. G. Liversidge and E. R. Cooper. Nanosizing: a formulation approach for poorly-water-soluble compounds. European Journal of Pharmaceutical Sciences, 2003;18:113-120

O. Mert, S. K. Lai, L. Ensign, M. Yang, Y.-Y. Wang, J. Wood and J. Hanes. A poly(ethylene glycol)-based surfactant for formulation of drug-loaded mucus penetrating particles. Journal of Controlled Release, 2012;157:455-460

G. Mittal, D. K. Sahana, V. Bhardwaj and M. N. V. Ravi Kumar. Estradiol loaded PLGA nanoparticles for oral administration: Effect of polymer molecular weight and copolymer composition on release behavior in vitro and in vivo. Journal of Controlled Release, 2007;119:77-85

S. Monjed, P. Gilles and F. Elias. Particle uptake by Peyer's patches: a pathway for drug and vaccine delivery. Expert Opinion on Drug Delivery, 2004;1:141-163

B. Morakul, J. Suksiriworapong, J. Leanpolchareanchai and V. B. Junyaprasert. Precipitation-lyophilization-homogenization (PLH) for preparation of clarithromycin nanocrystals: Influencing factors on physicochemical properties and stability. International Journal of Pharmaceutics Special Section: Formulating Better Medicines for Children, 2013;457:187-196

V. Nadeau, G. Leclair, S. Sant, J.-M. Rabanel, R. Quesnel and P. Hildgen. Synthesis of new versatile functionalized polyesters for biomedical applications. Polymer, 2005;46:11263-11272

D. E. Owens and N. A. Peppas. Opsonization, biodistribution, and pharmacokinetics of polymeric nanoparticles. International Journal of Pharmaceutics, 2006;307:93-102

A. Panoyan, R. Quesnel and P. Hildgen. Injectable nanospheres from a novel multiblock copolymer: Cytocompatibility, degradation and in vitro release studies. Journal of Microencapsulation, 2003;20:745-758

V. B. Patravale, A. A. Date and R. M. Kulkarni. Nanosuspensions: a promising drug delivery strategy. Journal of Pharmacy and Pharmacology, 2004;56:827-840

V. J. Pranav Shah, Tamishraha Bagchi, Ambianandan Misra. Role of Caco-2 Cell Monolayers in Prediction of Intestinal Drug Absorption. Biotechnology Progress, 2006;22:186-198

S. Ramachandran, S. Nandhakumar and M. D. Dhanaraju. Formulation and Characterization of Glutaraldehyde Cross-Linked Chitosan Biodegradable Microspheres Loaded with Famotidine. Tropical Journal of Pharmaceutical Research, 2011;10:309-316

H. M. Redhead, S. S. Davis and L. Illum. Drug delivery in poly(lactide-co-glycolide) nanoparticles surface modified with poloxamer 407 and poloxamine 908: in vitro characterisation and in vivo evaluation. Journal of Controlled Release, 2001;70:353-363

A. d. Rieux, V. Fievez, M. Garinot, Y.-J. Schneider and V. Preat. Nanoparticles as potential oral delivery systems of proteins and vaccines: A mechanistic approach. Journal of Controlled Release, 2006;116:1-27

V. Rozehnal, D. Nakai, U. Hoepner, T. Fischer, E. Kamiyama, M. Takahashi, S. Yasuda and J. Mueller. Human small intestinal and colonic tissue mounted in the Ussing chamber as a tool for characterizing the intestinal absorption of drugs. European Journal of Pharmaceutical Sciences, 2012;46:367-373

N. G. Sahoo, M. Kakran, L. A. Shaal, L. Li, R. H. Muller, M. Pal and L. P. Tan. Preparation and characterization of quercetin nanocrystals. Journal of Pharmaceutical Sciences, 2011;100:2379-2390

S. K. Sahoo, J. Panyam, S. Prabha and V. Labhasetwar. Residual polyvinyl alcohol associated with poly (d,l-lactide-co-glycolide) nanoparticles affects their physical properties and cellular uptake. Journal of Controlled Release, 2002;82:105-114

S. Sant, S. Poulin and P. Hildgen. Effect of polymer architecture on surface properties, plasma protein adsorption, and cellular interactions of pegylated nanoparticles. Journal of Biomedical Materials Research Part A, 2008;87A:885-895

S. Sepassi, D. J. Goodwin, A. F. Drake, S. Holland, G. Leonard, L. Martini and M. J. Lawrence. Effect of polymer molecular weight on the production of drug nanoparticles. Journal of Pharmaceutical Sciences, 2007;96:2655-2666

Q. Shen, Y. Lin, T. Handa, M. Doi, M. Sugie, K. Wakayama, N. Okada, T. Fujita, et al. Modulation of intestinal P-glycoprotein function by polyethylene glycols and their derivatives by in vitro transport and in situ absorption studies. International Journal of Pharmaceutics, 2006;313:49-56

S. Shilpa, N. Ve´ronique and P. Hildgen. Effect of porosity on the release kinetics of propafenone-loaded PEG-g-PLA nanoparticles. Journal of Controlled Release, 2005;107:203-214

M. Shoaib, S. Al Sabah Siddiqi, R. Yousuf, K. Zaheer, M. Hanif, S. Rehana and S. Jabeen. Development and Evaluation of Hydrophilic Colloid Matrix of Famotidine Tablets. AAPS PharmSciTech, 2010;11:708-718

K. S. Soppimath, T. M. Aminabhavi, A. R. Kulkarni and W. E. Rudzinski. Biodegradable polymeric nanoparticles as drug delivery devices. Journal of Controlled Release, 2001;70:1-20

M. Tobio, R. Gref, A. Sanchez, R. Langer and M. J. Alonso. Stealth PLA-PEG Nanoparticles as Protein Carriers for Nasal Administration. Pharmaceutical Research, 1998;15:270-275

A. Vila, H. Gill, O. McCallion and M. Ì. a. J. Alonso. Transport of PLA-PEG particles across the nasal mucosa: effect of particle size and PEG coating density. Journal of Controlled Release, 2004;98:231-244

K. Yoncheva, E. Lizarraga and J. M. Irache. Pegylated nanoparticles based on poly(methyl vinyl ether-co-maleic anhydride): preparation and evaluation of their bioadhesive properties. European Journal of Pharmaceutical Sciences, 2005;24:411-419

L. Yu. Amorphous pharmaceutical solids: preparation, characterization and stabilization. Advanced Drug Delivery Reviews Characterization of the Solid State, 2001;48:27-42

Page de liaison

The results of the first article have demonstrated usefulness of synthesized grafted polymer (PLA-g-PEG) to prepare Famotidine loaded NPs to be used as P-gp efflux inhibitor of Famotidine. It was reported that PEG has an inhibition effect of P-gp efflux. The impact of PEG of two molecular weights (750 Da and 2000 Da) at two grafting ratios (1% and 5%) on P-gp efflux was evaluated. CaCo-2 cell monolayer *in vitro* model was used to evaluate the effect of different NPs formulations on P-gp. It was thought the NPs formulations that containing more PEG will have more inhibition effect on P-gp efflux, therefore it was assumed that NPs having PEG 2000 Da at 5% grafting ratio will have significant effect on P-gp efflux of Famotidine. Even though there is no a clear explanation for PEG mechanism by which it inhibits the P-gp function, PLA-g-5%PEG was found more effective irrespective to the tested PEG molecular weights. As mentioned in the hypothesis section increased PEG concentration improved the inhibition effect on P-gp. Thus, in continuation with the results obtained from the first study, further studies were planned to explore the applications of selected 5% grafted NPs formulations. In this second article, the development of a tablet formulations based on NPs was undertaken to evaluate their effect on P-gp compared to a reference commercial Famotidine tablet formulation. Thus, the work of the second article focuses on developing tablet formulation, evaluating transport study across Caco-2 and evaluating the impact of compressing forces on NPs properties.

Chapter Four : Tablet Formulation of Famotidine loaded P-gp inhibiting Nanoparticles using PLA-g-PEG Grafted Polymer.

Mohamed Mokhtar[1], Patrick Gosselin[2], Lacasse François-Xavier[1]

and Patrice Hildgen*[1]

[1] Faculté de pharmacie, Université de Montréal, Montréal, QC, H3C 3J7, Canada;

[2] Corealis Pharma Inc, Laval, QC, H7V 4A6, Canada

Submitted to Journal of Drug Development and Industrial Pharmacy on Janaury,18th, 2015. Manuscript Number: (LDDI-2015-0037)

Résumé :

L'objectif de cette étude est d'évaluer les nanoparticules de famotidine inhibitrices de P-gp ((NPs) comme une partie de la formulation d'un dosage solide. Les nanoparticules de famotidine ont été préparées par évaporation d'émulsion de solvants en utilisant le polymère PLA-g-5%PEG de poids moléculaire de 750 et 2000 Da. Les comprimés renfermaient 40% de nanoparticules famotidine, 52.5% de cellulose microcristalline, 7% d'amidon prégélatinisé comme agent liant/désintégrant et 0.5% stéarate de magnésium comme lubrifiant. Les comprimés contenant 1.6 mg de famotidine ont été préparés avec une moyenne de 500 mg, une épaisseur allant de 6.2 à 6.5 mm, une dureté de 5 à 8 kp et un temps de désintégration de moins d'une minute. Les résultats obtenus suggèrent que les NPs contenant la famotidine peuvent être formulés comme une formulation orale solide toute en inhibant les P-gp quelque soit le poids moléculaire du PEG et peut alors améliorer la perméabilité orale ainsi que la biodisponibilité.

4.1. Abstract

The objective of this study was to evaluate the use of P-gp inhibiting Famotidine (P-gp substrate drug model) loaded nanoparticles (NPs) as a part of a suitable oral solid dosage form. Famotidine loaded NPs were prepared by solvent emulsion evaporation method using PLA-g-5%PEG grafted polymer using two PEG molecular weights 2000 and 750 Da. Tablet formulation was composed of 40 % Famotidine loaded NPs, 52.5 % microcrystalline cellulose as filler, 7 % pregelatinazed starch as binder/disintegrant and 0.5 % magnesium stearate as lubricant. Tablet containing 1.6 mg of Famotidine were prepared at an average weight of 500 mg, thickness of 6.2 to 6.5mm, hardness of 5 to 8 kp and disintegration time was less than one minute. The obtained results suggest that NPs from grafted PEG-g-PLA polymers loaded with Famotidine can be formulated as an oral solid dosage form while effectively inhibit P-gp efflux irrespective to PEG molecular weights and therefore could represent a formulation alternative to enhance oral permeability and oral bioavailability of P-gp substrate.

4.2. Introduction

Bioavailability is defined as the fraction of dose which could reach the systemic circulation. Generally, orally administrated drug could be affected by many factors such as drug solubility, absorption, permeability and gut wall metabolism(1). The most studied transporter protein responsible for efflux drug from cells is permeability

glycoprotein P-gp(2-4). P-gp acts as a pump to lower drug intracellular concentration by secretion of drug molecules from intracellular to lumen side so it reduces permeability and bioavailability of drug (P-gp efflux)(3, 4). Famotidine is a histamine H2-receptor antagonist used to treat peptic ulcer; gastroesophageal reflux; and Zollinger-Ellison syndrome(5). Although Famotidine was reported to be more potent that Ranitidine and Cimetidine, its oral bioavailability is low due mainly to P-gp efflux(6, 7). Poly lactic acid (PLA) and Polyethylene glycol (PEG) are used as drug delivery pharmaceutical excipients in a wide range of pharmaceutical formulations(8). PEG is also used to modify nanoparticles (NPs), dendrimers and excipients surface to avoid cell recognition and to inhibit P-gp efflux(9-11). Nanoparticles (NPs) generally are used to protect and stabilize drug molecules in GIT(12). To overcome P-gp efflux of Famotidine, dispersion within pegylated (PEG5%-g-PLA) nanoparticles (NPs) can be used to protect, stabilize and block P-gp pump activity(13). CaCo-2 as *in vitro* model was used to evaluate NPs ability to inhibit P-gp efflux. The aim of the study was to develop a tablet formulation based on those Famotidine loaded NPs and to evaluate its inhibition function on P-gp efflux. Dry granulation was used to improve NPs flow properties therefore it was necessary to find suitable excipients with good compactability and disintegrating ability. Tablets were assessed for *in vitro* evaluation of Famotidine permeability and compared to commercial Famotidine (Pepcid®).

4.3. Materials and Methods

4.3.1. Materials

Famotidine (lot no: 02-0024), microcrystalline cellulose 200 (Blanver lot no:12122/10), starch pregelatinazed (Starch 1500, Colorcon) and magnesium stearate (Ligamed MF-2-V, Peter Greven,) were obtained from Corealis Pharma Inc (Montreal, Canada). Commercial Famotidine tablet 10 mg (Pepcid®) was purchased from Pharmaprix (Montreal, Canada). All other materials and solvents were purchased from Laboratoire MAT (Montreal, Canada) and Sigma-Aldrich (St-Louis, USA) and used without further purification. All materials for cell culture were purchased from Invitrogen (Burlington, Canada).

4.3.2. Polymer Synthesis and Characterization

Poly(ethylene glycol) (PEG) grafted randomly on poly (D,L)-Lactide were synthesized in the laboratory and details procedure is described in the previous work(14-16). PEG grafting of two molecular weights (750 and 2000 Da) was performed at 5 % density ratio (mol/mol of lactic acid). In brief, the homopolymer ploy (D, L)-lactide was synthesized by ring-opening polymerization of dilactide under argon at 180 °C for 6 h using tetraphenyltin as catalyst. The synthesized polymer with allyl group was oxidized to hydroxyl group by hydroboration then to carboxylic acid groups by Jones reagent. Finally, methoxy poly (ethylene glycol) (MePEG) was grafted onto the polymer. ^{1}H

NMR spectra were recorded using a Bruker ARX 400 spectrometer (Germany). 10 to 20 mg samples of each polymer were dissolved in $CDCl_3$ and Chemical shift (d) was measured in ppm using tetramethylsilane (TMS) as an internal reference. The number (Mn) and the weight average molecular weights (Mw) of synthesized polymers were determined by gel permeation chromatography (GPC). Waters associate chromatography system model 717 (Waters, USA) equipped with a refractive index detector model 410 and a Phenogel 5 μm column (Phenomenex, USA) was used. Polystyrene standards were used for calibration with chloroform as a mobile phase at a flow rate of 0.6 mL/min. Fourier transform infrared (FTIR) spectroscopy was used to characterize the functional groups of PLA and PEG of PLA-g-PEG polymers. The spectra of polymers were recorded using a Nicolet iS10spectrometer (Madison, WI). All spectra were recorded at ambient temperature at a resolution of 2 cm^{-1} and 64 times scanning for each measurement to obtain an adequate signal-to-noise ratio. The IR spectra were recorded in transmission mode with dry powder of polymers, which were spread on a sample holder stage and scanned from 4000 cm^{-1} to 400 cm^{-1}.

4.3.3. Nanoparticles Preparation and Characterization

NPs preparation is described in previous work (13). Briefly, NPs were prepared by dissolving the drug and PEG-g-PLA polymer in solvents (DCM/DMF) and 0.5% of PVA was used to produce stable emulsion droplets. NPs were prepared by (oil/water) emulsion-solvent evaporation method using high-pressure homogenizer (HPH) Emulsiflex C30 (Avestin, ON, Canada). The emulsion was collected then solvents

were evaporated under vacuum pressure. Suspensions were centrifuged then lyophilized to obtain dry NPs. Same process was used for blank NPs except for the addition of Famotidine.

4.3.3.1. Particle Size and Size Distribution

Loaded NPs before, after compression and placebo blend (same excipients without NPs) were measured to evaluate the impact of tablet compressing on NPs. NPs size and size distribution were measured by dynamic light scattering (DLS) using a ZetaSizer Nanoseries ZS (Malvern instrument, Worcester, UK). NPs were resuspended in Milli-Q water (0.01%w/v) and ultrasonicated for three minutes prior to measurement in order to break aggregates. Three runs and three measurements of particle size analysis were performed at 25°C.

4.3.3.2. Surface Charge (Zeta Potential)

Surface charges of NPs were measured in triplicate using a Zeta Sizer Nanoseries ZS (Malvern instrument, Worcester, UK). NPs were suspended in 10 mM sodium chloride aqueous solutions and measurements were carried out at 25°C. The mean value and standard deviation were calculated from triplicate measurements of each sample.

4.3.3.3. Drug Loading and Encapsulation Efficiency

Encapsulation efficiency NPs was determined by adding 10 mL of 1N NaOH aqueous solution to 10 mg of NPs under stirring for 30 min. Sample analysis were performed in triplicate using high performance liquid chromatography (Shimadzu LC-2010HT, Kyoto, Japan) with SPD-20A UV/vis detector, and a Hyperclone 5 microns packing 130 A pore size BDS C18 column (Phenomenex, CA,USA). The mobile phase used was composed of a mixture of phosphate buffer solution pH 6.0 and methanol (10/90 %v/v) at a flow rate of 1 mL/min and Famotidine was measured at 267 nm. Encapsulation efficiency (EE) was calculated as the percentage of drug entrapped in NPs compared to the initial amount of drug in the solvent phase using the following Equation 4.1

Equation 4.1

$$EE\% = \frac{\text{Amount of drug entrapped in NPs}}{\text{Initial amount of drug added into the solvent phase}} \text{x}100$$

Drug loading (DL) of NPs was calculated as percentage of drug entrapped in NPs compared to the total weight of NPs using the following Equation 4.2:

Equation 4.2

$$DL\% = \frac{Assay\ of\ Famotidine\ entrapped\ in\ NPs}{Total\ weight\ \ of\ NPs}\ X\ 100$$

4.3.4. Tablet formulation

4.3.4.1. Excipients Selection

Tablet dosage form was chosen in this study because of it represents the most popular route amongst other dosage forms and also to ease comparison with commercial Famotidine tablet formulation(17). Generally the pharmaceutical excipients are added to aid the formulation manufacture, facilitate the preparation and ensure active ingredient uniformity, stability, patient compliance and proper drug delivery. Therefore the excipients in this study were selected to develop an oral formulation based on their known compatibility with the drug and in order to ensure immediate release of Famotidine. Microcrystalline cellulose (MCC) was chosen as diluent because of its good compressibility. Pregelatinized starch was used as disintegrant and magnesium stearate as a lubricant. Those inactive ingredients are used in Famotidine commercial tablet Pepcid®.

4.3.4.2. Tablet Formulation

Two tablet formulations based on Famotidine loaded NPs loaded were prepared. First formulation (F1) was composed of NPs prepared from PLA-g-5%PEG2000Da and second formulation (F2) was composed of NPs prepared from PLA-g-5%PEG750Da. Formulation composition consists of 40 % Famotidine loaded NPs with a weights of 200 mg (containing 1.6 mg Famotidine), 52.5% of micro crystalline cellulose (MCC) (262 mg) as a diluents, 7% of pregelatinized starch or 35 mg and 0.5% magnesium

stearate as lubricant (2.5 mg). The tablets contained high quantity of NPs due to low encapsulation efficiency of prepared Famotidine loaded NPs.

4.3.4.3. Dry Granulation

NPs had very poor flow properties and low density values as per small particle size. Therefore dry granulation technique was chosen to improve those properties(18, 19). NPs, MCC and starch were sieved over 30 mesh, weighed then mixed in V-shape blender Blend master Lab Patterson-Kelley (East Stroudsburg, PA, USA) for 5 minutes at 25 rpm. Single station carver press (Carver Laboratory Press, MN, USA) was used to fabricate slugs after weighing. Slugs were directly compressed at a constant compression force (300 lbs).

4.3.4.4. Tablet Compression

Compressed slugs from dry granulation technique were gently crushed in the mortar and sieved with 35 mesh screen. Mg stearate was added to powder blend and mixed using the same V-shape blender for 2 minutes. Finally powder blend was compressed using a Carver type single punch tablet press at 500 Lbf force to fabricate 500 mg standard concave 12 mm diameter tablets (Sami Precision Machining tooling, Canada).

4.3.4.5. Tablet Formulation Characterization

4.3.4.5.1. Bulk & Tapped Density, Powder Flow

Powder flow is a very critical parameter in tablets and capsules production to obtain a uniform feed, reproducible matrix filling and tablet weight. Carr's index and Hausner's ratios were characterized in order to evaluate the flow properties of powder blends containing NPs to be compressed into tablets. Density measurements were done with a Vankel tap density tester model 10700 (Edison, NJ, USA) according to USP(20). To carry out bulk density, fixed weights of powder were placed in a 50 mL graduated cylinder and the volume occupied was measured. For tapped density, graduated cylinder was then tapped at a constant velocity until a constant volume is obtained. Carr's compressibility index and Hausner's ratio were calculated for NPs powder and formulation blend powders before and after dry granulation. The Carr's compressibility index was calculated by following Equation 4.3:

Equation 4.3

$$\text{Carr's Index} = \frac{\text{Tapped density} - \text{Bulk density}}{\text{Tapped density}}$$

and Hausner's ratio was calculated by the following Equation 4.4 :

Equation 4.4

$$\text{Hausner ratio} = \frac{\text{Tapped density}}{\text{Bulk density}}$$

4.3.4.5.2. Particle Size and Size Distribution of Powder Blends

The size and particles size distribution (PSD) of the blend powder before and after dry granulation of F1 and F2 were determined in dry-dispersion mode using a Malvern Mastersizer 2000 equipped with a Scirocco 2000 module (measuring range of 0.02 to 2000μm). The measurement parameters of this method are air pressure (4 bar), feed rate (50 %), sample tray and sample mass (100 mg). The size and particle size distribution are reported in term of volume.

4.3.4.5.3. Tablet Weight, Thickness and Hardness

Tablet weights were measured using a precision balance (Mettler Toledo AG104, Switzerland). The thickness of tablets were measured using a Mitutoyo micrometer (Kanagawa, Japan). The crushing strength of the tablets were measured using a Vander Kamp tablet hardness tester model VK 200 (Edison, NJ, USA). The mean and the relative standard deviation values of tablets produced were calculated.

4.3.4.5.4. Tablet Disintegration

Tablet disintegration was measured by QC-21 disintegration test system Hanson Research (Chatsworth, CA, USA) as directed by USP(20). A tablet was placed in each six tubes of the basket apparatus in 900 mL of water at 37 ± 2°C as immersion fluid. The time was monitored for complete disintegration of all tablets with no palpable mass remaining in the apparatus.

4.3.4.5.5. Thermal Properties by Differential Scanning Calorimetry (DSC)

Thermal characterizations were carried out using a TA Universal analysis Q20 (TA instruments, DE, USA). Samples of approximately 8 mg of polymers, NPs, two NPs based crushed tablets formulations (F1&F2) and commercial Famotidine were sealed in flat bottom aluminum pans with lids. Samples were analyzed in triplicate at a temperature range from -35 to 200°C at a heating rate of 10°C /min under a nitrogen purge of 50 mL/min. Indium was used as the calibration standard.

4.3.4.5.6. Crystallinity of Famotidine in Tablets Formulations by XRPD

The crystal structure was studied by X-ray powder diffractometry using Bruker X-ray diffractometer model D2 phaser (Karlsrushe, Germany), with a CuKα radiation source (ʎ= 1.59A°) at 30 kv and 10 mA equipped with LynxEye detector angular opening 2.49239°. The opening slit, scatter plate and detector windows were 0.6 mm, 1.0 mm and 3 mm, respectively. The measurements were made over a range of 4 to 40° 2θ at

an increment of 0.02°, and the time per step 0.5s at a scanning speed of 3.4° per min. Samples of two NPs based powder blends and crushed commercial Famotidine tablets were analyzed using a low volume sample holder.

4.3.4.6. Drug Release

In vitro Famotidine release from two NPs, two NPs based tablet formulations and commercial Famotidine were evaluated by dialysis bag diffusion technique described in details in previous work(13). Tablets were gently crushed in mortar with pestle then, known amount of samples were evaluated to quantify Famotidine at predetermined time intervals (5, 15, 30, 60, 120 and 240 min). HPLC method described earlier in encapsulation efficiency section was used to quantify Famotidine released from NPs.

4.3.4.6.1. Tablet Release Stability

Tablets of the two formulations (F1 and F2) in HDPE bottles closed with induction seal PP caps were subjected to 4 weeks accelerated stability study by exposing the samples at 40 ± 2° C and relative humidity of 75 ± 5 % in programmable test chamber (Thermo Scientific forma environmental chamber model 39-40). Thermal analysis and drug release were evaluated after the storage period.

4.3.4.7. Drug Dissolution

The *in vitro* dissolution studies were carried out and the dissolution rates of Famotidine from NPs tablets and commercial tablet formulations were determined using USP dissolution test apparatus type II rotating paddle (Distek 2100 C, USA). The apparatus containing 900 ml of pH 4.5 (0.1 M phosphate buffer 13.6g/L of monobasic potassium phosphate) at 37 ± 0.5 °C(20). Six tablets of each formula were placed in individual 900 ml vessels. The paddle rotated at 50 rpm, then, 3 ml from the dissolution medium were withdrawn at predetermined time intervals(5, 10, 15, 30, 45 and 60 min). Samples were filtered through 0.45 μm and analyzed by HPLC described in section 1.3.3.3.

4.3.4.8. *In-Vitro* Permeability Evaluation of Oral Tablet Formulations

4.3.4.8.1. Cell Culture

Caco-2 cells were cultured at 37°C in DMEM as described in details in previous work (13). Culture medium was changed in both compartments the day after seeding and every successive day (Apical volume 0.5 ml, Basolateral volume 1.5 ml). Caco-2 cells

monolayer were used 21-28 days postseeding. The integrity of the cell monolayers during the growth phase was monitored by TEER reading using an EVOM™ epithelail Tissue voltohmmter and a Millipore Corp Endohm-12 electrode (Sarasota, USA).

4.3.4.8.2. Transport Study

Transport study was done to evaluate the effect of tablet formulations on the Famotidine P-gp efflux across CaCo-2 *in vitro* model compared to commercial formulation. Transport study was carried out for five different formulations, first formulation (F1) loaded NPs prepared from PLA-g-5%PEG2000Da, second formulation (F2) loaded NPs PLA-g-5%PEG750Da, first physical mixtures formulation (PM1) blank NPs of PLA-g-5%PEG2000Da with Famotidine, second physical mixture formulation (PM2) blank NPs of PLA-g-5%PEG750Da with Famotidine and commercial Famotidine. Physical mixtures were prepared with the same excipients used in F1 and F2 with respect to the quantity of NPs and Famotidine. Gently crushed tablets using mortar and pestle were used in the transport study. Cell monolayers were pre-incubated for 30 minutes at 37º C in transport Hanks Buffer supplement solution (HBSS). Basolateral to apical and apical to basolateral transport experiments were performed by adding 1.5 and 0.4 mL of solutions, respectively, containing 80 μg/mL Famotidine or its corresponding quantities of different combinations. Transport study was carried out in triplicate for each formulation. High

performance liquid chromatography method described in section 4.3.3.3 was used to quantify Famotidine in basolateral and apical compartments over four hours. From these results, calculations allowed to obtain the apparent permeability coefficients in both directions as well as the asymmetry index of the transport. The apparent permeability coefficient is determined from the amount of Famotidine diffused with time. Papp is calculated according to the following Equation 4.5:

Equation 4.5

$$Papp\ (cm\ s^{-1}) = (dQ/dt)\ (1/(AC_0))$$

Where dQ/dt is the rate of permeation, C_0 is the initial concentration of Famotidine in the donor cell (either basal or apical compartment), and A is the area of the cells monolayer. The asymmetry index allows identification of potential P-gp substrates. Indeed, this efflux ratio is determined by dividing the Papp value in the BL-AP direction by the corresponding value in AP-BL direction. An index greater than 1.0 indicates predominance of secretory transport suggesting the presence and action of an efflux transporter such as P-gp.

4.3.4.9. Data Analysis

All the experiments were conducted at least in triplicate (n=3) and results were expressed as mean ± standard deviation unless otherwise noted. Statistical significance was evaluated by one-way analysis of variance(ANOVA) using SigmaStat software version 3.1. The effect of PEG from all formulations on the P-gp efflux of Famotidine from transport study was evaluated using one-way analysis of variance (ANOVA) with the Holm-Sidak comparisons versus control (Pure Famotidine). The significant effect of treatment/level of statistical significance was judged as being $p < 0.05$, with a confidence limit of 95%.

4.4. Results and Discussion

4.4.1. Polymer Characterization

^{1}H NMR spectrums (Figure 4.1) of grafted polymers (PLA-g-PEG) showed the two main peaks of PLA. First PLA peak at 5.2 pmm (1) corresponding to the tertiary PLA proton (m, –CH), and another peak at 1.5 ppm (3) for the pendant methyl group of the PLA chain (m, $–CH_3$). Moreover, spectrum showed PEG peak at 3.6 pmm (2) for the protons of the repeating units in the PEG chain (m, $OCH_2–CH_2O$). ^{1}H NMR spectrums for grafted polymers was consistent with previous findings(13, 14). GPC analysis (Table 4.1) showed consistency with PEG molecular weight grafting ratio used. Indeed, average molecular weights were 16621 and 12905 Da and the average number molecular weight were 21137 and 17330 Da, respectively, for PLA-g-5%PEG750Da and PLA-g-5%PEG2000Da grafted polymers. Polydispersity index (PDI) results (Table 4.1) were similar for both polymers and showed narrow molecular weights distribution. FTIR scans were done for pure PLA, pure PEG and the two grafted PEG-g-PLA polymers. The characteristic stretch bands of PLA and PEG, at 1747 cm^{-1} and at 2883 cm^{-1} respectively, were used as a reference to be compared to the spectrum from PLA-g-5%PEG grafted polymers(21, 22). FTIR scans of the two synthesized polymers from Figure 4.2 showed that both characteristic peaks of PLA and PEG were detected. DSC results (Table 4.1) showed only PLA glass transition temperature (Tg) for PLA-g-5%PEG750Da was detected at 29.68°C, while PLA Tg could not be measured due to the interference with PEG melting point at 53.42ºC for PLA-g-5%PEG2000Da polymer. More details on polymer synthesis and characterization can be found in previous work(13)

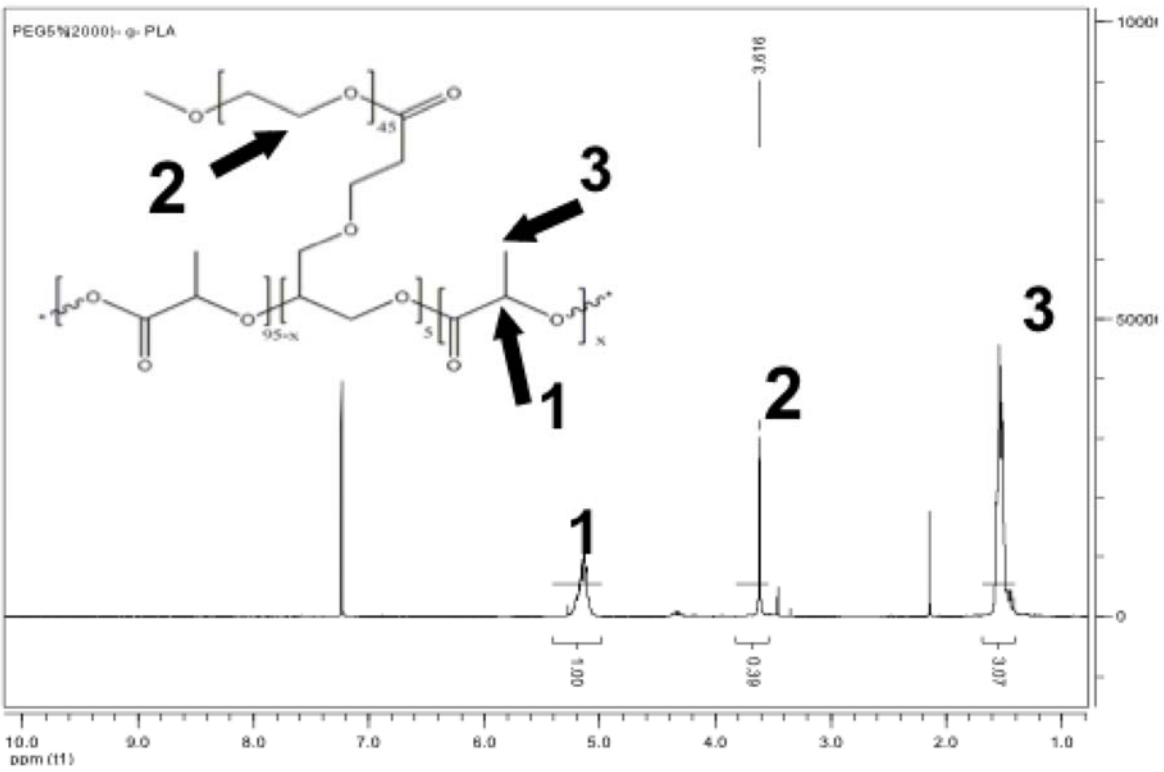

Figure 4.1 NMR for grafted PLA-g-5%PEG2000Da polymer

Polymer Composition	Mw (Da)	Mn (Da)	PDI	PEG m.p (°C)	PLA Tg (°C)
PLA-g-5%PEG750Da	16621	12905	1.29	N/D	29.68 ± 1.87
PLA-g-5%PEG2000Da	21137	17330	1.22	53.42 ± 0.39	N/D

m.p=melting point, Tg= glass transition temperature, N/D Not detected, (n=3)

Table 4.1 Molecular weights, PDI and DSC results for PEG-PLA grafted polymers

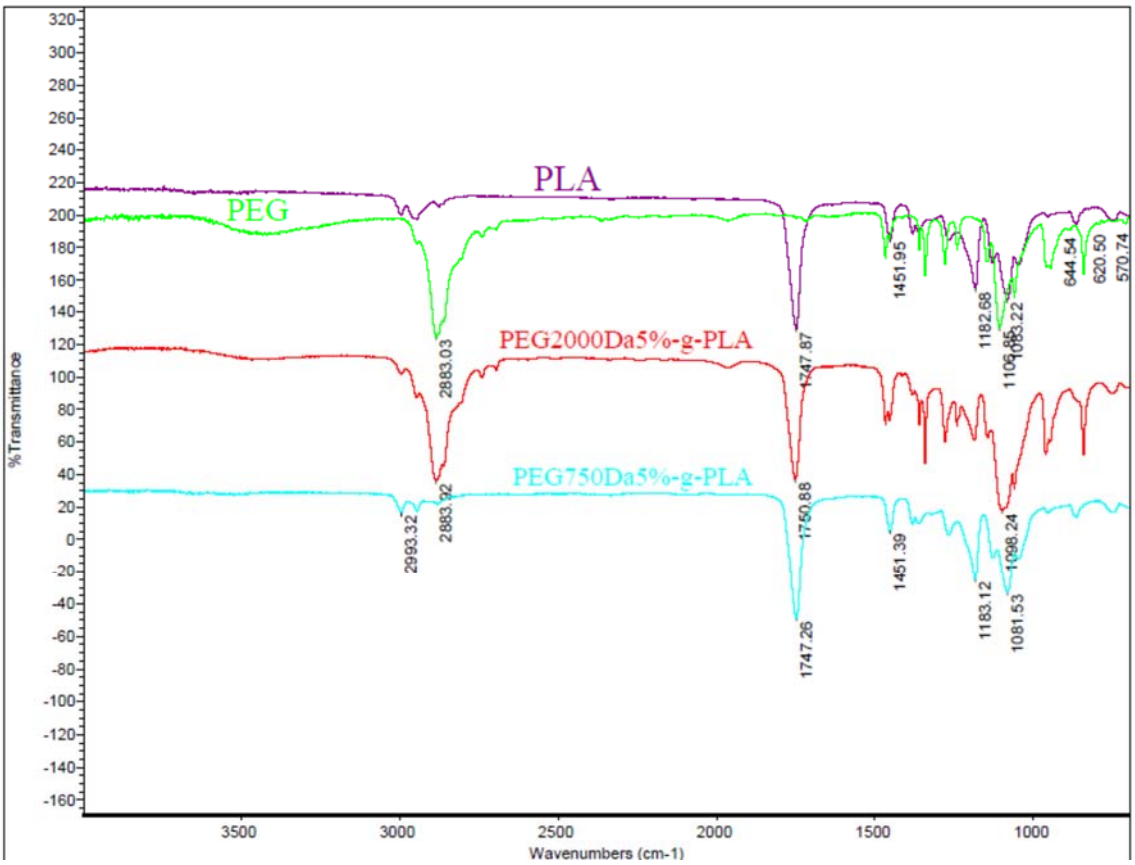

Figure 4.2 FTIR Spectrum of pure PLA, PEG and two grafted polymers

4.4.2. Nanoparticles Characterization

Particle size and size distribution obtained by dynamic light scattering of two NPs formulations are shown in Table 4.2. PLA-g-5%PEG750Da and PLA-g-5%PEG2000Da NPs had similar mean particle size of 211 and 217 nm, respectively. The polydispersity index (PI) values were 0.11 for NPs prepared from PLA-g-5%PEG750Da and 0.05 for NPs prepared from PLA-g-5%PEG2000Da. NPs had low PI value (homogenous samples) which demonstrated a unimodal size distribution(23).

Table 4.2 showed that zeta potential of loaded NPs prepared from PLA-g-5%PEG750Da and PLA-g-5%PEG2000Da were -4.6 and -7.7 mV, respectively. The observed low zeta potential values of NPs were attributed mainly due to the residual PVA amount associated with NPs preparation(24, 25). Low zeta potential values of NPs in agreement with reported results for similar polymers(26). Table 4.2 also shows that NPs formulations had low encapsulation efficiency at approximately 15% and drug loading at 0.8 %. The hydrophilic nature of drug model Famotidine might resulted in significant loss of drug during NPs preparation involving solvents. Improving encapsulation efficiency and/or drug loading of NPs is an approach to improve tableting process.

NPs formulation	NP Size mean ± SD	PI ± SD	Zeta potential (mV) ± SD	EE (%) ± SD	DL (%) ± SD
PLA-g-5%PEG750Da	211 ± 18	0.11±0.03	-4.6 ± 0.4	14.5 ± 3.6	0.8 ± 0.2
PLA-g-5%PEG2000Da	217 ± 14	0.05±0.03	-7.7 ± 1.0	15.3 ± 2.5	0.8 ± 0.3

PI=polydispersity Index, EE=Encapsulation Efficiency, DL=Drug Loading

Table 4.2 The mean particles size, PI, Zeta Potential and Drug Loading of Two NPs Formulations (n=3)

4.4.3. Tablet Formulation

A pharmaceutical dosage form typically consists of active pharmaceutical ingredient and excipients. The excipients are added to aid the formulation stability, manufacture, facilitate the preparation, patient acceptability and drug delivery(8). Some properties of final dosage form, such as bioavailability and stability, are dependent on the excipients chosen, concentrations and interactions with each other and the active ingredients (27). Therefore the excipients in this study were selected to develop an oral solid dosage formulation, based on their known compatibility(20). The formulation of a tablet based on Famotidine loaded PLA-g-PEG NPs is the aim of the study. A tablet formulation was developed to be composed of 40 % of loaded NPs (corresponding to 1.6 mg of Famotidine per tablet), 52.5% of microcrystalline cellulose (MCC), 7% of pregelatinized starch and 0.5 % of magnesium stearate. MCC was added to the formulation as diluent and to improve flow property and also as a binder(28). Pregelatinized starch was added to the formulation as a binder (to facilitate the agglomeration of powder), as a tablet disintegrant and also to improve powder flow. Magnesium stearate was added as a lubricant, which is usually used to reduce the frictional forces between particles and between particles and metal contact surface of tablet punches and dies(29). High quantity of NPs with very poor flow powder was needed to compensate the low drug loading of 0.8%.. This was considered as an obstacle in developing a tablet formulation. Improving NPs drug loading would be effective approach to reduce NPs quantity then improve blend powder flow properties and decrease tablet weight. Both tablets formulations PLA-g-5%PEG2000Da (F1) and

PLA-g-5%PEG750Da (F2) were prepared by dry granulation in order to densify NPs with poor density and flow properties. Commercial Famotidine (Pepcid® 10 mg) was used as a comparator with NPs based tablets.

4.4.4. Dry Granulation

Dry granulation process is preferably used to prepare granules and to densify the powder blend, for proper flow and compressibility properties. Dry granulation process involves compaction and densification of powders, using a roller compactor or tablet press that is employed as a slugging tool for powders that may not have a sufficiently uniform stream in the die cavity. In this study, slugging was chosen to perform dry granulation. Dry granulation consists in compacting powder to form a slug with a heavy duty, rotary tablet press or a solid strip, using a roller compactor and then reducing its size by milling or screening to achieve a desired granule(18, 30). NPs have a very poor flowability, therefore dry granulation was chosen to improve NPs powder blend flow. The fine particles (<100 um) tend to be more cohesive and less flowing, while large dense particles tend to be free flowing(31, 32).

4.4.5. Formulation Characterization

4.4.5.1. Bulk, Tapped Density and Powder Flow

Powder flowability is a very important property in tablets-production process and for product uniformity. The dosage and pharmacological effect of the products depends on

powder flow(19, 30, 33-35). Powder flowability is influenced by factors such as particle size, size distribution and shape. Some characterizations of particle properties such as flowability and compactibility are very crucial to achieve a successful tablet compression(30, 33, 34, 36, 37). Consequently, powder flow properties was evaluated as part of the formulation development. Tapping test, a common and easy method, is widely used in pharmaceutical industry to measure flowability. It also provides Carr's index of the powder bed(35). The bulk and tapped density were measured for NPs powder, powder blend before and after dry granulation for two NPs formulations (F1&F2). Table 4.3 shows results of bulk/tapped density, Hausner ratio and Carr's index of two NPs powders formulations with very poor flowability. Table 4.4 presents qualitative interpretation of Hausner ratio and Carr's index results(20). Poor flow of NPs was expected, due to small particles size. Table 4.3 shows that both NPs PEG5%-g-PLA had similar and very low bulk density values of 0.02 g/mL and tapped density of 0.05 g/mL, which indicate a very poor powder flow based on calculated Carr's index 57-59 (Hausner ratio above 1.9), which is related to inter particles fraction (20). The formulated blend powder density slightly increased but still a very poor powder flow was observed after adding the excipients to NPs powder, probably because of high proportion of NPs within the formulations. Following dry granulation process, the blend powder showed a significant increase in bulk density of 0.33-0.34g/mL and tapped density of 0.46-0.48 g/mL and the calculated Carr's index was 28-32 (Hausner ratio was 2), not optimal but passable powder flow. Both NPs formulations had similar values of bulk and tapped density before and after dry granulation process. Even thought Carr’s index values after dry granulation showed powder flow properties for

both NPs formulations had a qualitative very poor flow, powder blends were practically sufficiently dense to be properly compressed. The very poor flow of powder blend even after dry granulation due to high proportion of NPs within tablet formulation drive to find another approach to improve powder flow. For instance, increase drug loading of NPs could be one approach in order to reduce NPs quantity per tablet and therefore improve powder flow.

	Bulk Density(g/ml)	Tapped Density(g/ml)	Carr's index	Hausner Ratio
F1 based on PLA-g-5%PEG2000Da NPs				
NPs	0.02 ± 0.01	0.05 ± 0.01	59 ± 3.0	2.46 ± 0.16
Blend powder	0.08 ± 0.07	0.16 ± 0.01	48 ± 7.3	2 ± 0.16
Dry-granulated	0.33 ± 0.01	0.48 ± 0.05	32 ± 8.5	2 ± 0.22
F2 based on PLA-g-%%PEG750Da NPs				
NPs	0.02 ± 0.01	0.05 ± 0.01	57 ± 2.08	1.89 ± 0.19
Blend powder	0.08 ± 0.07	0.17 ± 0.01	52 ± 7.60	2.13 ± 0.12
Dry-granulated	0.34 ± 0.02	0.46 ± 0.05	28 ± 3.21	2.00 ± 0.19

Table 4.3 Powder flow characterization of NPs, powder blend and dry granulated powder

Carr's Index	Flow character	Hausner ratio
1 to 10	Excellent	1.00 to 1.11
11 to 15	Good	1.12 to 1.18
16 to 20	Fair	1.19 to 1.25
21 to 25	Passable	1.26 to 1.34
26 to 31	Poor	1.35 to 1.45
32 to 37	Very poor	1.46 to 1.59
> 38	Very, very poor	> 1.6

Table 4.4 Hausner ratio and Carr's index interpretation(20)

4.4.5.2. Particle Size and Size Distribution of Powder blends

The particles size and size distribution (PSD) were evaluated for NPs formulations F1 and F2 after dry granulation and the placebo blend powder (only excipients, no NPs). Particles sizing of the powder blends was evaluated by laser diffraction. The test was carried out at high pressure (4) bars to break down any agglomerates and at 50% feed rate. The particles size and size distribution are reported in terms of volume. Volume-based methods are very sensitive to the appearance of a few large particles. Figure 4.3 shows results obtained for F1, F2 and placebo blend formulations. They respectively showed a Gaussian-like distribution of the particles size. Results (Figure 4.3) clearly showed that the average particle size of NPs tablet formulations is in the same range as standard pharmaceutical excipients. F1 particles were sized between 156 and 440 μm with a mean of 284 μm. For F2, results showed d(0.1) is 105 and d(0.9) is 440 μm with

mean of 265 µm. While for placebo formulation composed of standard excipients, similar particles sizes between 112 and 405 µm with a mean of 242 µm were observed. PSD results of powder blend after dry granulation of both NPs tablet formulations with placebo were found similar, suggesting a proper formulation and densification process.

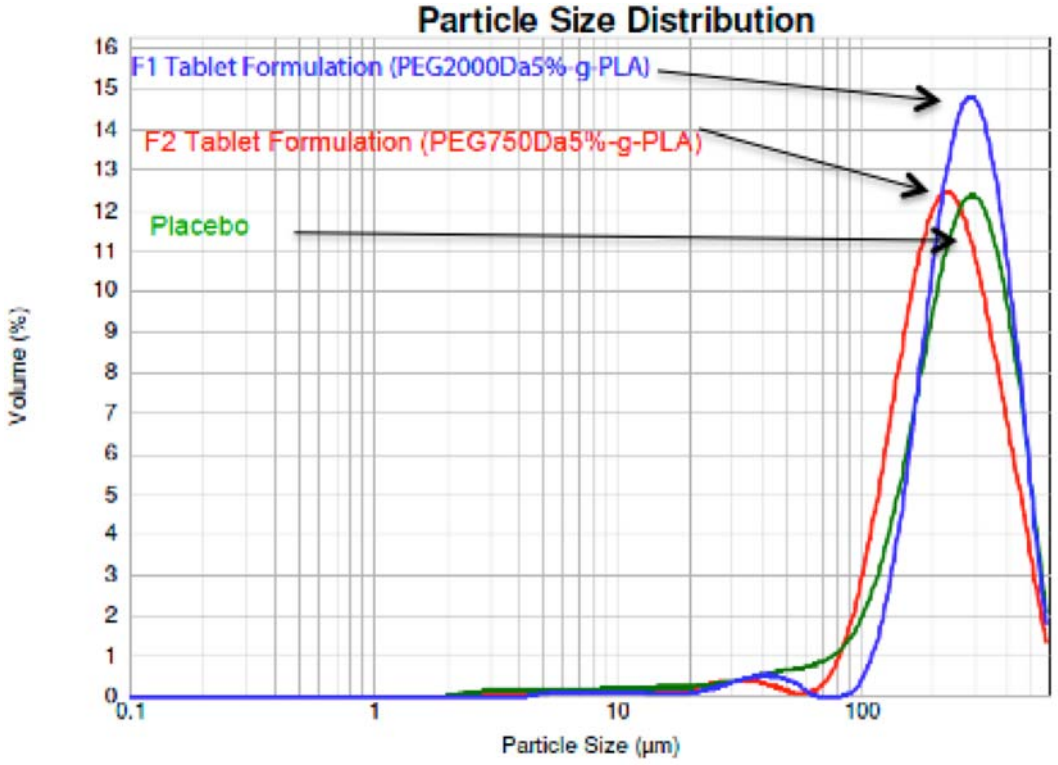

Figure 4.3 Particle size distribution of F1,F2 and Placebo formulations

4.4.6. Tablets Characterization

F1 and F2 tablets were characterized for their tablet thickness, weight, hardness and tablet disintegration, and compared with commercial Famotidine formulation (Table 4.5). Finally powder blend was compressed at 500 Lbf force to fabricate 500 mg tablets with 12mm. NPs Tablet formulations (F1&F2) possessed good mechanical strength with sufficient hardness. Table 4.5 showed that tablets prepared from PLA-g-5%PEG750Da NPs (F2) had average thickness of 6.46 ± 0.11 mm, tablet average weight of 504 ± 3.25 mg and hardness of 8 ± 0.2 kp. On the other hand, tablets of the F1 formulation had average thickness of 6.33 ± 0.12 mm, average weight of 503 ± 3.48 mg and a hardness of 5.2 ± 0.26 kp. Tablet hardness and thickness for F2 NPs PLA-g-5%PEG750Da were statistically significant difference (p=<0.001) from F1 PLA-g-5%PEG2000Da. Table 4.5 shows disintegration time for NPs formulations of less than one minute (20 seconds average) typical of immediate release dosage forms and 2.2 minutes for commercial Famotidine at a increased hardness of 20.95 kp for the latter.

Formulation Compositions	Weight (mg)	FMT Dosage (mg)	Thickness (mm)	Hardness (Kp)	Disintegration (min)
Commercial Famotidine (n=10)	208 ± 2.81	10	4.19 ± 0.05	20.9 ± 1.05	2.17 ± 0.017
F1 Tablets NPs (PLA-g-5%PEG2000Da)	503 ± 3.48 (n=30)	1.6	6.33 ± 0.12 (n=30)	5.2 ± 0.26 (n=6)	17 ± 1.0 (n=6)
F2 Tablets NPs (PLA-g-5%PEG750Da)	504 ± 3.25 (n=30)	1.6	6.46 ± 0.11 (n=30)	8.0 ± 0.29 (n=6)	18 ± 1.6 (n=6)

Table 4.5 Tablets characterization of Commercial Famotidine, F1 and F2 NPs formulations

4.4.7. NPs Size Analysis Before and After Tablet Compression

The mean particle size of powder blends and after tablet compressing were characterized to examine the influence of compressing force on NPs. The average of the mean particle size of NPs formulations after tablet compressing showed that PLA-g-5%PEG750Da had mean particle size at 201 nm and PLA-g-5%PEG2000Da had 215nm. Results (Table 4.6) of NPs size showed there was no significant different, therefore the compression force used had no influence on NPs.

Tablet Formulations	Mean of NP size (nm) ± SD
NPs(PLA-g-5%PEG750Da)	211 ± 18.7
after compressing	201 ± 3.5
NPs(PLA-g-5%PEG2000Da)	217 ± 14.3
after compressing	215 ± 19.3
Placebo (excipients without NPs)	1613 ± 125.0

Table 4.6 The mean particles size values of NPs tablet formulations before and after tablet manufacturing (n=3)

4.4.8. Thermal Properties by Differential Scanning Calorimetry (DSC)

Based on the literature review, Famotidine exists in two crystal forms (A and B) and the form B is the metastable, kinetically favored form (38). Melting points of different crystals of Famotidine are 171.43 and 164.4°C, respectively, for forms A and B.

Famotidine loaded NPs formulations had Tg value at 43 and 48°C, respectively, for PLA-g-5%PEG750Da and PLA-g-5%PEG2000Da. Tablet formulations of NPs (F1 and F2) and commercial Famotidine were characterized by DSC. Figure 4.4 and Table 4.7 shows a163°C melting point that was detected for commercial Famotidine while For NPs formulations (F1) Famotidine, it was detected at 188°C and 186°C for (F2). F1 and F2 had sharp melting point of Famotidine and the peak had shifted from the original position to a higher melting temperature. It could be possibly due to solvents impact on Famotidine crystals form or presence of other functional groups of polymers. Further investigation need to be carried out to verify the reasons whereas it so not the main focus of the study.

Formulation Composition	Glass transition temperature (°C)	Famotidine melting point (°C)
F1 Tablet NPs (PLA-g-5%PEG2000Da)	48 ± 2.0	188 ± 1.9
F1 after Stability study	49 ± 1.3	188 ± 1.0
F2 Tablet NPs (PLA-g-5%PEG750Da)	43 ± 0.6	186 ± 3.1
F2 after Stability study	44 ± 2.6	188 ± 0.6
Commercial Famotidine tablet	NA	166 ± 1.5

Table 4.7 DSC characterization of Tablet formulations (n=3)

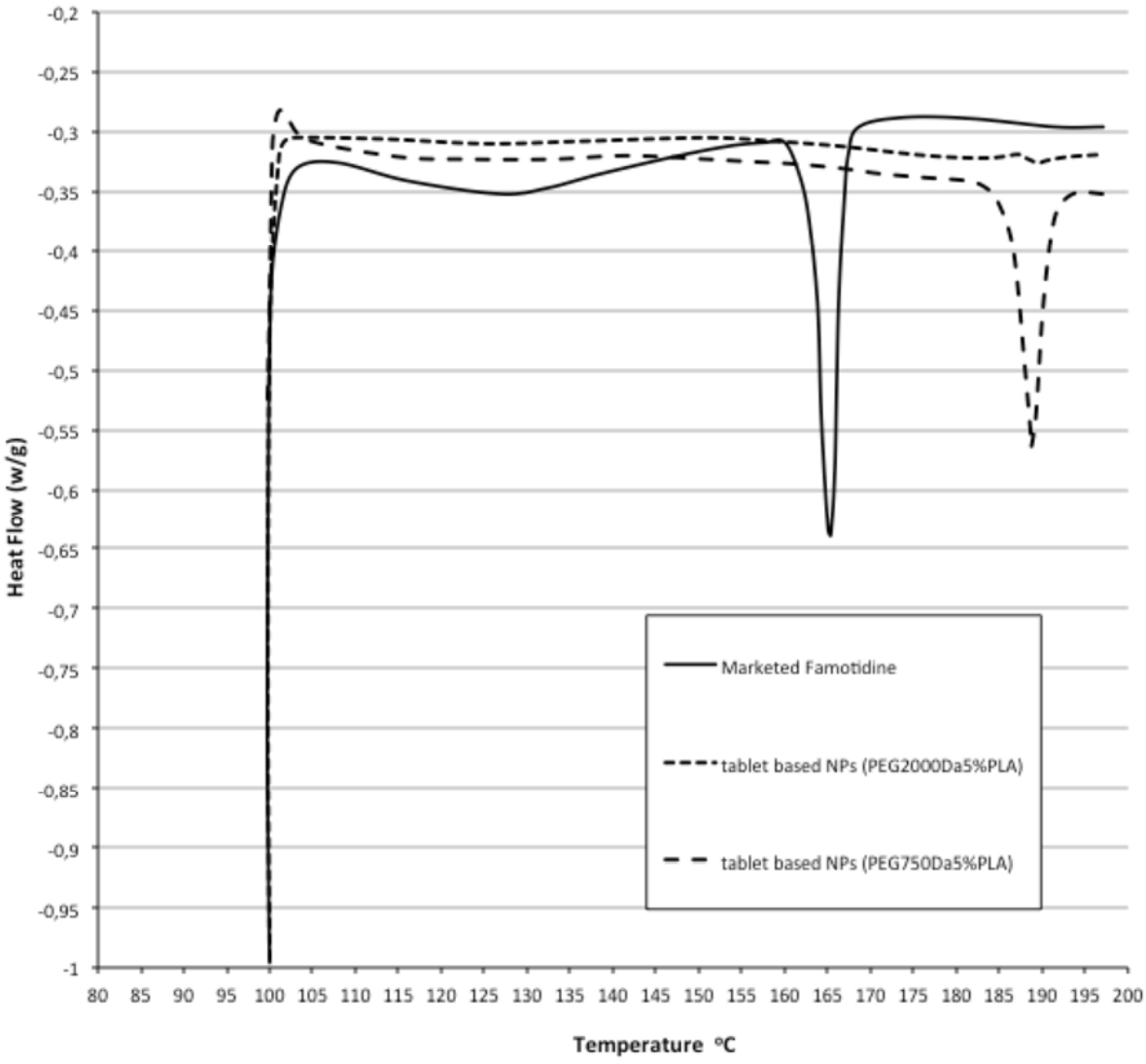

Figure 4.4 Thermograms of Famotidine from different tablet formulations

4.4.9. Crystallinity of Famotidine in Tablets Formulations by X-Ray Powder Diffraction (XRPD)

X-ray powder diffraction technique was used to identify Famotidine crystal state after encapsulation in NPs. Famotidine form B used in this study has distinct major

characteristic peaks at 5.96, 11.5, 15.7, 17.5 19.5, 20.5, 22.5 and 24.5° 2ϴ (39, 40). X-ray diffraction patterns scans revealed that pure Famotidine was clearly in crystalline state, since it showed sharp, distinct peaks. XRPD scans of Famotidine loaded NPs (Figure 4.5) showed two Famotidine minor peaks at 21.50 and 23.50° 2ϴ.

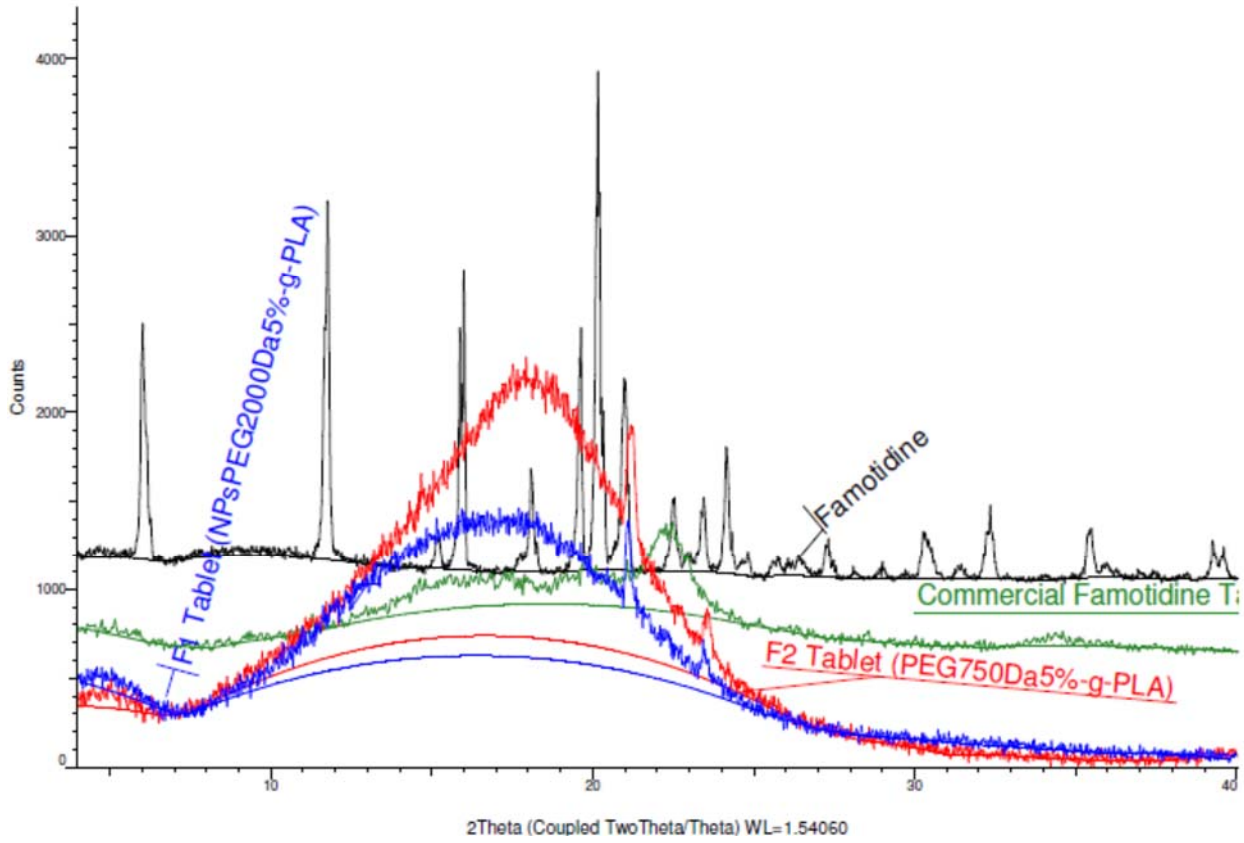

Figure 4.5 X-ray Diffractograms of Famotidine from different tablet formulations

Commercial Famotidine ablets showed a peak at 23° 2Θ with very low intensity compared to pure Famotidine peak. Such low intensity and decrease number of peaks it might be attributed to change in Famotidine from crystal to amorphous state or that XRPD could not detect all Famotidine peaks (41-45). But based on the DSC characterization where Famotidine melting peak were detected, such absence might be due to the limit of detection of the machine used for this low drug loading.

4.4.10. Drug Release

The purpose of studying kinetic release of Famotidine from two NPs tablet formulations and comparing it with commercial Famotidine formulation was to evaluate the effect of NPs matrix and compressing force on Famotidine release. The kinetic release of Famotidine from different tablet formulations was carried out at same conditions as kinetic release of Famotidine from corresponding unformulated/uncompressed NPs formulations. It was found that Famotidine showed a total fast release profile from all tablets formulations in pH 7.4 medium, consistent with NPs results and reported results (46-48). Famotidine release profile showed a biphasic release behavior as previously reported(49), the first phase up to 30 min where 35 to 40 % of drug was released followed by a slower release from 30 min and up to 4 h. Figure 4.6 showed that there is no difference of Famotidine release rate amongst different formulations. It was found that 75 % of Famotidine was released within 2 h. Famotidine released from NPs tablet formulation prepared by dry granulation and commercial Famotidine showed no differences in dissolution profiles,

suggesting that the tablet manufacturing technique had no effect on Famotidine drug release(48). NPs tablet formulations demonstrated that they provide an immediate release of Famotidine that is comparable with commercial Famotidine formulations.

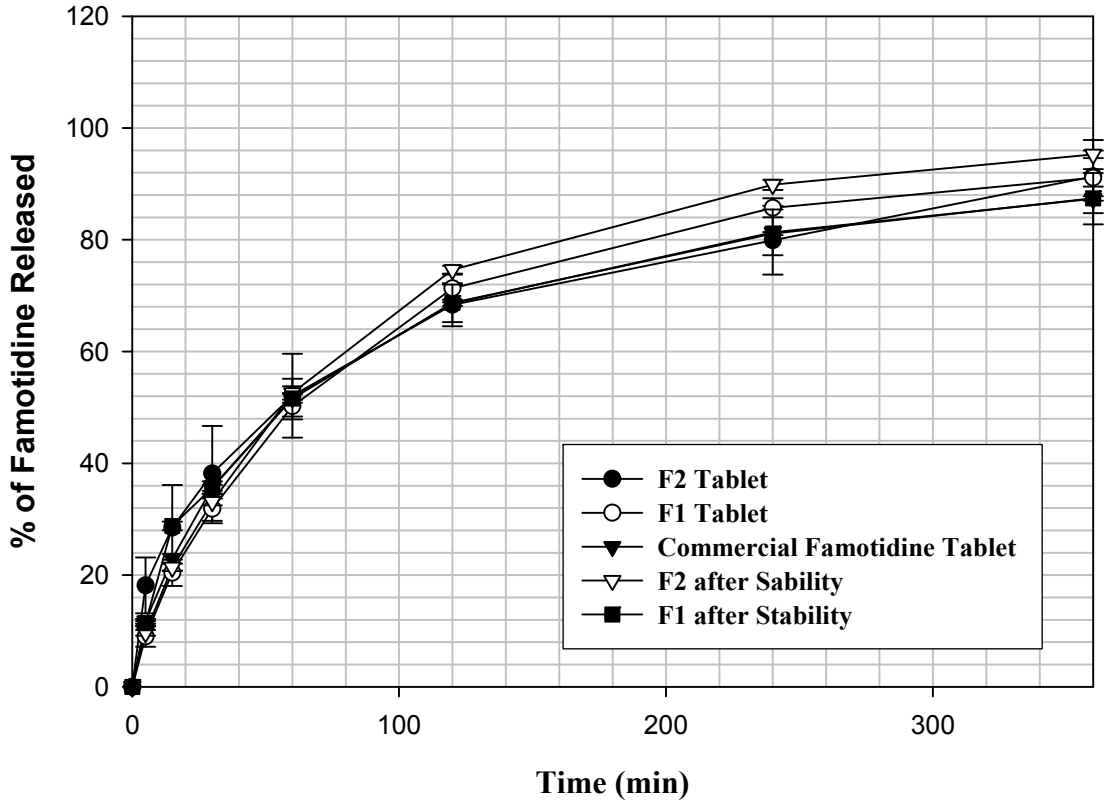

Figure 4.6 Percentage of Famotidine Released at pH 7.4 from different tablet formulations

4.4.11. Stability Study

Results from DSC and drug release results (Figure 4.6 and Table 4.7) from NPs based tablet formulations (F1 and F2) showed no change neither for Famotidine melting point, Tg and Famotidine release in pH 7.4 PBS medium over 4 weeks storage under accelerated conditions.

4.4.12. Drug Dissolution

Famotidine release (Figure 4.7) from F1, F2 and commercial tablet formulations showed fast release from 0.1M phosphate buffer pH 4.5 (13.6g/L of monobasic potassium phosphate). All formulations achieved above 90 % of Famotidine dissolution after 5 min of dissolution. The percentage of Famotidine released showed no significant difference amongst all formulations except at five minutes sampling time. Indeed, at five minutes time points, commercial Famotidine had a significantly ($p=0.034$) higher release than NPs formulations, which might be attributed to short term entrapment of drug molecules within NPs polymeric matrix. The fast release was attributed to fast disintegration time for all tablet formulations that enhanced wetting of dissolution medium into the tablet and thus promoting Famotidine release. Complete Famotidine release from all tablet formulations occurred less than 30 min therefore NPs tablets formulations demonstrate an immediate release. Dissolution test clearly showed no impact of NPs on Famotidine release comparing to Famotidine commercial tablet formulation. The different in Famotidine release profiles from both

release study drug release pH 7.4 and dissolution study pH4.5 is due to different pH medium.

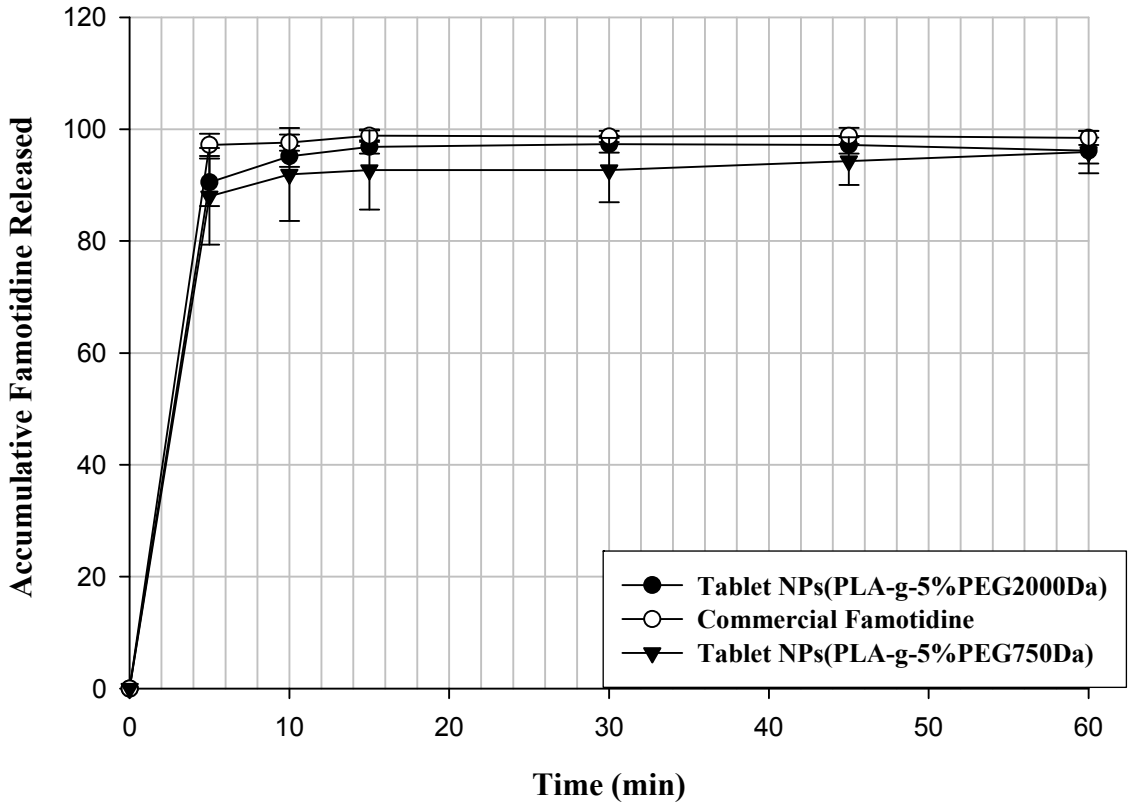

Figure 4.7 Famotidine Dissolution Profile from Different Tablet Formulations

4.4.13. Transport Study

The transport experiments were conducted to evaluate permeability of Famotidine and to examine the potential effect of PEG on P-gp efflux of Famotidine loaded NPs tablets formulations across CaCo-2 cells *in vitro* model. A total of five formulations were used in this study to examine these effects on Famotidine permeability across CaCo-2. Gently crushed tablets loaded with NPs formulations were prepared from PLA-g-5%PEG2000Da (F1) and PLA-g-5%PEG750Da (F2), two formulations of physical mixtures (PM1&PM2) of blank NPs formulations (corresponding to loaded formulations) with Famotidine and commercial Famotidine formulation were used. The transport results from commercial Famotidine and pure Famotidine (no PEG) were used as references to evaluate the effect of PEG to inhibit or decrease P-gp efflux on Famotidine. Transport experiments in bidirectional sides were carried out in triplicate for all formulations and average results were reported. CaCo-2 well is divided into upper part, the apical (serosal) side representing the lumen side, and a lower part, the basolateral (mucosal) side. In the mucosal intestine, lower part in CaCo-2 model, where secretory transport of Famotidine occurs, the effect of PEG as P-gp inhibitor would be expected either by decreasing or inhibition of P-gp function. Asymmetry index (AI) is the ratio of secretory (BL-to-AP) side to absorptive (AP-to-BL) which reflects P-gp efflux on Famotidine. AI also showed PEG inhibition on P-gp efflux of Famotidine. Our study (Table 4.8) showed an asymmetric index value of 1.01 for pure Famotidine had which means the secretion level (BL-to-AP) slightly higher but mostly similar than absorption level (AP-to-BL) as reported(50). Results (Table 4.8) showed

that the AI value of tablets loaded NPs of PLA-g-5%PEG2000Da (F1) and PLA-g-PEG750Da (F2) were 0.07 and 0.43, respectively, while the AI value for commercial Famotidine was 1.02. Both tablets loaded NPs showed inhibition effect of P-gp efflux of Famotidine compared to commercial and pure Famotidine, F1 being the most effective formulation. AI results of 0.06 and 0 for physical mixtures formulations (PM1&PM2) showed also an inhibition of P-gp efflux of Famotidine which it can be attributed to PEG content. The secretory results (BL-to-AP) demonstrated that all formulations containing PEG showed a decrease of P-gp efflux of Famotidine back to apical side, compared to commercial and pure Famotidine. Tablet formulations containing NPs prepared from polymer grafted with PEG 2000Da either in loaded or blank NPs were found to be more effective to inhibit P-gp efflux of Famotidine than corresponding formulations containing PEG 750Da. Even if tablet formulations containing blank NPs showed good transport results, loaded NPs have advantages over blank NPs such as protecting drug from harsh environment, improving drug absorption and altering drug release(12). Those results confirmed our hypothesis that loaded NPs formulated as tablets can inhibit P-gp Famotidine efflux. In this study the presence of hydrophilic polymers (PEG) on the surface of NPs grafted at 5 % PEG, irrespective to molecular weights, provided an effective way to control the interface between NPs and the biological systems (P-gp in this case) as they are designed to interact with. To summarize transport results, it was observed that P-gp efflux inhibition of Famotidine is attributed to PEG content. Indeed, as PEG increased, the inhibition effect increased which is consistent with the hypothesis of the study(9, 51-55). The studies presented herein suggest that commonly used pharmaceutical

excipients such as PEG (750 Da and 2000 Da) are capable of inhibiting efflux transporter (P-gp) activity. Even though PEG's mechanism inhibits P-gp efflux still not clear, PEG has demonstrated its capability to inhibit the P-gp efflux mechanism. PEG might interfere with interaction between Famotidine molecules and drug substrate binding site of P-gp occurs principally in the trans-membrane domain(amino acid residues).

Formulation and Combination	AP-BL ($x10^{-6}$cm/sec)	BL-AP ($x10^{-6}$cm/sec)	AI
Pure Famotidine	10.3 ± 0.7	10.4 ± 0.6	1.01 ± 0.6
Commercial Famotidine	4.9 ± 1.4	5.0 ± 0.3	1.02 ± 0.05
loaded NPs PLA-g-5%PEG750Da	1.7 ± 0.1	0.7 ± 0.6	0.43 ± 0.3
Blank NPs PLA-g-5%PEG750Da	6.3 ± 0.2	0.4 ± 0.2	0.06 ± 0.004
Loaded NPs PLA-g-5%PEG2000Da	4.1 ± 0.8	0.3 ± 0.2	0.07 ± 0.01
Blank NPs PLA-g-5%PEG2000Da	4.0 ± 0.1	0	0.000
AI=Asymmetric Index, AP=apical, BL=basolateral			

Table 4.8 Bidirectional results from Marketed Famotidine,F1&F2 NPs tablets formulations, pure Famotidine and tablet physical mixtures across CaCo-2 monolayer cells

4.5. Conclusion

Grafted PLA-g-5%PEG polymers were synthesized and loaded NPs were prepared. The mean average size of prepared loaded NPs were 211 and 217 nm and demonstrated a unimodal size distribution with low negative surface charge values ranging from -4.6

and -7.7mV. Dry granulation achieved improvement of powder blend flow properties due to the intrinsic poor properties of NPs. Prepared tablets had adequate physical properties typical of an immediate release dosage form. Particle size, drug release and drug transport results of NP based tablet formulations showed that the manufacturing process did not influence NPs properties. Famotidine released from NPs and from tablets made of NPs showed a similar biphasic release behavior with no significant difference of compressed NPs on Famotidine release compared to commercial formulation at pH 7.4. Transport study results of all tablet formulations containing PEG showed their capability to inhibit the P-gp efflux of Famotidine. The permeability results demonstrated the concept of connecting hydrophilic Me.PEG with hydrophobic PLA capable to inhibit P-gp efflux. Generally in addition to PEG's inhibitory effect, drug loaded within PEGylated NPs could offer a protection from stomach harsh environments. Thus, NPs prepared from PLA-g-5%PEG could be an effective formulation tool to enhance drug permeability through inhibit P-gp efflux then improve oral bioavailability.

4.6. References

1. Aulton ME. Aulton's pharmaceutics : the design and manufacture of medicines. 3rd ed. Edinburgh ; New York: Churchill Livingstone; 2007.

2. Hediger MA, Romero MF, Peng JB, Rolfs A, Takanaga H, Bruford EA. The ABCs of solute carriers: physiological, pathological and therapeutic implications of human membrane transport proteins - Introduction. Pflugers Archiv-European Journal of Physiology 2004;447(5):465-468.

3. Akhtar N, Ahad A, Khar RK, Jaggi M, Aqil M, Iqbal Z, et al. The emerging role of P-glycoprotein inhibitors in drug delivery: a patent review. Expert Opinion on Therapeutic Patents 2011;21(4):561-576.

4. Estudante M, Morais JG, Soveral G, Benet LZ. Intestinal drug transporters: An overview. Advanced Drug Delivery Reviews 2013;65(10):1340-1356.

5. McNally GP, Roche EJ. Stabilized composition of famotidine and sucralfate for treatment of gastrointestinal disorders. In: Google Patents; 1997.

6. Thakker KLaDR. Saturable Transport of H2-Antagonists Ranitidine and Famotidine Across Caco-2 Cell Monolayers. Journal of Pharmaceutical Sciences 1999;88(7):680-687.

7. Bourdet D, Thakker D. Saturable Absorptive Transport of the Hydrophilic Organic Cation Ranitidine in Caco-2 Cells: Role of pH-Dependent Organic Cation Uptake System and P-Glycoprotein. Pharmaceutical Research 2006;23(6):1165-1177.

8. Rowe RC, Sheskey PJ, Quinn ME. Handbook of pharmaceutical excipients. In. 6th ed. London ; Chicago, Washington,DC: Pharmaceutical Press ;American Pharmacists association; 2009.

9. Hugger ED, Novak BL, Burton PS, Audus KL, Borchardt RT. A comparison of commonly used polyethoxylated pharmaceutical excipients on their ability to inhibit P-glycoprotein activity in vitro. Journal of Pharmaceutical Sciences 2002;91(9):1991-2002.

10. Gref R, L M, Quellec P, Marchand M, Dellacherie E, Harnisch S, et al. Stealth corona-core nanoparticles surface modified by polyethylene glycol (PEG): influences of the corona (PEG chain length and surface density) and of the core composition on phagocytic uptake and plasma protein adsorption. Colloids and Surfaces B: Biointerfaces 2000;18(3-4):301-313.

11. Liu Y, Chiu GNC. Dual-Functionalized PAMAM Dendrimers with Improved P-Glycoprotein Inhibition and Tight Junction Modulating Effect. Biomacromolecules 2013;14(12):4226-4235.

12. Wehrung D, Geldenhuys WJ, Oyewumi MO. Effects of gelucire content on stability, macrophage interaction and blood circulation of nanoparticles engineered from nanoemulsions. Colloids and Surfaces B: Biointerfaces 2012;94(0):259-265.

13. Mokhtar M, Gosselin P, Lacasse F-X, and Hildgen P. Design of PEG-grafted-PLA nanoparticles as oral permeability enhancer for P-gp substrate drug model Famotidine. Journal of Microencapsulation 2014.

14. Nadeau V, Leclair G, Sant S, Rabanel J-M, Quesnel R, Hildgen P. Synthesis of new versatile functionalized polyesters for biomedical applications. Polymer 2005;46(25):11263-11272.

15. Essa S, Rabanel JM, Hildgen P. Effect of polyethylene glycol (PEG) chain organization on the physicochemical properties of poly(d, l-lactide) (PLA) based nanoparticles. European Journal of Pharmaceutics and Biopharmaceutics 2010;75(2):96-106.

16. Shilpa S, Ve´ronique N, Hildgen P. Effect of porosity on the release kinetics of propafenone-loaded PEG-g-PLA nanoparticles. Journal of Controlled Release 2005;107:203-214.

17. Abebe A, Akseli I, Sprockel O, Kottala N, Cuitino AM. Review of bilayer tablet technology. International Journal of Pharmaceutics 2014;461(1-2):549-558.

18. Kleinebudde P. Roll compaction/dry granulation: pharmaceutical applications. European Journal of Pharmaceutics and Biopharmaceutics 2004;58(2):317-326.

19. Leuenberger H, Lanz M. Pharmaceutical powder technology from art to science: the challenge of the FDA's Process Analytical Technology initiative. Advanced Powder Technology 2005;16(1):3-25.

20. USP. United States Pharmacopeia and National Formulary (USP-NF). Rockville, MD, USA,; 2014.

21. Choi K-m, Choi M-C, Han D-H, Park T-S, Ha C-S. Plasticization of poly(lactic acid) (PLA) through chemical grafting of poly(ethylene glycol) (PEG) via in situ reactive blending. European Polymer Journal 2013;49(8):2356-2364.

22. Elmowafy E, Awad G, Mansour S, El-Shamy A. Release Mechanisms Behind Polysaccharides-Based Famotidine Controlled Release Matrix Tablets. Aaps Pharmscitech 2008;9(4):1230-1239.

23. Patravale VB, Date AA, Kulkarni RM. Nanosuspensions: a promising drug delivery strategy. Journal of Pharmacy and Pharmacology 2004;56(7):827-840.

24. Yoncheva K, Lizarraga E, Irache JM. Pegylated nanoparticles based on poly(methyl vinyl ether-co-maleic anhydride): preparation and evaluation of their bioadhesive properties. European Journal of Pharmaceutical Sciences 2005;24(5):411-419.

25. Vila A, Gill H, McCallion O, Alonso MÌaJ. Transport of PLA-PEG particles across the nasal mucosa: effect of particle size and PEG coating density. Journal of Controlled Release 2004;98(2):231-244.

26. Sant S, Poulin S, Hildgen P. Effect of polymer architecture on surface properties, plasma protein adsorption, and cellular interactions of pegylated nanoparticles. Journal of Biomedical Materials Research Part A 2008;87A(4):885-895.

27. Panakanti R, Narang AS. Impact of Excipient Interactions on Drug Bioavailability from Solid Dosage Forms. Pharmaceutical Research 2012;29(10):2639-2659.

28. Li Q, Rudolph V, Weigl B, Earl A. Interparticle van der Waals force in powder flowability and compactibility. International Journal of Pharmaceutics 2004;280(1-2):77-93.

29. Sepassi S, Goodwin DJ, Drake AF, Holland S, Leonard G, Martini L, et al. Effect of polymer molecular weight on the production of drug nanoparticles. Journal of Pharmaceutical Sciences 2007;96(10):2655-2666.

30. Parrott EL. Densification of powders by concavo-convex roller compactor. Journal of Pharmaceutical Sciences 1981;70(3):288-291.

31. Mckenna A, Mccafferty DF. Effect of particle size on the compaction mechanism and tensile strength of tablets. Journal of Pharmacy and Pharmacology 1982;34(6):347-351.

32. Dolenc A, Kristl J, Baumgartner S, Planinsek O. Advantages of celecoxib nanosuspension formulation and transformation into tablets. International Journal of Pharmaceutics 2009;376(1-2):204-212.

33. Teng Y, Qiu Z, Wen H. Systematical approach of formulation and process development using roller compaction. European Journal of Pharmaceutics and Biopharmaceutics 2009;73(2):219-229.

34. Sandler N, Lammens RF. Pneumatic dry granulation: potential to improve roller compaction technology in drug manufacture. Expert Opinion on Drug Delivery 2011;8(2):225-236.

35. Camboìn A, Brea J, Loza MI, Alvarez-Lorenzo C, Concheiro A, Barbosa S, et al. Cytocompatibility and P-glycoprotein Inhibition of Block Copolymers: Structure-Activity Relationship. Molecular Pharmaceutics 2013.

36. More PK, Khomane KS, Bansal AK. Flow and compaction behaviour of ultrafine coated ibuprofen. International Journal of Pharmaceutics 2013;441(1-2):527-534.

37. Sáska Z, Dredán J, Luhn O, Balogh E, Shafir G, Antal I. Evaluation of the impact of mixing speed on the compressibility and compactibility of paracetamol-isomalt containing granules with factorial design. Powder Technology 2011;213(1-3):132-140.

38. Hassouna F, Raquez J-M, Addiego Fdr, Dubois P, Toniazzo Vr, Ruch D. New approach on the development of plasticized polylactide (PLA): Grafting of poly(ethylene glycol) (PEG) via reactive extrusion. European Polymer Journal 2011;47(11):2134-2144.

39. McDevitt CA, Callaghan R. How can we best use structural information on P-glycoprotein to design inhibitors? Pharmacology & Therapeutics 2007;113(2):429-441.

40. Ferenczy GG, Parkanyi L, Angyan JG, Kalman A, Hegedus B. Crystal and electronic structure of two polymorphic modifications of famotidine. An experimental and theoretical study. Journal of Molecular Structure: (Theochem) 2000;503(1-2):73-79.

41. Sahoo NG, Kakran M, Shaal LA, Li L, Muller RH, Pal M, et al. Preparation and characterization of quercetin nanocrystals. Journal of Pharmaceutical Sciences 2011;100(6):2379-2390.

42. Morakul B, Suksiriworapong J, Leanpolchareanchai J, Junyaprasert VB. Precipitation-lyophilization-homogenization (PLH) for preparation of clarithromycin nanocrystals: Influencing factors on physicochemical properties and stability. International Journal of Pharmaceutics Special Section: Formulating Better Medicines for Children 2013;457(1):187-196.

43. Liu P, Rong X, Laru J, van Veen B, Kiesvaara J, Hirvonen J, et al. Nanosuspensions of poorly soluble drugs: Preparation and development by wet milling. International Journal of Pharmaceutics 2011;411(1-2):215-222.

44. Jiang T, Han N, Zhao B, Xie Y, Wang S. Enhanced dissolution rate and oral bioavailability of simvastatin nanocrystal prepared by sonoprecipitation. Drug Development and Industrial Pharmacy 2012;38(10):1230-1239.

45. Hecq J, Deleers M, Fanara D, Vranckx H, Amighi K. Preparation and characterization of nanocrystals for solubility and dissolution rate enhancement of nifedipine. International Journal of Pharmaceutics 2005;299(1-2):167-177.

46. Shoaib M, Al Sabah Siddiqi S, Yousuf R, Zaheer K, Hanif M, Rehana S, et al. Development and Evaluation of Hydrophilic Colloid Matrix of Famotidine Tablets. AAPS PharmSciTech 2010;11(2):708-718.

47. Mady FM, Abou-Taleb AE, Khaled KA, Yamasaki K, Iohara D, Ishiguro T, et al. Enhancement of the aqueous solubility and masking the bitter taste of famotidine using drug//SBE-b-CyD//povidone K30 complexation approach. Journal of Pharmaceutical Sciences 2010;99(10):4285-4294.

48. Baseer AB, Abdul), Hassan FH, Fouzia), Hassan SH, Syed Muhammad Fareed), Jabeen SJ, Sabahat), Israr FI, Fozia), Murtaza GM, Ghulam), et al. Physico-chemical comparison of famotidine tablets prepared via dry granulation and direct compression techniques. Pakistan Journal of Pharmaceutical Sciences 2013;26(3):439-443.

49. Avgoustakis K, Beletsi A, Panagi Z, Klepetsanis P, Karydas AG, Ithakissios DS. PLGA-mPEG nanoparticles of cisplatin: in vitro nanoparticle degradation, in vitro

drug release and in vivo drug residence in blood properties. Journal of Controlled Release 2002;79(1-3):123-135.

50. Rozehnal V, Nakai D, Hoepner U, Fischer T, Kamiyama E, Takahashi M, et al. Human small intestinal and colonic tissue mounted in the Ussing chamber as a tool for characterizing the intestinal absorption of drugs. European Journal of Pharmaceutical Sciences 2012;46(5):367-373.

51. Hugger ED, Cole CJ, Raub TJ, Burton PS, Borchardt RT. Automated analysis of polyethylene glycol-induced inhibition of P-glycoprotein activity in vitro. Journal of Pharmaceutical Sciences 2003;92(1):21-26.

52. Shen Q, Lin Y, Handa T, Doi M, Sugie M, Wakayama K, et al. Modulation of intestinal P-glycoprotein function by polyethylene glycols and their derivatives by in vitro transport and in situ absorption studies. International Journal of Pharmaceutics 2006;313(1-2):49-56.

53. Iqbal J, Hombach J, Matuszczak B, Bernkop-Schnurch A. Design and in vitro evaluation of a novel polymeric P-glycoprotein (P-gp) inhibitor. Journal of Controlled Release 2010;147(1):62-69.

54. Brendan M. Johnson, William N. Charman, Porter CJH. An In Vitro Examination of the Impact of Polyethylene Glycol 400, Pluronic P85, and Vitamin E d-a-Tocopheryl Polyethylene Glycol 1000 Succinate on PGlycoprotein Efflux and Enterocyte-Based Metabolism in Excised Rat Intestine. AAPS Pharmscitech 2002;4(4):13.

55. Kin-Kai H, Giesing DH, Hurst GH. Aventis Pharmaceuticals, Inc. Method of enhancing bioavailability of fexofenadine and its derivatives. US6451815 2002.

56. Mundargi RC, Babu VR, Rangaswamy V, Patel P, Aminabhavi TM. Nano/micro technologies for delivering macromolecular therapeutics using poly(d,l-lactide-co-glycolide) and its derivatives. Journal of Controlled Release 2008;125(3):193-209.

Chapter Five

General Discussion, Conclusion and Perspectives

5.1. General Discussion

The choice of PEG grafting ratio (1% and 5%) was based on previous works(1-4). GPC results of grafted polymers showed that average molecular weight of grafted PEG750Da1%-g-PLA polymer has the lowest molecular weight while PEG2000Da5%-g-PLA has the largest molecular weight (in consistency with PEG molecular weight and grafting ratio used). The actual grafting % obtained for PEG 750 grafting was lower than theoretical ones, whereas PEG 2000Da grafting was higher than expected. The better obtained results was using PEG 2000 Da compared to PEG 750 Da, it might be explained by reactivity of the different PEG with pendant carboxylic compared to ended carboxylic group. Mechanistic study could demonstrate the following hypothesis, PEG 750 Da reacts with lactic carboxylic group at the end of polymer backbone while PEG 2000 Da reacts more with pendant carboxylic group. PEG750Da1%-g-PLA thermograms (Table 3.1) show Tg at -1.77 °C but pure PEG have Tg at - 21°C, PLA at 50 °C and PLA-g-PEG at 29.68 °C, this results could be due to a low grafting efficiency of PEG as pendant group. The large amount of unreacted PEG could also plasticizes the polymer but PEG is very soluble in aqueous washing phase and it does not appear in GPC distribution. PEG molecular weight of 750 Da and 2000 Da were chosen for optimal biocompatibility. PEG with higher molecular weight become too big to be eliminated. A lower grafted % of PEG molecular weight smaller than 750 Da is possibly not enough to increase the hydrophilicity of the NPs surface.

^{1}H NMR spectrum and FTIR scans for the four synthesized grafted polymers PEG-g-PLA were obtained and the grafted polymers were used to prepare different NPs formulations. The average particle size is consistent by measurement using two different methods and with previous work(1-4). It does not seem that the amount of PEG nor Famotidine change the size of NPs. Chemical surface studies would be helpful to quantify the amount of PEG and to determine this self organized structure. Residual PVA was observed in many studies but the actual influence of this surfactant is not clearly demonstrated(2, 5). Our previous works do not show significant difference in size with NPs made by a method without any surfactant (nanoprecipitation)(6, 7). The advantage of emulsion/solvent evaporation method is an easy scalling up comparing to nanoprecipitation. Changing to another surfactant FDA approved should be done in future development. Nanoprecipitation do not allow to prepare enough NPs for tablet preparation. Famotidine is hydrophilic drug since the octanol/water partition coefficient is log P = -0.64 and it has ionisable guanidine basic group (pKa= 8.44). Famotidine is very hydrophilic at working pH (7.4) since calculated log D = -3,0 and actual water solubility is 1 g/l ; that could explain low drug loading. Polymorphic crystal form B of Famotidine is used in the commercial tablet form. DSC results of different loaded NPs formulations showed a shift of melting point of Famotidine to a higher temperature (180 °C). This suggests the presence of a crystalline form however no polymeric form at this melting point has been described in literature. The possible explanation is an interaction between the drug molecules and the polymer yielding a complex. For NPs as well as tablet with low loading, no melting point can be detected, then Famotidine could be molecularly dispersed as well as in

amorphous or nanocrystalline state. The XRPD scans of loaded NPs showed two pattern types that varied more with grafting ratios rather than with PEG molecular weight. XRPD scans of NPs prepared from PEG1% showed Famotidine form B characteristic peaks. While for PEG5%, Famotidine exhibited only two minor peaks at 21.50° and at 23.50° 2Θ, suggesting that Famotidine exists below XRPD limit of detection(8-11). Famotidine from NPs formulations showed fast release profiles which might be attributed to the hydrophilic nature of Famotidine(12, 13). Famotidine released profile did not show significant influence of polymer molecular weights, PEG molecular weights, PEG grafting ratios, particle size, and PVA on Famotidine released from different NPs formulations. Polymers and NPs characterizations results of different loaded NPs formulations showed Famotidine was encapsulated for the four different grafted polymers. The asymmetry index, namely the ratio of secretory (basolateral-to-apical) to absorptive (apical-to-basolateral) transport, reflects the overall effect of P-gp. For P-gp function inhibition it will be expected from the formulation that has lower AI value. Asymmetry index (AI) results from transport experiments of loaded NPs showed that NPs of PLA-g-5%PEG2000Da had the lowest AI value (0.007), followed by NPs prepared from PLA-g-5%PEG750Da (0.01), then PLA-g-1%PEG750Da (0.58). It can be noticed from asymmetry index results that increased P-gp inhibition were obtained from formulations containing PEG 5%, irrespective to molecular weights which is consistent with other findings(14-16). Therefore the two Famotidine loaded NPs formulations prepared from PEG-g-PLA grafted at 5% were selected to develop two NPs based tablet formulation. The tablet formulation was developed to be composed of 40 % of loaded NPs (corresponding to

1.6 mg of Famotidine per tablet), 52.5% of microcrystalline cellulose (MCC), 7% of pregelatinized starch and 0.5 % of magnesium stearate. The reason why tablets based on NPs (F1 and F2) had a weight of 500 mg is that they contained high quantity of NPs (40%) due to NPs low drug loading (0.8%). Therefore, high quantities of NPs with very poor powder flow quality were needed to compensate the low drug loading. Rapid partition of Famotidine into external phase during NPs preparations, therefore decreased Famotidine entrapment into NPs during polymer deposition(17). This was considered an obstacle in developing a tablet formulation for this study. Moreover high quantity of NPs was used to obtain detectable Famotidine concentration from drug transport study and for tablet characterization tests. Improving NPs drug loading would be effective approach to reduce NPs quantity then improve blend powder flow properties and decrease tablet weight. Famotidine is very hydrophilic therefore famotidine partition from oil into the aqueous phase, that could explain low drug loading. To avoid or minimize such partitioning of drug between two immiscible phases, w/o/w double-emulsion method would be preferred in producing NPs loaded to encapsulate hydrophilic drug(18). Both tablets formulations PLA-g-5%PEG2000Da (F1) and PLA-g-5%PEG750Da F2) were prepared by dry granulation in order to densify NPs powder with poor flow property. The bulk and tapped density were measured for NPs powder, powder blend before and after dry granulation for two NPs formulations (F1&F2). Results of bulk, tapped density, Hausner ratio and Carr's index of two NPs powder formulations showed very poor flowability. By comparing the results of Carr's index of NPs powder versus dry granulated ones, a significant improvement in powder flow was noticed. Even thought Carr’s index values after dry

granulation showed powder flow properties for both NPs formulations had a very poor flow, powder blends were practically sufficiently dense to be properly compressed. The size and particles size distribution (PSD) results obtained for F1, F2 and placebo blend formulations showed a Gaussian-like distribution of the particle size. PSD results of powder blend after dry granulation of both NPs tablet formulations with placebo were found similar, suggesting a proper densification process. Commercial Famotidine (Pepcid® 10 mg) was used as a comparator with NPs formulations. Tablet formulations (F1&F2) possessed good mechanical strength with sufficient hardness. Disintegration time for NPs tablet formulations (F1&F2) was less than one minute (20 seconds average) and 2.2 minutes for commercial Famotidine. NPs based tablet formulations had rapid disintegration time probably attributed to the dry granulation and the lower compression force. The mean particle size of NPs after tablet compressing were characterized to examine the influence of compressing force on NPs and results of NPs size showed that tablet compression process does not affect morphology of NPs. Despite the large amount of NPs, the size was not modified during compression. To obtained enough Famotidine in the tablet with NPs, large amount of NPs modified the properties of the powder and making tablet. Moreover, kinetic release of Famotidine from tablet formulations was studied to evaluate the effect of NPs matrix and compressing force. Comparing Famotidine released from NPs tablet formulation prepared by dry granulation and commercial Famotidine showed no differences, suggesting that the tablet manufacturing technique had no effect on Famotidine drug release. Stability results of tablet formulations (F1 and F2) showed no change neither for Famotidine melting point, Tg and Famotidine release in pH 7.4 PBS medium. Drug

dissolution Famotidine from F1, F2 and commercial tablet formulations showed fast released from 0.1 M phosphate buffer pH 4.5. The fast release was attributed to fast disintegration time for all tablet formulations that enhance penetrating of dissolution medium into the tablet and thus promote Famotidine release. There no modification of dissolution profile which are all immediate release. The transport study results (AI) of tablet formulations showed that the AI value of tablet of loaded NPs of PLA-g-5%PEG2000Da (F1) and PLA-g-5%PEG750Da (F2) were 0.07 and 0.43, respectively, while the AI value for commercial Famotidine was 1.02. F1 showed the most effective formulations (0.07) to inhibit P-gp function. Commercial Famotidine (no PEG) was used as a reference to evaluate the effect of PEG to inhibit or decrease P-gp efflux on Famotidine. Transport results of NP-based tablet formulations showed no impact of tabletting process on NPs to inhibit P-gp efflux. Transport results of tablet formulations containing NPs prepared from polymer grafted demonstrate that PEG 2000Da to be more effective to inhibit P-gp efflux of Famotidine than formulations containing PEG 750Da. There are three possible mechanisms for P-gp inhibition(19, 20). Even though pegylated NPs mechanism inhibits P-gp efflux is not clear, free PEG inhibits P-gp function(14). Aoun et al demonstrated also an inhibition of P-gp on fungus cells when using similar polymer as nanocarrier(4). To summarize transport results, it was observed that P-gp efflux inhibition of Famotidine is attributed to PEG content and results of loaded NPs and tablet formulations showed that P-gp efflux inhibition of Famotidine can be attributed to PEG content. Indeed, as PEG content increased, the inhibition effect increased which is consistent with the general hypothesis of the study(15, 21-23). The studies presented herein suggest that commonly used

pharmaceutical excipients such as PEG (750 Da and 2000 Da) are capable to inhibit efflux transporter (P-gp) activity. Those results confirmed our hypothesis that inhibition of P-gp Famotidine efflux by loaded NPs formulated as tablets is efficient and open a way to increase the bioavailability of drugs that are P-gp substrate. It has been reported that NPs transported via transcellular transport in which NPs up taken by endocytic process takes place at cell apical membrane intracellular trafficking toward exocytic release at basolateral compartment(24-26). Tablet made with NPs containing P-gp inhibitor allow formulator to use of less drug.

References

1. Essa S, Rabanel JM, Hildgen P. Effect of polyethylene glycol (PEG) chain organization on the physicochemical properties of poly(d, l-lactide) (PLA) based nanoparticles. European Journal of Pharmaceutics and Biopharmaceutics 2010;75(2):96-106.

2. Shilpa S, Ve´ronique N, Hildgen P. Effect of porosity on the release kinetics of propafenone-loaded PEG-g-PLA nanoparticles. Journal of Controlled Release 2005;107:203-214.

3. Sant S, Poulin S, Hildgen P. Effect of polymer architecture on surface properties, plasma protein adsorption, and cellular interactions of pegylated nanoparticles. Journal of Biomedical Materials Research Part A 2008;87A(4):885-895.

4. Valéry Aoun CD, Fabrice Pagniez, Jean-Michel Rabanel, Patrice Le Pape, V. Gaëlle Roullin, Grégoire Leclair, and Patrice Hildgen. Enhanced Pulmonary Administration of Amphotericin B Loaded in PEG-g-PLA Nanoparticles: In Vitro Proof-of-Concept and Susceptibility Against Candida spp. and Aspergillus spp. Journal of Nanopharmaceutics and Drug Delivery 2014:Accepted.

5. Sahoo SK, Panyam J, Prabha S, Labhasetwar V. Residual polyvinyl alcohol associated with poly (d,l-lactide-co-glycolide) nanoparticles affects their physical properties and cellular uptake. Journal of Controlled Release 2002;82(1):105-114.

6. Tobio M, Gref R, Sanchez A, Langer R, Alonso MJ. Stealth PLA-PEG Nanoparticles as Protein Carriers for Nasal Administration. Pharmaceutical Research 1998;15(2):270-275.

7. Rabanel J-M, Faivre J, Tehrani SF, Lalloz A, Hildgen P, Banquy X. Effect of the Polymer Architecture on the Structural and Biophysical Properties of PEGâ€“PLA Nanoparticles. ACS Applied Materials & Interfaces
ACS Appl. Mater. Interfaces 2015;7(19):10374-10385.

8. Sahoo NG, Kakran M, Shaal LA, Li L, Muller RH, Pal M, et al. Preparation and characterization of quercetin nanocrystals. Journal of Pharmaceutical Sciences 2011;100(6):2379-2390.

9. Morakul B, Suksiriworapong J, Leanpolchareanchai J, Junyaprasert VB. Precipitation-lyophilization-homogenization (PLH) for preparation of clarithromycin nanocrystals: Influencing factors on physicochemical properties and stability. International Journal of Pharmaceutics Special Section: Formulating Better Medicines for Children 2013;457(1):187-196.

10. Liu P, Rong X, Laru J, van Veen B, Kiesvaara J, Hirvonen J, et al. Nanosuspensions of poorly soluble drugs: Preparation and development by wet milling. International Journal of Pharmaceutics 2011;411(1-2):215-222.

11. Jiang T, Han N, Zhao B, Xie Y, Wang S. Enhanced dissolution rate and oral bioavailability of simvastatin nanocrystal prepared by sonoprecipitation. Drug Development and Industrial Pharmacy 2012;38(10):1230-1239.

12. Shoaib M, Al Sabah Siddiqi S, Yousuf R, Zaheer K, Hanif M, Rehana S, et al. Development and Evaluation of Hydrophilic Colloid Matrix of Famotidine Tablets. AAPS PharmSciTech 2010;11(2):708-718.

13. Abdul Baseer FH, Syed Muhammad Fareed Hassan, Sabahat Jabeen, Fozia Israr, Ghulam Murtaza, Naheed Haque. Physico-chemical comparison of famotidine tablets prepared via dry granulation and direct compression techniques. Pakistan Journal of Pharmaceutical Sciences 2013;26(3):439-443.

14. Hugger ED, Audus KL, Borchardt RT. Effects of poly(ethylene glycol) on efflux transporter activity in Caco-2 cell monolayers. Journal of Pharmaceutical Sciences 2002;91(9):1980-1990.

15. Hugger ED, Cole CJ, Raub TJ, Burton PS, Borchardt RT. Automated analysis of polyethylene glycol-induced inhibition of P-glycoprotein activity in vitro. Journal of Pharmaceutical Sciences 2003;92(1):21-26.

16. Hugger ED, Novak BL, Burton PS, Audus KL, Borchardt RT. A comparison of commonly used polyethoxylated pharmaceutical excipients on their ability to inhibit P-glycoprotein activity in vitro. Journal of Pharmaceutical Sciences 2002;91(9):1991-2002.

17. Govender T, Stolnik S, Garnett MC, Illum L, Davis SS. PLGA nanoparticles prepared by nanoprecipitation: drug loading and release studies of a water soluble drug. Journal of Controlled Release 1999;57(2):171-185.

18. Mundargi RC, Babu VR, Rangaswamy V, Patel P, Aminabhavi TM. Nano/micro technologies for delivering macromolecular therapeutics using poly(d,l-

lactide-co-glycolide) and its derivatives. Journal of Controlled Release 2008;125(3):193-209.

19. Werle M. Natural and Synthetic Polymers as Inhibitors of Drug Efflux Pumps. Pharmaceutical Research 2008;25(3):500-511.

20. Kaur V, Garg T, Rath G, Goyal AK. Therapeutic potential of nanocarrier for overcoming to P-glycoprotein. Journal of Drug Targeting 2014;22(10):859-870.

21. Shen Q, Lin Y, Handa T, Doi M, Sugie M, Wakayama K, et al. Modulation of intestinal P-glycoprotein function by polyethylene glycols and their derivatives by in vitro transport and in situ absorption studies. International Journal of Pharmaceutics 2006;313(1-2):49-56.

22. Iqbal J, Hombach J, Matuszczak B, Bernkop-Schnurch A. Design and in vitro evaluation of a novel polymeric P-glycoprotein (P-gp) inhibitor. Journal of Controlled Release 2010;147(1):62-69.

23. Kin-Kai H, Giesing DH, Hurst GH. Aventis Pharmaceuticals, Inc. Method of enhancing bioavailability of fexofenadine and its derivatives. US6451815 2002.

24. Monjed S, Gilles P, Elias F. Particle uptake by Peyer's patches: a pathway for drug and vaccine delivery. Expert Opinion on Drug Delivery 2004;1(1):141-163.

25. Rieux Ad, Fievez V, Garinot M, Schneider Y-J, Preat V. Nanoparticles as potential oral delivery systems of proteins and vaccines: A mechanistic approach. Journal of Controlled Release 2006;116(1):1-27.

26. M. Rabanel J, Aoun V, Elkin I, Mokhtar M, Hildgen P. Drug-Loaded Nanocarriers: Passive Targeting and Crossing of Biological Barriers. Current Medicinal Chemistry 2012;19(19):3070-3102.

5.2. Conclusion and Perspective

The PLA-g-PEG polymers with different grafting ratios 1 and 5 % were synthesized with molecular weights consistent with PEG molecular weight of 750 and 2000Da. The grafting of PEG on PLA was confirmed with ^{1}H NMR, FTIR and DSC results. NPs characterization results demonstrate that NPs formulations were prepared with mean particle size ranged from 156 to 211nm and a unimodal size distribution. NPs had zeta potential values ranging from -4.6 to -9.9 mV. Dry granulation was used to improve the powder blend flow properties due to the intrinsic poor flow properties of NPs.

Prepared tablets had adequate physical properties typical of an immediate release dosage form. NPs tablets formulation demonstrated that they provide an immediate release of Famotidine comparable to commercial Famotidine. Particle size, drug release and drug transport results of NP based tablet formulations showed that dry granulation and tabletting processes did not influence NPs properties. Transport study results showed that loaded NPs and tablet formulations prepared from PLA-g-5%PEG, irrespective of PEG molecular weights, are able to inhibit the P-gp efflux of Famotidine. Therefore, NPs prepared from PLA-g-5%PEG could be a promising oral solid formulation strategy to improve oral bioavailability of P-gp substrate. The permeability results of demonstrate the concept of connecting hydrophilic Me.PEG with hydrophobic PLA capable to inhibit P-gp efflux. Generally in addition to PEG inhibitory effect, drug loaded within PEGylated NPs could offer a protection from stomach harsh environment, increase drug dissolution and drug absorption. Thus, NPs prepared from PLA-g-5%PEG could be an effective formulation tool to enhance drug permeability by inhibition of P-gp efflux then improve oral bioavailability.

Encapsulation efficiency of NPs will be improved in order to decrease the quantity of NPs in the formulation due to poor flow of NPs. Results from PLA-g-5%PEG NPs formulations may or may not be relevant to in vivo situations such as pharmacokinetic studies on human formulations containing PEG or exploratory formulations containing PEG. Further studies (e.g. gut perfusion studies and pharmacokinetic studies in animal models) should be conducted to establish a possible in vitro/in vivo correlation. For a

broader use of PLA-g-PEG copolymers as delivery systems, we may try to encapsulate other drugs (e.g. anticancer drugs) into those types of particles. Long term chemical and physical stability will be carried out for NPs based tablet formulations.